THESIS APPROVAL

GRADUATE SCHOOL, KASETSART UNIVERSITY

Doctor of Philosophy (Chemistry)

DEGREE

Chemistry | Chemistry

FIELD | **DEPARTMENT**

TITLE: Quantum Chemical Calculations and ONIOM Studies on Cyclopropane Synthase, Succinate Dehydrogenase and Cyclooxygenase

NAME: Miss Darinee Sae-Tang

THIS THESIS HAS BEEN ACCEPTED BY

THESIS ADVISOR

(Associate Professor Supa Hannongbua, Dr.rer.nat.)

COMMITTEE MEMBER

(Mr. Chak Sangma, Ph.D.)

COMMITTEE MEMBER

(Mr. Prasat Kittakoop, Ph.D.)

COMMITTEE MEMBER

(Miss Sumalee Kamchonwongpaisan, Ph.D.)

COMMITTEE MEMBER

(Professor Peter Wolschann, Dr.rer.nat.)

DEPARTMENT HEAD

(Assistant Professor Noojaree Prasitpan, Ph.D.)

APPROVED BY THE GRADUATE SCHOOL ON .....

DEAN

(Associate Professor Gunjana Theeragool, D.Agr.)

THESIS

QUANTUM CHEMICAL CALCULATIONS AND ONIOM STUDIES ON CYCLOPROPANE SYNTHASE, SUCCINATE DEHYDROGENASE AND CYCLOOXYGENASE

DARINEE SAE-TANG

A Thesis Submitted in Partial Fulfillment of
the Requirements for the Degree of
Doctor of Philosophy (Chemistry)
Graduate School, Kasetsart University
2009

Darinee Sae-Tang 2009: Quantum Chemical Calculations and ONIOM Studies on Cyclopropane Synthase, Succinate Dehydrogenase and Cyclooxygenase. Doctor of Philosophy (Chemistry), Major Field: Chemistry, Department of Chemistry. Thesis Advisor: Associate Professor Supa Hannongbua, Dr.rer.nat. 127 pages.

The application of computational calculations to biological systems has become interesting to describe enzyme/ligand interaction. Three enzymes, cyclopropane synthase, succinate dehydrogenase and cyclooxygenase, were investigated using performance of quantum chemical calculations and ONIOM approach. Firstly, the interaction energies of the cofactor in the methylation with the cyclopropane synthase, SAM, SAH, and sinefungin were performed. The important residues are found to be Asp70 and Glu121 in which SAM shows a stronger interaction than sinefungin and SAH, respectively. Moreover, twenty five systematic ONIOM2 calculations were performed for the cyclopropane synthase with various model systems. The SAM cofactor obviously strongly interacts in the cofactor binding site than SAH product as a consequent of the methyl substituent at the sulfur atom resulting in positive charge around sulfur and neighboring atoms in the system. Secondly, the ONIOM calculations of succinate dehydrogenase and 3-NP inhibitor, were investigated and compared with succinate, in the substrate binding site of succinate dehydrogenase flavoprotein subunit.The obtained results showed that the succinate establishes more tight binding than 3-nitropropionate of about 3 times. The individual interaction calculations between 3-NP/succinate, including FAD, and various amino acids indicated that the interaction energy with Arg409 is the main contributor and the flavin derivatives FAD play an important role in the binding pocket of the complex. Finally, the binding energy calculations of flurbiprofen to the binding pocket of cyclooxygenase were performed. Comparison of interaction energies between flurbiprofen with COX-1 and COX-2 binding site was studied. The results showed that the main interaction between flurbiprofen and two COX isozymes are due to Arg120. In addition, selective COX-2 inhibitor, SC558, was also compared and it was found that repulsive interaction plays significant role for specific interaction of this inhibitor to COX-2 inhibition. Taken into account, ONIOM2 method can be useful to describe specific interaction of the inhibitor and helpful for design of specific potent inhibitors.

_____ _____ ___ / ___ / ___

Student's signature Thesis Advisor's signature

ACKNOWLEDGMENTS

I would like to express my gratitude to my advisor, Associate Professor Dr. Supa Hannongbua who shared me a lot of her experience and research insight. I greatly appreciate her extensive knowledge and teach me many things. She is the model of a virtuous and successful researcher. I also like to express for her tremendous support and meticulous attention throughout the duration of my PhD studied. I also wish to express my acknowledge to my co-advisor Dr. Sumalee Kamchonwongpaisan, Senior Researcher at National Center for Genetic Engineering and Biotechnology (BIOTEC), for invaluable helping and providing a wealth of advice. She is then the model of goodness and ethics for me. I especially thank my co-advisor Dr. Prasat Kittakoop, researcher at Chulabhorn Research Institute for his direction, suggestion and encouragement of my research. I would like to thank Prof. Simon Mackay, Prof. Peter Wolschann, Dr. Chak Sangma and Associate Professor Supanna Techasakul for their worthy suggestion and constructive criticism**.** I am in sincere appreciation to my entire committees for the most generous of generous of gifts, their time and experience. I wish to thank my friends Nahoum and Stephanie Anthony, for helping me get through the lively times, and caring which they provided me in Scotland.

I recognize that this research would not have been possible without the financial support from Thailand Graduate Institute of Science and Technology, (TGIST), Kasetsart University Research and Development Institute (KURDI). I am deeply grateful to the my colleagues at Laboratory for Computational and Applied Chemistry (LCAC) for their providing helpful assistance, sharing useful ideas and providing a loving environment and I would also like to thank all of staffs at Department of Chemistry, Faculty of Science, Kasetsart University for research facilities.

Lastly, and most importantly, I wish to thank my parent and my sister. They supported me, encouraged me and love me.

Darinee Sae-Tang
March, 2009

TABLE OF CONTENTS

LIST OF TABLES

LIST OF TABLES (Continued)

LIST OF TABLES (Continued)

LIST OF TABLES (Continued)

LIST OF FIGURES

LIST OF FIGURES (Continued)

LIST OF FIGURES (Continued)

LIST OF ABBREVIATIONS

3-NP	=	3-nitropropionic
AA	=	Arachidonic acid
AA5	=	Atpenin A5
Ala	=	Alanine
Arg	=	Arginine
Asp	=	Aspartic acid
B3LYP	=	Becke's three parameter hybrid functional using the LYP
BBF	=	Backbone Atoms Fixing
BCG	=	Bacillus Calmette-Guerin
BE	=	Binding Energy
BSSE-CP	=	Basis set superposition error based on counterpoise
CmaA1	=	Cyclopropane mycolic acid synthase1
CmaA2	=	Cyclopropane mycolic acid synthase2
CoMFA	=	Comparative molecular field analysis
CoMSIA	=	Comparative molecular similarity indices analysis
COX	=	Cyclooxygenase
CTAB	=	Cetyltrimethylammonium bromide
Cys	=	Cysteine
DDDMAB	=	Didecyldimethylammonium bromide
DEF	=	Deformation Energy
DFT	=	Density Functional Theory
F	=	Fix water
FLP	=	Flurbiprofen
FAD	=	Flavin adenine dinucleotide
FADH2	=	1,5-dihydro-flavin adenine dinucleotide
HAF	=	Heavy Atoms Fixing
His	=	Histidine
HIV	=	Human Immunodeficiency Virus

LIST OF ABBREVIATIONS (Continued)

HF	=	Hartree-Fock
IC50	=	Inhibitory Concentration 50%
Ile	=	Isoleucine
INT	=	Interaction Energy
KDH	=	Ketoglutarate dehydrogenase
Kgd	=	Ketoglutarate decarboxylase
LAM	=	lipoarabinomannan
Lys	=	Lysin
MC	=	Monte Carlo
MD	=	molecular dynamics
Met	=	Methionine
MP2	=	Møller- Plesset perturbation
M.tuberculosis	=	Mycobacterium tuberculosis
N	=	Neutral form of cofactor
NSAID	=	Nonstereoidal anti-inflammatory drug
ONIOM	=	Our own N-layered Integrated molecular Orbital and molecular Mechanics
PcaA	=	Proximal Cyclopropanation of Alpha-mycolates
PG	=	Prostaglandin
Phe	=	Phenylalanine
Pro	=	Proline
PM3	=	MNDO Parametric Method number3
PYR	=	Pyrimidine part of adenine cofactor
Q	=	Ubiquinone
QH_2	=	Ubiquinol
QM	=	Quantum Mechanics
QSAR	=	quantitative structure-activity relationship
R	=	Relax water

LIST OF ABBREVIATIONS (Continued)

SC558	=	4-[5-(4-bromophenyl)-3-trifluoromethyl-1H-1-pyrozolyl-benzenesulfonamide
SDH	=	Succinate dehydrogenase
SAM	=	S-adenosyl-L-methionine
SIN	=	Sinefungin
SAH	=	S-adenosyl-L-homocysteine
SdhA	=	Succinate dehydrogenase chain A
SdhB	=	Succinate dehydrogenase chain B
SdhC	=	Succinate dehydrogenase chain C
SdhD	=	Succinate dehydrogenase chain D
SQRs	=	Succinate:Ubiquinone Oxidoreductase
TB	=	Tubercuclsis
TCA	=	Citric acid cycle
Trp	=	Triptophan
Tyr	=	Tyrosine
Val	=	Valine
Z	=	Zwitterionic form of cofactor

QUANTUM CHEMICAL CALCULATIONS AND ONIOM STUDIES ON CYCLOPROPANE SYNTHASE, SUCCINATE DEHYDROGENASE AND CYCLOOXYGENASE

INTRODUCTION

The application of computational calculations to biological systems has become interesting to describe an interaction of an enzyme/ligand. The excellent increase in computer power has applied many atoms to calculate for quantum chemical methods to perform of the large systems. An Our-own-N-layered Integrated molecular Orbital and Molecular mechanics (ONIOM) method is one of the challenge methods that combines a quantum mechanical (QM) with the quantum mechanical (QM) or the molecular mechanical (MM) methods. This method is very powerful for study biological system that has large number of atoms while pure quantum mechanical cannot operate due to it needs more computational cost. Moreover, this method is very reliable and efficient, adopted by Morokuma group (Dapprich *et al.*, 1999; Feliu Maseras, 1995; Svensson *et al.*, 1996). The concept of this approach is divide the system in two or three layers (ONIOM2 and ONIOM3) look like partition of onion skin. Many areas of chemistry and biology take this advantage method to study many biological systems to perform detail of interaction. In this study, quantum chemical calculation and ONIOM hybrid method were implemented and applied in two targets; tuberculosis and anti-inflammatory.

Tuberculosis

Tuberculosis (TB) keeps a major public health concern in spite of the availability of effective chemotherapy. This disease is mainly caused by *Mycobacterium Tuberculosis* (*M. tuberculosis* and one of the oldest and most devastating of human affliction. It infects two billion people and kills more than 2 million people annually, more than any other infectious disease (WHO, 2005). The rise in TB incidence over the two last decades is due to Human Immunodeficiency

Virus (HIV) pandemic and due to the spread of multi-drug resistant strains of the bacteria. While several antibiotics are effective in treating mycobacterial infections, these drugs target a surprisingly small number of essential functions in the cell and there has been no new TB drugs introduced since 1960s. Unfortunately, drug companies are not interested in developing anti-TB drugs because it has a relatively small incident in industrialized countries not when comparing to that developing countries. *M. tuberculosis* is susceptible to effective anti-microbacteria.

Tuberculosis drugs are classified into two categories. The first-line drugs of treatment of tuberculosis are isoniazid (INH), ethambutol (EMB), rifampicin (RIF), pyrazinamide (PZA), streptomycin and combination of these drugs. Targets for treatment drugs are various such as cell wall biogenesis and chromosomal replication. For example, isoniazid acts on the mycolic acid cell wall by inhibiting the synthesis of mycolic acids while ethambutol acts on lipoarabinomannan (LAM), a complex mole extending from the plasma membrane to the surface. Rifampicin binds to bacterial RNA polymerase. However, these drugs are not effective, current treatment of tuberculosis also needed to shorten the 6 month, lack of patient compliance with chemotherapy and problem from multi-drug-resistant infections. Next, the second line drugs, para-aminosalicylic acid (PAS), ethionamide (ETA), cycloserine (CS), fluroquinolones and kanamycin, are contributed due to mutation resistance from *M. tuberculosis* pathogen despite even though they have side effects.

There is much number of genes for *M. tuberculosis* genomes which can be new possible drug targets to resistant this pathogen. For instance, attractive targets of *M. tuberculosis* are metabolism, persistence, cell wall synthesis, etc (George *et al.*, 1995; Smith and Norton, 1980). In this study, we focused two enzyme targets, cyclopropane synthase that related with mycolic acids synthesis and succinate dehydrogenase that may be involved in respiration of bacteria.

1. Cyclopropane Synthase

Cyclopropane synthase is a promising target for tuberculosis drugs related with cell wall synthesis of bacteria. The cell envelope of *M. tuberculosis* is gram-positive organism which shows unique membrane and highly complex hydrophobic consisting of glycolipids and mycolic acids. This pathogen is strongly acid-alcohol-fast rod and has hydrophobic lipid surface. The mycolic acids of *M.tuberculosis* are very distinctive and make up more than 40% of mycobacterial cell wall. Mycolic acids are α-alkyl-β-hydroxyl long chain fatty acids with 60 to 90 carbon atoms (Barry *et al.*, 1998; Yuan *et al.*, 1995). Branch of side chain consists of methyl group, double bonds and cyclopropane rings as shown in Figure 1.

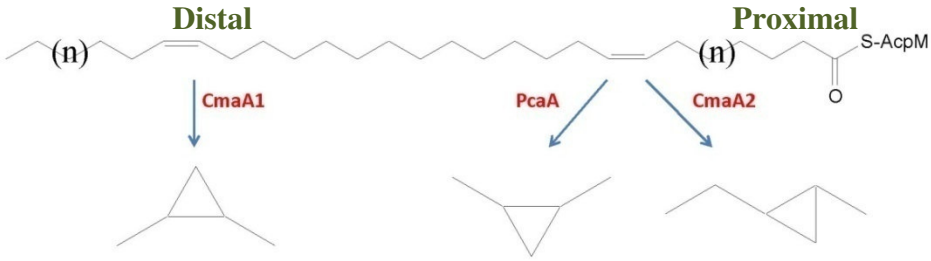

Figure 1 Reactions catalyzed by CmaA1, PcaA and CmaA2.

At least seven homologous genes of H37Rv have been identified.(Cole *et al.*, 1998) Only three enzymes are investigated in this study, Proximal Cyclopropanation of Alpha-mycolates (PcaA), Cyclopropane mycolic acid synthase1 (CmaA1) and Cyclopropane mycolic acid synthase2 (CmaA2). PcaA, CmaA1 and CmaA2 are the enzyme that required for cording and mycolic acid cyclopropane ring in the cell wall of *M. tuberculosis*. PcaA is the enzyme required for the synthesis of the proximal cyclopropane of alpha mycolic acid. CmaA1 is involved in carrying out cyclopropane ring at either the distal or the proximal position, and only proximal position in CmaA2.

Cyclopropane synthase from *M. tuberculosis* introduces a cyclopropane ring into the unsaturated alkyl chain of a fatty acid substrate via the transfer of a methylene group from the ubiquitous methylating cofactor S-adenosyl-L-methionine (SAM) to a (Z)-double bond as shown in Figure 2. These enzymes are considered essential targets for new antituberculosis drugs because cyclopropanation of mycolic acids is associated with the virulence and persistence of the mycobacterium.

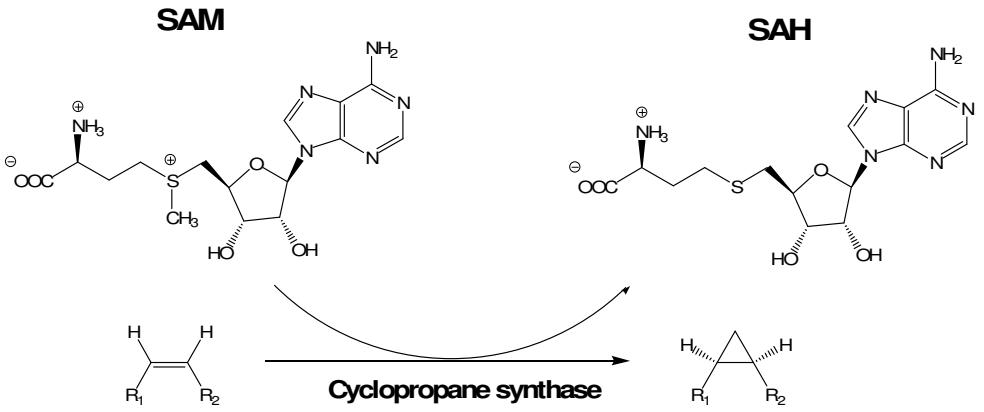

Figure 2 Reaction of cyclopropane synthase.

Cyclopropanation of unsaturated mycolic acids to cyclopropane mycolic acid uses SAM cofactor. S-adenosyl-L-methionine (SAM), a methyl donor, has been found to involved in methyltransferases of many macromolecules (Salvatore, 1977). Analogues of SAM have been recognised as potential inhibitors of the methylation process in many diseases including cancer, primarily through the action of methyltransferases on nucleic acid substrates. With respect to the cyclopropanation of fatty acids in *M. tuberculosis*, competition with the methylating cofactor offers the possibility of developing small molecule inhibitors with drugable character. Indeed, the reaction product S-adenosyl-L-homocysteine (SAH) and the natural product sinefungin both entirely inhibit in vitro methylene transfer in low μM concentrations (at levels similar to those seen with other methyltransferases) in *M. Tuberculosis*. Sulfone analogues of SAM inhibit a related cyclopropane fatty acid synthases in *E. coli*, which is considered a model for the development of *M. tuberculosis* inhibitors.

Sinefungin is a natural nucleoside antibiotic whose structure similar to S-adenosylhomocysteine and S-adenosylmethionine (see Figure 3). It has been shown to inhibit the development of fungi and parasite (Smith and Norton, 1980). Therefore, in this study, this compound is found because it is structurally similar to SAM as shown in Figure 3. Moreover, many biological activities of sinefungin have been shown to be related to inhibition of the methyltransferases enzymes. In an attempt to correlate with SAM structure and sinefungin using its analogues suggested that a positive charge on the sulfur atom is not required for high affinity, while the adenosine moiety is necessary for strong binding in the active site (Guérard *et al.*, 2004).

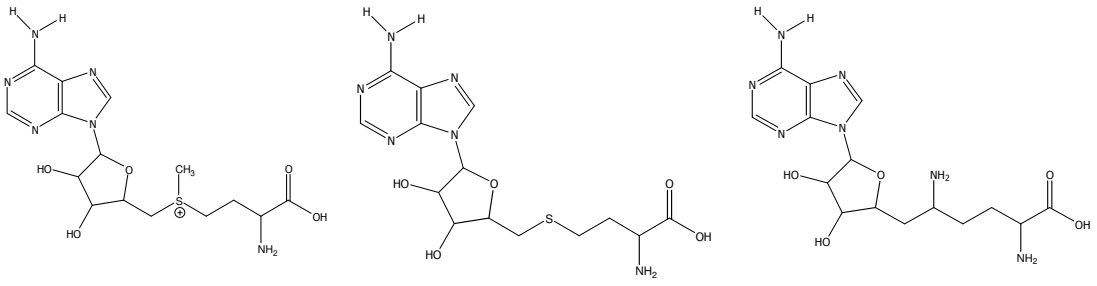

(a) (b) (c)

Figure 3 Structure of SAM (a), SAH (b) and sinefungin (c).

If the *M. tuberculosis* cyclopropane synthases are to be pursued as targets in tuberculosis therapy, then characterisation of SAM/SAH binding site is required for designing small molecules to effectively compete with the cofactor. We have performed an in-depth modelling analysis based on quantum chemical calculations, of three cyclopropane synthases with bound SAM, SAH and sinefungin to identify those residues that must be targeted by any small molecule to effectively compete and ensure inhibit of the methylation process.

2. Succinate Dehydrogenase

Succinate dehydrogenase (SDH) is an enzyme system has been found in the matrix part of the inner mitochondrial membrane. The enzyme complex has two main parts, one contribute to the citric acid (TCA) cycle with the task to catalyse the reversible interconversion between succinate and fumarate, a reaction involves an enzyme-bound FAD/FADH2 couple and the other is complex II of the electron transport chain, which uses electrons freed from succinate, to iron-sulfur clusters inside the enzyme and release the $2H^+$ back into the mitochondrial matrix. The iron-sulfur clusters will reduce ubiquinone, Q, to ubiquinol, QH_2.

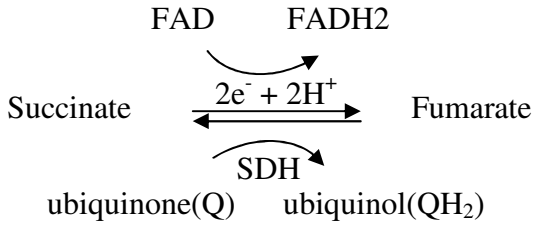

Figure 4 Reaction pathway of succinate to fumarate via succinate dehydrogenase.

Complex II has been well characterized in bacteria, fungi, and mammals and is known to be the simplest of all the complexes of the electron transport chain, with composed of 4 subunits (Lemire and Oyedotun, 2002; Yankovskaya *et al.*, 2003). It contains two peripheral membrane proteins, a flavoprotein subunit (SdhA) and an iron-sulfur protein subunit (SdhB), and two small integral membrane proteins (SdhC and SdhD), respectively. The succinate binding site is formed by the SdhA polypeptide, which is linked covalently to a FAD molecule acting as acceptor of a hydride ion at an early step of succinate oxidation. This flavoprotein subunit interacts with the SdhB subunit that contains three nonheme iron-sulfur centers acting as conductors of electrons from the flavoprotein to the membrane. The two small integral proteins anchor the SdhA-SdhB subcomplex to the matrix side of the inner membrane

and contain a b-type heme and the ubiquinone-binding site (Yankovskaya *et al.*, 2003).

The TCA cycle can be blocked at the level of succinate dehydrogenase using the competitive active site directed inhibitor 3-NP, 3-nitropropionic (Alston *et al.*, 1977). The inhibition by 3-NP has been widely found in plants (Patocka *et al.*, 2000; Salem *et al.*, 1995; Williams *et al.*, 1975) and some fungi (Nielsen and Smedsgaard, 2003; Paterson and Kemmelmeier, 1990). 3-NP inactivated SDH in the TCA cycle by covalently and irreversibly binding to its active site. Furthermore, 3-NP inhibits SDH in complex II of the mitochondrial electron transport chain.

3-NP is an also exhibited potent anti-mycobacterial activity against *M. tuberculosis* H37Ra (Chomcheon *et al.*, 2005). The mode of action of 3-NP for antimycobacterial activity may be related to the inhibition of mycobacterial succinate dehydrogenase. Recent proteomic studies of *M. tuberculosis* revealed the presence of a succinate-semialdehyde dehydrogenase gene in the bacterium (Schmidt *et al.*, 2004), and therefore 3-NP could be a potential lead chemotype for this enzyme target. Moreover, 3-NP has been known as a potent neurotoxic agent (Brouillet E, 1993). Such this inhibitor has a potential to be developed into drugs against persistent bacteria. In addition, understanding the resistant mechanisms in *M. tuberculosis* should lead to increase understanding of drug targets.

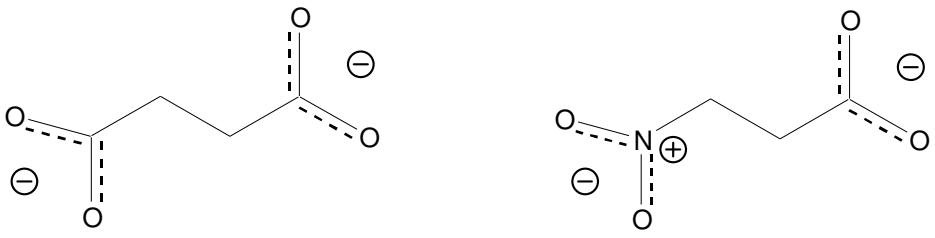

Succinate 3-Nitropropionate

Figure 5 Chemical structure of succinate and 3-nitropropionate

Anti-Inflammatory

1. Cyclooxygenase

Nonstereoidal anti-inflammatory drugs (NSAIDs) (Mantri and T.Witiak, 1994; Vane and Botting, 1996) such as aspirin, ibuprofen, flurbiprofen, and naproxen are commonly used for the treatment of pain, fever, and inflammatory. Their principal pharmacological effect is their ability to inhibit prostaglandin synthesis. They display their anti-inflammatory action mainly through inhibition of cyclooxygenase (COX), transforming arachidonic acid into prostaglandins (Smith *et al.*, 1996). Beyond their therapeutic utility, traditional NSAIDs possess predictable side effects including dyspepsia, gastrointestinal (GI) ulceration, and antiplatelet activity. Because of the widespread use of NSAIDs, these toxicities are one of the most prevalent drug-associated health risks.

The discovery of two isoforms of COXs (Xie *et al.*, 1991), COX-1 and COX-2, has helped in understanding the side effects associated with NSAIDs. COX-1 is constitutively expressed in most tissues and, particularly, in the gastrointestinal tract and kidneys where it is mainly responsible for the synthesis of cytoprotective prostaglandins. COX-2 is selectively induced by proinflammatory cytokines (IL-1) and growth factors (TNFR) and facilitates the release of prostaglandins involved in the inflammatory process (Katori *et al.*, 1998; Vane and Botting, 1996). This discovery led to the hypothesis that side effects such as ulcers and renal failure associated with the clinically useful NSAIDs are caused by the inhibition of COX-1, whereas the anti-inflammatory properties result from the inhibition of the inducible COX-2. Therefore, specific COX-2 inhibitors provided a new class of anti-inflammatory, analgesic and antipyretic drugs with significantly reduced side effects.

The development of the new generation of NSAIDs (Figure 6) began with the unexpected discovery of a second cyclooxygenase isozyme. Two groups of researchers, one studying genes elevated in transformed chicken fibroblasts (Simmons *et al.*, 1989) and another studying genes induced by phorbol esters in murine

fibroblasts (Kujubu *et al.*, 1991), had independently discovered a second cyclooxygenase gene that appeared, based on its pattern of regulation and expression, to be the sole isozyme that produced prostaglandins responsible for potentiating inflammatory processes (Smith *et al.*, 1996). The realizations that inhibition of COX-2 might be sufficient to achieve the therapeutic benefits of NSAID therapy and, conversely, that the indiscriminate inhibition of COX-1 likely resulted in the side effects commonly associated with NSAIDs stimulated an intense and highly competitive race to identify compounds that would selectively inhibit only COX-2.

The first few COX-2 selective compounds identified were DuP697 (Copeland *et al.*, 1994) and NS398 (Futaki *et al.*, 1994). These two NSAIDs had already in development when COX-2 was discovered. These compounds had been singled out for their gastrointestinal sparing properties in animal models. When tested using recombinant human cyclooxygenases (Meade *et al.*, 1993) Barnett *et al*., 1994; O'Neill *et al*., 1994; Kargman *et al*., 1996b; Riendeau *et al*., 1997), they were shown to be 80- and 1000- fold more selective, respectively, for inhibition of COX-2 (Gierse *et al*., 1995). Although the development of NS398 and DuP697 was later discontinued, the structure of DuP697 served as a starting point for the synthesis of the diarylheterocyclic family of selective inhibitors, which include SC58635 (celecoxib) and MK-966 (rofecoxib) (Hunt *et al.*, 2003; Smith and Baird, 2003).

A second generation of NSAIDs has been developed for the treatment of rheumatoid arthritis and osteoarthritis. These drugs selectively inhibit the COX-2 isozyme by having a reduced incidence of gastrointestinal irritation. In fact, celecoxib has been approved by the FDA as the first drug for treatment of familial adenomatous polyposis, a hereditary disease that leads to colorectal cancer. In addition, epidemiological studies suggest that COX-2 selective anti-inflammatory drugs may become a new option in treatment of cancer and the treatment of Alzheimer's disease (Sawdy *et al.*, 1997; Kutchera *et al.,* 1996; Stewart *et al*., 1997).

The COX-2 inhibitors can structurally be restricted to only two classes, (1) the acidic methane sulphonamide containing diphenyl ethers, represented by nimesulfide and NS398, and (2) the vicinal diaryl heterocycles having essentially either sulfonamide (SO_2NH2) or methylsulfonyl (SO_2Me) substitution at one of the phenyl ring, represented by SC558, celecoxib, rofecoxib and valdecoxib. The two adjacent phenyl rings of these COX-2 inhibitors orient in rigid cis-stilbene geometry and the phenyl ring having SO_2NH_2/SO_2Me group extends towards hydrophilic region of Val523 on COX-2 binding pocket. This feature has thus been proposed to be the primary determinant for the COX-2 selectivity. Furthermore, lack of this rigid geometry can also be reasoned for conventional NSAIDs to be nonselective.

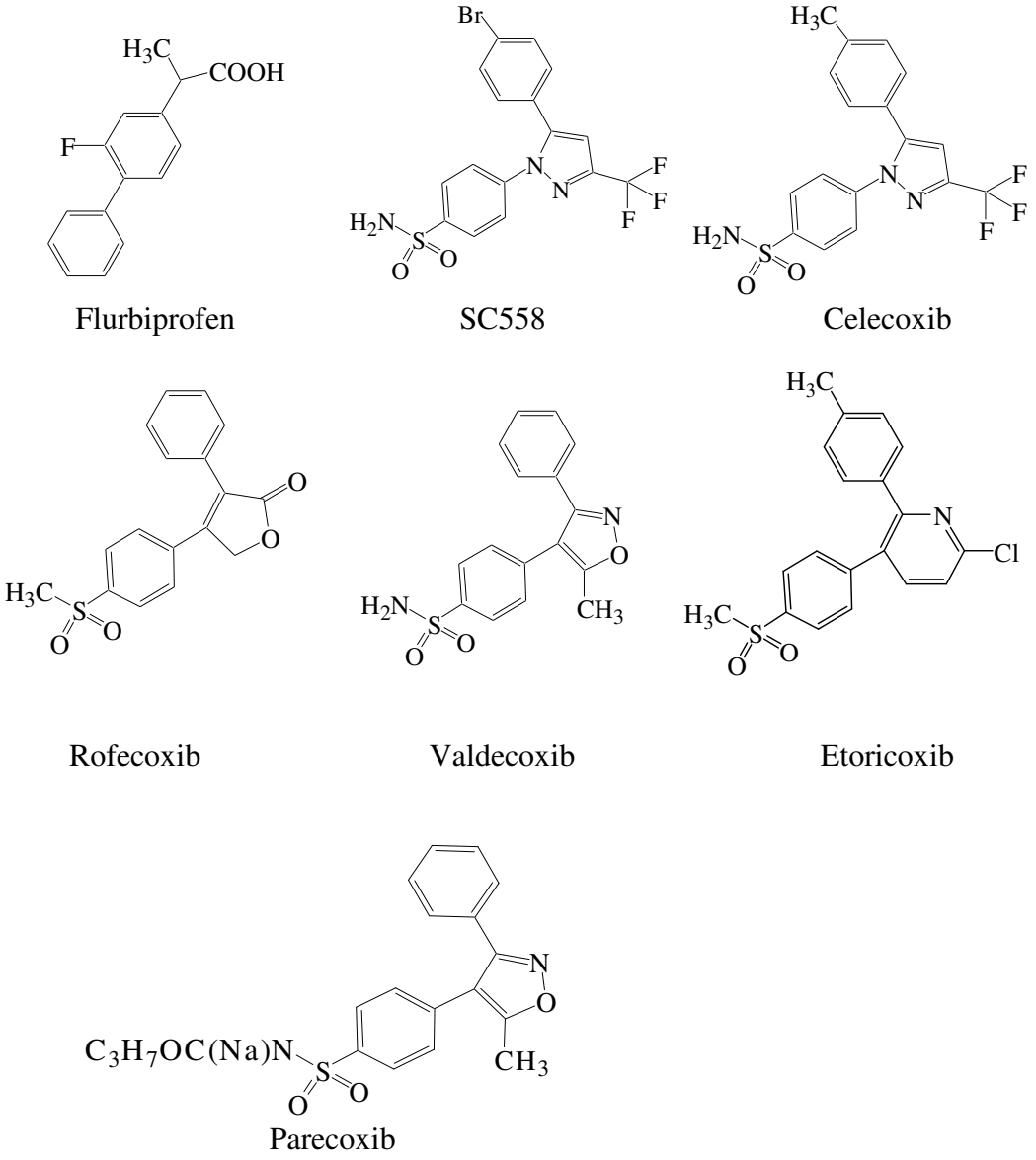

Figure 6 Molecular structures of NSAIDs and coxibs.

The cyclooxygenase binding site in both isozymes is a long, narrow hydrophobic channel extending from the membrane binding region of the protein. At the entrance of the channel, Arg120, Glu524, Tyr355 and Arg513 form a network of hydrogen bonds that acts as a gate to the binding site. Traditional NSAIDs that contain a carboxylate moiety that interacts with the salt bridge between Glu524 and Arg120, the trifluoromethyl group in SC558 does not provide this charge-charge interaction. In the eastern side of the binding site, the sulfonamide group extends into a relatively

polar side pocket that is somewhat restricted in COX-1. Based on site-directed mutagenesis experiments, the primary factor contributing to the COX-2 selectivity of SC558 (Kurumbail *et al*., 1996) is the substitution of Ile523 in COX-1 for valine in COX-2. However, the nearby His/Arg513 replacement may also contribute to selectivity. Crystal structure data suggest that these residue differences improve access of the sulfonamide to a side pocket.

Most of non-selective COX inhibitors or NSAIDs have carboxylate group binds within the cyclooxygenase active site. These carboxylate of drugs form salt bridge and stabilizes the guanidinium group of Arg120. In this study, *(S)*-flurbiprofen was choosen for represent in non-selective COX inhibitor class. Flurbiprofen, +/- 2-(2-fluoro-4-biphenyl)-propionic acid, is a chiral 2-arylpro-pionic acid. For selective COX-2 inhibitor has a diaryl heterocyclic ring and a central of five member ring (celecoxib, rofecoxib, valdecoxib or etoricoxib) or six member ring (etoricoxib) with specificity for COX-2 binding site. SC558, 4-[5-(4-bromophenyl)-3-trifluoromethyl-1H-1-pyrozolyl-benzenesulfonamide, was picked on as representative in this work.

OBJECTIVES

Performance of quantum chemical calculation have been used for the study of large biochemical system in three enzymes, cyclopropane synthase, succinate dehydrogenase and cyclooxygenase with the aims of

1. To identify key residues that bind to SAM and SAH cofactor in the cyclopropane synthase.
2. To examine the important subunits of SAM and SAH cofactors.
3. To study the effect of water molecules in the cyclopropane synthase cofactor binding site.
4. To compare the interaction of succinate and 3-NP in the succinate dehydrogenase enzyme.
5. To investigate the interaction of flurbiprofen and SC558 in cyclooxygenase-2.
6. To investigate the effect of charge and neutral state in the cyclopropane synthase and cyclooxygenase systems.

LITERATURE REVIEW

1. Tuberculosis

Tuberculosis (TB), once considered eradicated has again become a major global health concern. It is a condition that if untreated, can last for several years during which patients are debilitated and may disseminate *M. tuberculosis*, the bacterium that causes the disease. Estimates indicate that one-third of the world's population is infected with latent or persistent form of the disease (Bloom and Small, 1998; Dye *et al.*, 1999) and that 8.9 million new cases of the disease and 1.7 million deaths were reported worldwide in 2004 (Dye, 2006). The resurgence of the disease is caused by an inadequate and extended chemotherapy that relies on drugs developed in the mid-twentieth century. The associated poor patient compliance and emergence of drug resistant forms of TB, coupled with a strong epidemiological co-existence with HIV/AIDS highlights the fundamental need for new, more effective drugs to treat the disease (Mitchison, 1992; Mitchison, 2004).

M. tuberculosis is a successful pathogen in part because it persists and maintains chronic infections in humans, not withstanding an active immune response. It persists by exhibiting diverse metabolic states, only few of which can be targeted by current anti-mycobacterials. While the growing bacteria can be eliminated by drugs specific for factors involved in cell growth and division, the slow growing or dormant sub-populations maintain a sub-clinical infection weeks after the start of therapy. Many of pathways involved in a persistent phase of infection and pathogenesis of *M. tuberculosis* such as glyoxylate shunt enzymes (McKinney *et al.*, 2000), isocitrate lyase (Sharma *et al.*, 2000), malate synthase (Smith *et al.*, 2003) and cyclopropane synthases (Huang *et al.*, 2002) that lead to new targets for drug development.

Interestingly, persistence depends on genes required for supplying metabolites that allow mycobacteria to adapt to the adverse environment within the active macrophages. Under these conditions, glycolysis pathway is an importance. It decreased and the glyoxylate shunt is significantly upregulated. The glyoxylate shunt converts isocitrate to succinate and glyoxylate by enzyme isocitrate lyase (ICL), followed by addition of acetyl-CoA to glyoxylate to form malate by malate synthase. The disruption of isocitrate lyase attenuates persistence of *M. tuberculosis* in mice or inflammatory macrophages. Most of the anti-mycobacterial target is the cell wall, especially in the later stage of cell wall biosynthesis (Banerjee *et al.,* 1994). Several metabolic enzymes are linked with persistence and antioxidant defense of *M. tuberculosis*. Isocitrate lyase (ICL) and glyoxylate dehydrogenase, two enzymes of the glyoxylate shunt, are activated during adaptation to microaerophilic conditions (Wayne *et al.,* 1982), and *icl* expression is enhanced during infection of macrophages (Honer *et al.,*1999). Two constituents of pyruvate dehydrogenase (PDH) serve also as components of one of the antioxidant and antinitrosative systems in Mtb; these are lipoamide dehydrogenase (Lpd; Rv0462) and dihydrolipoamide acyltransferase (DlaT; Rv2215; formerly SucB). Lpd and DlaT interact with two other proteins to constitute a four protein, NADH-dependent peroxidase and peroxynitrite reductase.

Furthermore, Complex II: Succinate:Ubiquinone Oxidoreductase (SQRs), a component of both the electron transport chain and the citric , is one of targets for respiration of bacteria. It has a covalently bound flavin adenine dinucleotide (FAD) and several FeS clusters. It takes part in transporting electrons (or removing 2 hydrogens) from succinate to the ubiquinone (Q) and produces fumarate (it has 2 hydrogens less than succinate) as the product. Recently, the structural homology at dicarboxylate binding sites of SQRs was investigated (Elena Maklashina *et al.,* 2006). An exception to the conservation of amino acids near the dicarboxylate binding sites of the two enzymes is that there is a Glu (FrdA Glu-49) near the covalently bound FAD cofactor in most fumarate oxidoreductase (QFRs), which is replaced with a Gln (SdhA Gln-50) in SQRs. The role of the amino acid side chain in enzymes with Glu/Gln/Ala substitutions at FrdA Glu-49 and SdhA Gln-50 has been studied. The data demonstrate that the mutant enzymes with Ala substitutions in either QFR or

SQR remain functionally similar to their wild type counterparts. There were dramatic changes in the catalytic properties when Glu and Gln were exchanged for each other in QFR and SQR. The QFR and SQR enzymes are more efficient succinate oxidases when Gln is in the target position and a better fumarate reductase when Glu is present. Overall, structural and catalytic analyses of the FrdA E49Q and SdhA Q50E mutants suggest that coulombic effects and the electronic state of the FAD are critical in dictating the preferred directionality of the succinate/fumarate interconversions catalyzed by the complex II superfamily. Moreover, the transfer of electrons and protons between membranebound respiratory complexes that facilitated by lipid-soluble redox-active quinone molecules (Q) were studied (Rob Horsefield *et al.,* 2005). A structural analysis of the quinone-binding site (Q-site) identified in oxidoreductase (SQR) from *E. coli* was presented. The interaction between ubiquinone and the Q-site of the protein appears to be mediated solely by hydrogen bonding between the O1 carbonyl group of the quinone and the side chain of a conserved tyrosine residue. SQR was co-crystallized with the ubiquinone binding-site inhibitor Atpenin A5 (AA5) to confirm the binding position of the inhibitor and reveal additional structural details of the Q-site. The electron density for AA5 was located within the same hydrophobic pocket as ubiquinone at, however, a different position within the pocket. AA5 was bound deeper into the site prompting further assessment using protein-ligand docking. The initial interpretation of the Q-site was re-evaluated in the light of the new SQR-AA5 structure and protein-ligand docking data. Two binding positions, the Q1-site and Q2-site, are proposed for the *E. coli* SQR quinone-binding site to explain these data. At the Q2-site, the side chains of a serine and histidine residue are suitably positioned to provide hydrogen bonding partners to the O4 carbonyl and methoxy groups of ubiquinone, respectively. This allows there to propose a mechanism for the reduction of ubiquinone during the catalytic turnover of the enzyme.

In case of studied in inhibitor of SDH, the 3-nitropropionate as the principal toxic agent of *Indigofera endecaphylla Jacq* was identified and showed a competitive inhibitor of the succinoferricyanide oxidoreductase activity of Keilin-Hartree particles from rat heart (Hylin and Matsumot *et al.,* 1964).

3-nitropropionate carbanion is a highly specific, time-dependent, and irreversible inhibitor of succinate dehydrogenase (Alston *et al*., 1977). By analogy with the reaction of nitroethane with 1-amino acid oxidase, the data are consistent with the hypothesis that the carbanionic inhibitor forms a covalent N-S adduct with the active site flavin. The reaction of 3-nitropropionate with succinate dehydrogenase was motivated generally by the advance that studies of nitroalkane carbanions have contributed to our understanding of flavoenzyme catalysis and, specifically, by the possibility that internal collapse of the covalent N-5 iminium adduct might be catalyzed by general base abstraction of the 2-hydrogen as a proton. This would lead to the N-5 enamine adduct which, being resistant to attack by H_2O, would explain the irreversible inhibition of the enzyme. 3-NP acts by nucleophilic addition to N-5 of the covalently bound flavin component of the enzyme (Christopher *et al.,* 1979). The inhibition developed slowly, and nearly complete inactivation occurred with a stoichiometric amount of 3-nitropropionate dianion. In accord with this, 3-nitroacrylate, the expected product of dehydrogenation by the enzyme, inactivates it extremely rapidly and irreversibly. Several lines of evidence suggest that the oxidation product, 3-nitroacrylic acid, reacts with an essential -SH group at the substrate site. It is suggested that the inactivation step involves a nucleophilic attack by this essential -SH group on the double bond of 3-nitroacrylate.

Investigation on effect of carbon resources on the living or respiration of tubercle bacilli have proposed compounds of the TCA and focused on the possibility of substrates or intermediary carbohydrate metabolism of this pathway. In a previous respiratory studies informed the utilization of many TCA intermediates and substrates (Holmgren *et al.,* 1954). Lactic, pyruvic, acetic, fumaric, malic, succinic, citric, oxalacetic and α-ketoglutaric acids were oxidized by cell-free extracts of the avirulent H37Ra strain. These reports showed citric and succinic acids were not oxidized by whole cells. No oxygen uptake with whole cells using two these substrates while high concentrations of these acids delivered oxygen uptake inhibition. Cofactors adenosine triphosphate, diphosphopyridine nucleotide, and coenzyme A had effect to increase the rate of oxygen uptake with all substrates except pyruvate and lactate.

Furthermore, concentrations of lactic, pyruvic, acetic, oxalosuccinic, α-ketoglutaric, and oxalacetic acids supported the growth of small inocula of these organisms, but that no growth occurred in the presence of cis-aconitic, citric, isocitric, succinic, fumaric, malic, glutamic, aspartic acids, and alanine were found (Youmans and Youmans, 1953). This report proposed that the bacterial cells may have been imper meable to the substrates which had not supported growth, rather than that the cells lacked the specific enzymes. In comparing the results obtained with the virulent H37Rv strain and its a virulent variant, H37Ra, virulence does not appear to be related to their terminal oxidative pathways. Both organisms contain enzymes which oxidize intermediates of the tricarboxylic acid cycle. However, the cells of the H37Ra strain appear to be more permeable to these intermediates (Holmgren, Millman, and Youmans, 1954) than whole cells of the H37Rv strain (Youmans and Youmans, 1953).

The glycolytic and citric acid cycles play important part in the metabolism of the acid fast bacteria and showed that many enzymes concerned with the metabolism of intermediates of the cycle (Edson *et al.,* 1951). An anaerobic dehydrogenation of succinic acid was ten times with the avian than with the H37Ra and BCG strains (Andrejew, 1952). However in 1953, the results of examined quantitative growth and a basal synthetic medium from normal carbon source showed that pyruvic, acetic, oxalacetic, oxalosuccinic, α-ketoglutaric, lactic and glycerol supported the growth of the H37Rv strain whereas cis-aconitic, isocitric, fumaric, succinic, L-malic and citric acids did not support growth. Moreover, there were not shown the growth of Mycobacterium tuberculosis H37Rv, from small inocula of the intermediates of the tricarboxylic acid cycle. This might be due rather to the impermeability of the bacterial cells to these compounds than to the fact that the cells lacked the corresponding enzymes.

Recently, Jing Tian *et al.* found *M. tuberculosis*. lack α-ketoglutarate dehydrogenase (KDH) acitivity and showed that citrate synthase, aconitase, isocitrate dehydrogenase, fumarase, malate dehydrogenase, and succinate dehydrogenase, except ketoglutarate dehydrogenase presented, raising the possibility of separate

oxidative and reductive half-cycles. As a potential link between the half-cycles, they found that Rv1248c, annotated as encoding SucA, the putative E1 component of KDH, instead encodes α-ketoglutarate decarboxylase (Kgd) and produces succinic semialdehyde. Succinic semialdehyde dehydrogenase activity was detected in *M. tuberculosis* lysates and recapitulated with recombinant proteins GabD1 (encoded by Rv0234c) and GabD2 (encoded by Rv1731). Kgd and GabD1 or GabD2 form an alternative pathway from α-ketoglutarate to succinate. Rv1248c, which is essential or required for normal growth of *M.tuberculosis* (Sassetti, C., Boyd, D. H. & Rubin, E. J. , 2003).

2. Cyclooxygenase

Marta *et al*. (1997) studied the structural features that dictate the selectivity of diverse nonsteroidal antiinflammatory drugs for the two isoforms of the human prostaglandin H2 synthase (PGHS), the three-dimensional (3D) structure of human COX-2 was assessed by means of sequence homology modeling. The ovine COX-1 structure, solved by x-ray diffraction methods and sharing a 61% sequence identity with human COX-2, was used as template. Both structures were energy minimized using the AMBER 4.0 force field and molecular dynamic simulations were also carrying out, to understand more deeply the structural origins of the selectivity. Moreover, docking *(S)*-Flurbiprofen and SC558 were studied in the cyclooxygenase binding site in both isozymes, evidencing the role of different residues in the ligand-protein interaction. More docking calculation, Akaho *et* al. (1999) used Dock4.0 investigates the binding mode of COX-2 selective NSAIDs that there existed one to three hydrogen bonds with the net total being at least twelve when inhibitors were bound to COX-2. Kothekar *et al*. (1999) studied interaction of two anti-inflammatory drugs (NSAIDs), indoprofen and NS398 with both cyclooxygenase. They have also investigated conformational flexibility of the two drugs by systematic search and simulated annealing molecular dynamics (SAMD) methods. The next were molecular study with molecular dynamic simulations, Melissa *et al.* (2000) used an approach that combines docking with Monte Carlo (MC) simulations for analogues of celecoxib. These report a novel docking method, based on a combined Tabu and Monte Carlo

protocol. Using the docking-predicted starting conformations, relative changes in binding free energies were computed for methyl, ethyl, hydroxymethyl, hydroxyl, thiomethyl, methoxy, trifluoromethyl, chloro, fluoro and unsubstituted derivatives with the MC free energy perturbation (FEP) method. In addition, the docking and FEP results have provided clarification of the binding conformation of the phenylsulfonamide moiety and the origin of COX-2/COX-1 selectivity. Sahi *et al.* (2000) reported molecular dynamics (MD) simulation results on complexes of two non-steroidal antiinflammatory drugs NS398 and indoprofen with cyclooxygenases (COX-1 and COX-2). Both the drugs were docked manually in the catalytic cavity of the enzymes on the basis of structural information on COX-1 and COX-2 with different inhibitors using energy grid based in-house docking program IMF-1. These are discussed in the differential activity of the two drugs.

Three-dimensional quantitative structure-activity relationship (3D-QSAR), comparative molecular field analysis (CoMFA) to applied by Chavatte *et al*. (2001) to an extensive series of varied diarylheterocyclic derivatives known as COX-2 selective inhibitors. The compounds retained belong to nine structurally different families depending on the central cyclic tensor, pyrrole, imidazole, cyclopentene, benzene, pyrazole, spiroheptene, spiroheptadiene, isoxazole and thiophene. X-ray crystal structure of COX-2 bound with SC558 was used to derive the putative bioactive conformation of these inhibitors. Moreover, Gregory *et al*. (2001) developed QSAR and classification models experimental for a diverse set of 314 selective cyclooxygenase-2 (COX-2) inhibitors used to develop quantization and classification models as a potential screening mechanism for larger libraries of target compounds. Experimental log (IC50) values ranged from 0.23 to $\geq$ 5.00. Numerical descriptors encoding solely topological information are calculated for all structures and are used as inputs for linear regression, computational neural network and classification analysis routines.

Desiraju *et al.* (2002) used comparative molecular field analysis (CoMFA) and comparative molecular similarity indices analysis (CoMSIA) were performed on 114 analogues of 1,2-diarylimidazole to optimize their COX-2 selective anti-inflammatory

activities. These studies produced models with high correlation coefficients and good predictive abilities. The CoMSIA models have slightly higher predictive abilities than the CoMFA. Docking studies were also carried out wherein these analogues were docked into the active sites of both COX-1 and COX-2 to analyze the receptor ligand interactions that confer selectivity for COX-2. The most active molecule in the series adopts an orientation similar to that of SC558 inside the COX-2 active site while the least active molecule optimizes in a different orientation. Additionally, a correlation of the quantitative structure-activity relationship data and the docking results is found to validate each other and suggests the importance of the binding step in overall drug action. Combined molecular modeling, Hong Liu *et* al. (2002) reported the lamarckian genetic algorithm of AutoDock 3.0 employed to dock 1,5-diarylpyrazole class compounds into the active sites of COX-2 and COX-1 and predictive 3D QSAR models were developed by performing CoMFA and CoMSIA.

For quantum chemical calculation study, the mechanism for prostaglandin G2 synthesis in the cyclooxygenase active site of prostaglandin H synthase was investigated using hybrid density functional theory (B3LYP) (Blomberg *et al.*, 2003). The calculations show that the six step radical mechanism for the transformation of arachidonic acid to prostaglandin G2, starting from an active-site tyrosyl radical and the arachidonic acid substrate. Soliva *et al*. (2003) studied the mechanism of binding of different nonsteroidal anti-inflammatory drugs to the cyclooxygenase active site of cyclooxygenase-2 by molecular dynamics and free energy calculations. It is found that theoretical methods predict accurately the binding of different drugs based on different scaffolds. The study reported the unique characteristics of the COX-2 binding site. In COX-2 inhibitors related to DUP697, it has been shown that depending on the nature of the five member ring unit, local rearrangements in the binding site are possible, which can modify the pattern of drug-protein interactions. According to their simulations, different patterns are possible, leading to slightly different pharmacophores for COX-2 inhibitors and concluded that the recognition site of COX-2 is very flexible and can adapt its structure to very subtle structural changes in the drug. Recently in 2006, the molecular dymamics study of SC558 in COX-2 enzyme were studied. They performed a movement of SC558 from active site and

found role of important of water molecule in the active site. Moreover, these results provided a confirmation for the existence of a cavity near open gate protein surface.

METHODS OF CALCULATIONS

1. System Studies

1.1 Cyclopropane Synthase

Three different X-ray crystallographic structures of the cyclopropane synthase are shown in Table1 (Huang *et al.*, 2002). Based on the limitation of accuracy on calculations, the selective systems were focused on a cofactor binding site of enzyme within a 7.0 Å diameter centered on the cofactor. CTAC and DDDMAB existed in the X-ray crystallographic structure of CmaA1 and CmaA2 were removed.

Table 1 Details of X-ray structures of the cyclopropane synthase

PDB code	Protein/Enzyme	Ligands	Resolution(Å)
1L1E	PcaA	SAH	2.0
1KPG	CmaA1	SAH+CTAB	2.0
1KPI	CmaA2	SAH+DDDMAB	2.5

First, for PcaA enzyme, 26 residues were identified as binding site; Thr32, Tyr33, Ser34, Cys35, Asp70, Ile71, Gly72, Cys73, Gly74, Trp75, Leu93, Thr94, Leu95, Ser96, Gln99, Glu121, Gly122, Trp123, Glu124, Ser135, Ile136, Gly137, Ala138, His141, Phe142 and Arg146. Second, for CmaA1 enzyme, 30 residues were consisted of Pro7, His8, Val12, Tyr16, Thr32, Tyr33, Ser34, Asp70, Val71, Gly72, Cys73, Gly74, Trp75, Ala77, Thr78, Leu93, Thr94, Leu95, Ser96, Gln99, Ala121, Gly122, Trp123, Glu124, Ser135, Ile136, Gly137, Ala138, His141, and Phe142. Third, the enzyme in this study, CmaA2, 32 residues were listed as Pro15, Pro16, Val20, Tyr24, Met39, Thr40, Tyr41, Ser42, Asp78, Ile79, Gly80, Cys81, Gly82, Trp83, Gly84, Ser85, Thr86, Leu101, Thr102, Leu103, Ser104, Gln107, Gln129, Gly130, Trp131, Glu132, Ser143, Leu144, Gly145, Ala146, His149 and Phe150. The N and C terminal of the residues were capped with a methyl amino group (-$NHCH_3$) and an acetyl group (CH_3CO-), respectively. All side chains of residue were set as

naturally form of cyclopropane synthase enzyme at pH 7.0, therefore, Glu, Asp, Arg and Lys were leading to zwitterionic form. Hydrogen atoms were added to these systems using the Sybyl 7.0 program. Consequently, the structures were subsequently optimized with the semi-empirical PM3 method (Stewart *et al.,*1989) and the obtained structures were used as the starting geometries for all calculations, which were implemented in the Gaussian03 program (Gaussian 03, 2004). As there is no SAM and sinefungin structure complexed with these three enzymes, x-ray structure of SAH complex was adapted and modeled the structure for starting geometry of SAM and sinefungin complexes. The optimized SAH cofactor is converted to SAM and sinefungin by direct replacement using Sybyl7.0(SYBYL 7.3) for innovate SAH structure to SAM and sinefungin. After that these structures were optimized by ONIOM2 method (Dapprich *et al.*, 1999; Feliu Maseras, 1995; Svensson *et al.*, 1996). The SAM and sinefungin were treated at inner layer of ONIOM2 in high level of calculation using B3LYP/6-31G(d):PM3, and used these structures for further the quantum calculations.

1.2 Succinate Dehydrogenase

The molecular structure of succinate dehydrogenase was obtained from X-ray structure of 3-nitropropionate bound into mitochondrial respiratory complex by resolution 3.5Å (1ZP0.pdb) (Sun *et al.*, 2005). Based on this structure, we adopted the system consisting of 20 residues within a 7.0 Å diameter centered at inhibitors. The residues were Ala61, Gln62, Gly63, Gly64, PHE131, Gln252, Phe253, His254, Leu264, Ile265, Thr266, Glu267, Gly268, Arg298, His365, Tyr366, Arg409, Leu410, Gly411 and Ala412. All residues, assumed to be in ionic form at pH 7.0 thus Arg, Glu, FAD and $FADH_2$ cofactors were taken in their ionic form. The C- and N-terminal ends of cut amino acid residues were capped with acetyl group and methyl amino group from the adjacent amino acid residues were terminated, respectively. For the succinate-succinate dehydrogenase complex, succinate was constructed from 3-nitropropionate where replacing nitro group to carboxylate group as shown in Figure 7 using Sybyl7.0 program. Then, the optimized structure was performed using PM3 method of calculation.

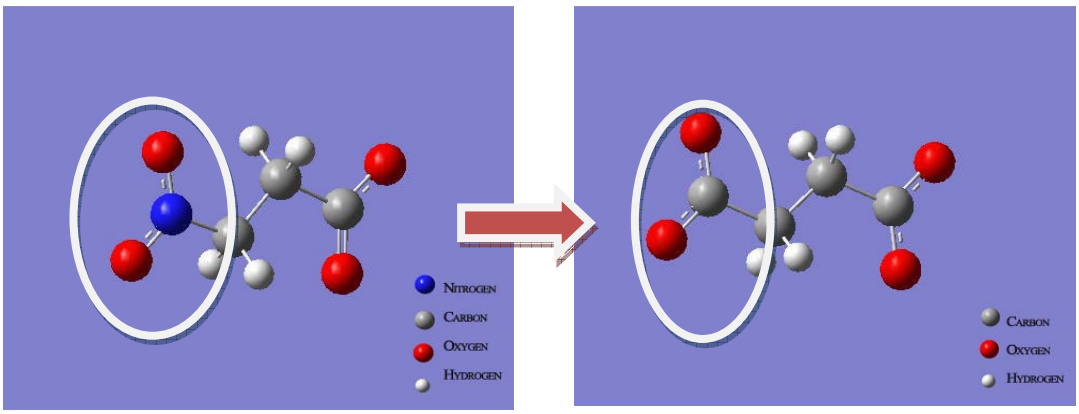

Figure 7 Replacing functional group, nitro to carboxylate group from 3-nitropropionate to succinate.

1.3 Cyclooxygenase

The molecular structures of complex of flurbiprofen with COX-1 and COX-2 were obtained from the 3.10 and 2.50Å resolved crystal structure 1CQE.pdb and 3PGH.pdb (Kurumbai *et al.* 1996), respectively. Based on these structures, the system studied consisting of 32 residues in COX binding pocket was adopted. For flurbiprofen inhibitor, only residues in 6 Å in binding pocket that consist of fourteen amino acids,Val116, Arg120, Val349, Leu352, Ser353, Tyr355, Leu359, Tyr385, Met522, Val523, Gly526, Ala527, Ser530 and Leu531. In neutral system, all residues were assumed to be in their neutral form. In case of charge system, all residues were assumed to be in ionic form at pH 7. In order to compare different interaction of enzyme/inhibitor, SC558 was selected. This system was set up as the same criteria as flurbiprofen complex. The SC558 structure was obtained from the 3.0 Å resolved crystal structure bound to COX-2 (1CX2.pdb) (Kurumbai *et al.* 1996). For SC558 inhibitor, seven amino acids in 6 Å in binding pocket of SC558 inhibitor was added due to largely structure form sulfonamide moiety. These residues are His90, Gln192, Arg513, Ala516, Ile517, Phe518 and Gly519. Terminated cutting residues, the N- and C-terminal ends of cut residues were capped with acetyl group (CH_3CO-) and methyl amino group (-$NHCH_3$) from the adjacent residues, respectively. Hydrogen atoms were added to the X-ray structure to generate the complete structure of the model by

Sybyl7.0 program. The structure was optimized with the semiempirical PM3 method which all the heavy atoms of the amino acids in the pocket were fixed at the X-ray structure and, therefore, only the geometry and position of the inhibitors molecules as well as the positions of all the hydrogen atoms were optimized and these structures were used to generate the starting geometries for all calculations.

2. Quantum Chemical Calculation

The individual interaction energy of the complex between cofactor with the individual amino acid (defined amino acid as X_i) was calculated from the optimized complex structures by ONIOM2:B3LYP/6-31G(d):PM3 method. These energies can be used to investigate the role of key amino acids involved in binding and describe both attractive and repulsive interactions. The interaction energy of each cofactor-X_i pair was calculated at the B3LYP/6-31G(d), B3LYP/6-31G(d,p) and MP2/6-31G(d) methods where the interaction energy (INT) is defined as in equation 1.

$$INT_{(Ligand\text{-}Xi)} = E_{(Ligand\ -Xi)} - [E_{(Ligand)} + E_{(Xi)}] \qquad 1)$$

Where $E_{(Ligand\ -Xi)}$ is the pair-summed energy of residue X_i with the cofactor, and $E_{(Ligand)}$ and $E_{(Xi)}$ are the energies of cofactor and each individual residue respectively. Energy values were corrected with the basis set superposition error (BSSE) for all calculations(Boys and Bernardi, 1970).

2.1 Cyclopropane Synthase

The quantum chemical calculations of cyclopropane synthase was studied in nine systems, SAM, SAH and sinefungin complexed with PcaA, CmaA1 and CmaA2 enzymes, respectively, as shown in Table 2.

Table 2 Nine quantum chemical calculation set up systems, consisting of three ligands and three enzymes.

Enzyme / Ligand	PcaA	CmaA1	CmaA2
SAM	✓	✓	✓
SAH	✓	✓	✓
Sinefungin	✓	✓	✓

In order to investigate the most important part of ligand stunt on the enzyme-ligand interaction, were divided SAM and SAH cofactors to four fragments consisting of adenine, ribose, sulfur and amino acid moieties. Studies with each fragment can suggest the most important part of cofactor showing strong interactions with key residues in the binding site of the enzyme. Only the sulfur subset of SAM and SAH cofactor is different. The sulfur moiety of SAM is a positive charge at a sulfur atom while the sulfur moiety of SAH is a neutral. The significant fragment differences between SAM and SAH are listed in Figure 8. In this study, interaction energies between fragment and cofactors have been carried out at MP2/6-31G(d) calculations in order to identify key important fragment of cofactor.

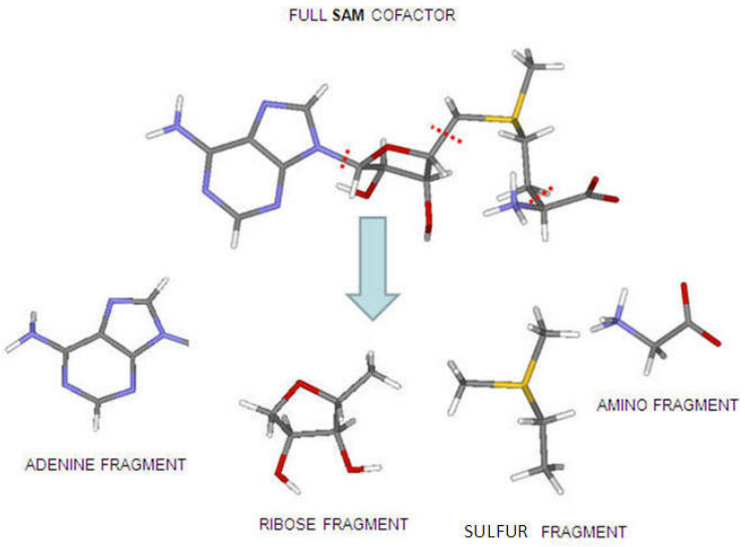

(a)

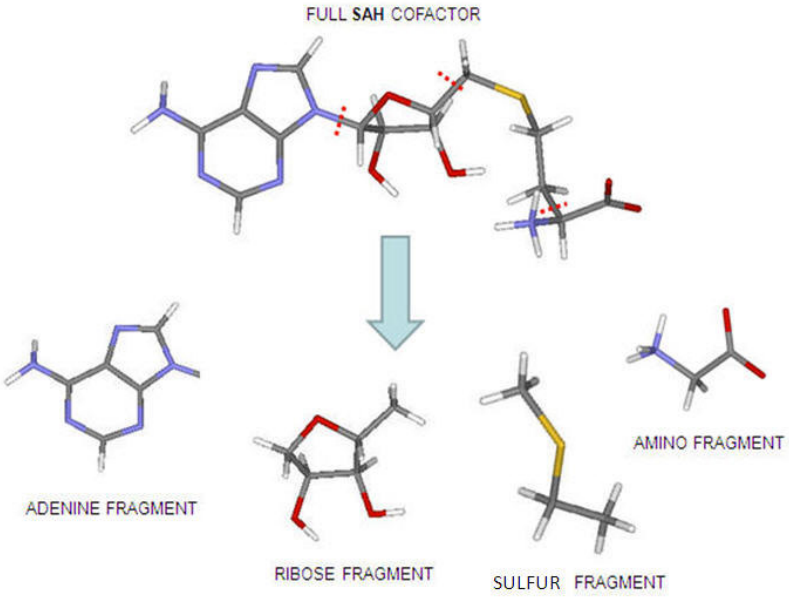

(b)

Figure 8 Fragment structures of cofactors of SAM (a) and SAH (b).

2.2 Succinate Dehydrogenase

Succinate, substrate, and 3-nitropropionate inhibitor were calculated and compared interaction energy in their ionic form. FAD cofactor was used in calculation to study how it paticipation in this system. The structure of FAD was assigned minus two charges at the oxygen adjacent to the phosphate atom.

2.3 Cyclooxygenase

Three levels of calculation; B3LYP/6-31G(d), B3LYP/6-31G(d) and MP2/6-31G(d), were studied to search for appropriate methods for this system. Second, neutral and zwitterionic forms of carboxylic group of flurbiprofen were investigated in COX-2 binding pocket. Moreover, two states of amino acids in binding pocket were characterized by neutral and charge state. Third, the interactions between two COX isoforms and flurbiprofen were considered. Finally, interaction energies between two inhibitors (flurbiprofen and SC558) and their residues were compared.

3. Interaction by ONIOM method

A two-layered ONIOM2 approach (Dapprich *et al.*, 1999; Feliu Maseras, 1995; Svensson *et al.*, 1996) was used to investigate the interaction between interesting cofactor and the amino acid residues in the binding site by dividing the system into two parts, inner and outer layers (see Figure 9). The inner layer or the interaction region was applied at a high level of calculation (region A), while the outer layer or the environmental region (region B) was applied at a lower level of calculation. The total ONIOM energy of the entire system (AB) was obtained from three independent energy calculations in ONIOM2 as shown in equations 2-6.

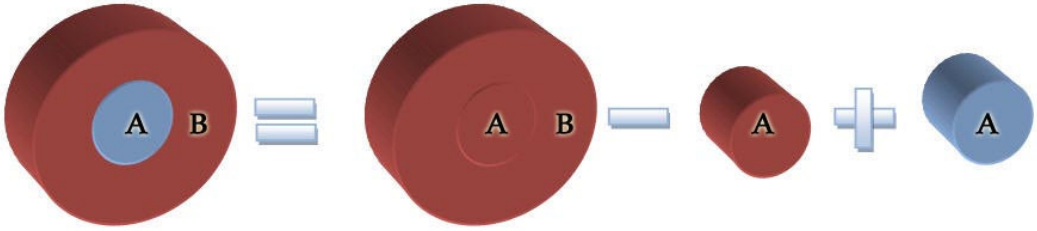

Figure 9 Idea representation of two-layer ONIOM or ONIOM2 method.

$$E_{\text{ONIOM2}} = E(low, real) - E(low, model) + E(high, model) \quad 2)$$

Or

$$E_{\text{ONIOM2(AB)}} = E(low, AB) - E(low, A) + E(high, A) \quad 3)$$

Here, the interaction energy between ligand or cofactor and its binding site was defined by:

$$\Delta E = E_{complex} - E_{pocket} - E_{ligand/cofactor} \quad 4)$$

Hence, the total energy obtained from the ONIOM2 calculations, $E^{ONIOM2}_{[AB]}$, can be expressed for Hartree Fock (HF) or density functional theory (DFT) for model region and PM3 for real region by:

$$E^{ONIOM2}_{[AB]} = E_{[PM3,AB]} - E_{[PM3.A]} + E_{[HF,A]} \quad 5)$$

$$E^{ONIOM2}_{[AB]} = E_{[PM3,AB]} - E_{[PM3.A]} + E_{[B3YLP,A]} \quad 6)$$

All the ONIOM calculations were corrected for basis set superposition error using the counterpoise correction (CP) method.

3.1 Cyclopropane Synthase

The ONIOM calculations have been used to calculate binding energies between SAM/SAH cofactors with PcaA cofactor binding site in which B3LYP method was used as the high level method and PM3 method was used for low level method. The details of system study are listed in Table 3. In this work, only PcaA

enzyme was chosen because mutant of this enzyme fails to persist within and kills infected mice despite normal initial replication (Glickman *et al.*, 2000). Investigation on the effect of two different forms of cofactor on the binding site, neutral and zwitterionic forms (see Figure 10), were performed together with inclusion of Glu124 in the inner layer (ONIOM 2A and 2B). Moreover, the effect of water molecules in the interaction energy was also considered in both fix position (F) and relaxed position (R), (ONIOM 2C, 2D, 2F and 2G). Comparison between inclusions of water molecules in the inner layer (ONIOM 2D) and outer layer (ONIOM 2E) was analyzed as well as on the cofactor system alone in the inner layer (ONIOM 2H and ONIOM 2I). Without PYR (pyrimidine moiety of cofactor) in the inner layer, we investigate the binding energy of the cofactor with PcaA in the similar manner as described above, resulting in ONIOM 2J, 2K and 2L. In addition, we found Asp70 plays strong interaction with SAH, therefore, the system was modeled as ONIOM 2M and 2N. Furthermore, inclusion of more residues (Thr32, Ser34, Asp70 and Glu124) in the layer together with three water molecules was investigated (ONIOM 2O and ONIOM 2P). Comparison with different cofactors, eight varied ONIOM models were generated for SAM cofactor, similar to that of SAH, resulting in ONIOM 2Q, 2R, 2S, 2T, 2U, 2V, 2W models and only one ONIOM model for sinefungin (ONIOM 2Y).

Table 3 Details of ONIOM2 models for cyclopropane synthase system

	Inner layer	**Outer layer**
ONIOM 2A	PYR- SAH(N) Glu124	Rest Residues
ONIOM 2B	PYR- SAH(Z) Glu124	Rest Residues
ONIOM 2C	PYR- SAH(N) Glu124 $3H_2O$(F)	Rest Residues
ONIOM 2D	PYR- SAH(Z) Glu124 $3H_2O$(F)	Rest Residues
ONIOM 2E	PYR- SAH(Z) Glu124	Rest Residues $3H_2O$(F)
ONIOM 2F	PYR- SAH(N) Glu124 $3H_2O$(R)	Rest Residues
ONIOM 2G	PYR- SAH(Z) Glu124 $3H_2O$(R)	Rest Residues

Table 3 (Continued)

	Inner layer	**Outer layer**
ONIOM 2H	SAH(Z) $3H_2O$(F)	Rest Residues
ONIOM 2I	SAH(Z)	Rest Residues $3H_2O$(F)
ONIOM 2J	SAH Glu124	Rest Residues
ONIOM 2K	SAH(Z) Glu124 $3H_2O$(F)	Rest Residues
ONIOM 2L	SAH Glu124	Rest Residues $3H_2O$(F)
ONIOM 2M	SAH(Z) Asp70	Rest Residues
ONIOM 2N	SAH Asp70 $3H_2O$(F)	Rest Residues
ONIOM 2O	SAH(Z) Glu124 Thr32 Ser34 Asp70 $3H_2O$(F)	Rest Residues
ONIOM 2P	SAH(Z) Glu124 Thr32 Ser34 Asp70 $3H_2O$(R)	Rest Residues

Table 3 (Continued)

	Inner layer	**Outer layer**
ONIOM 2Q	SAM	Rest Residues
ONIOM 2R	SAM $3H_2O$(F)	Rest Residues
ONIOM 2S	SAM	Rest Residues $3H_2O$(F)
ONIOM 2T	SAM	Rest Residues $5H_2O$(F)
ONIOM 2U	SAM	Rest Residues $5H_2O$(R)
ONIOM 2V	SAM Asp70	Rest Residues
ONIOM 2W	SAM Asp70 $5H_2O$ (F)	Rest Residues
ONIOM 2X	SAM Glu124 Thr32 Ser34 Asp70 $3H_2O$(F)	Rest Residues
ONIOM 2Y	Sinefungin $3H_2O$(F)	Rest Residues

PYR : Pyrimidine part of adenine cofactor
N : Neutral form of cofactor
Z : Zwitterionic form of cofactor
F : Fix water
R : Relax water

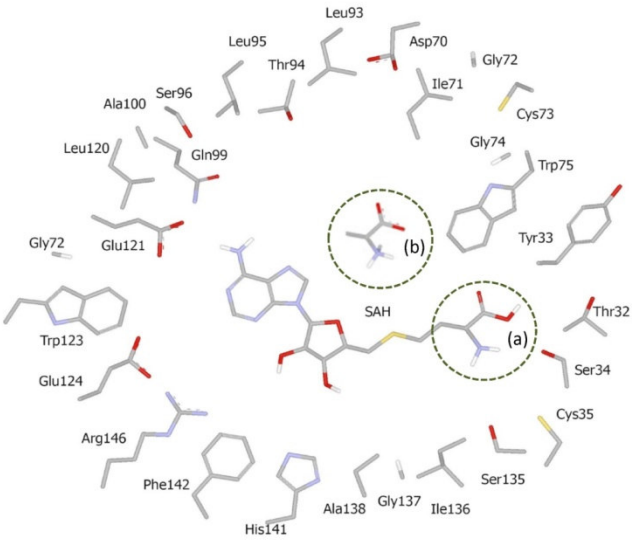

Figure 10 Structural schematic representation for the PcaA with neutral form (a) and zwitterionic form (b) of SAH.

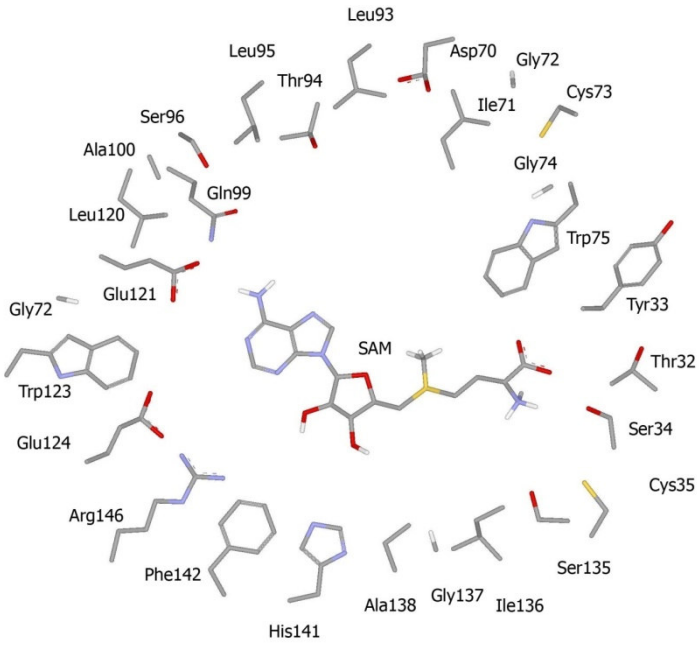

Figure 11 Structural schematic representation for the PcaA with zwitterionic form of SAM.

3.2 Succinate dehydrogenase

An ONIOM calculation of succinate dehydrogenase enzyme and its inhibitor, 3-NPA, has been investigated and compared with substrate, succinate, within 7 Å of the substrate site of succinate dehydrogenase flavoprotein subunit (SdhA). The representative structure of system was used to construct four systems following by:

3-NP	+	FAD	+	residues with in 7 Å
Succinate	+	FAD	+	residues with in 7 Å

with ionic forms of substrate and inhibitor. Therefore, a total of 2 model systems were generate and two approximations were performed to optimize structures; heavy atoms fixed (HAF) and backbone atoms fixed (BAF).

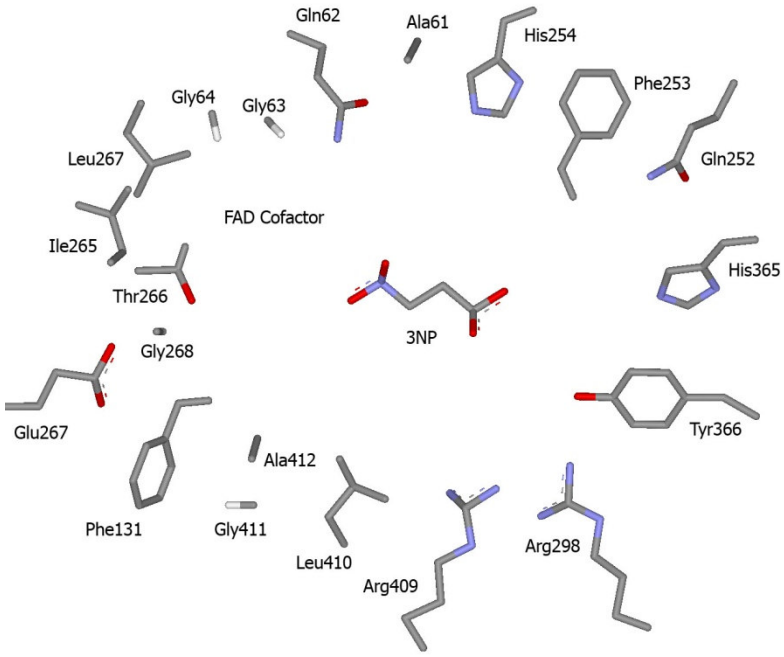

Figure 12 Structural schematic representation for the model of 3-NPA.

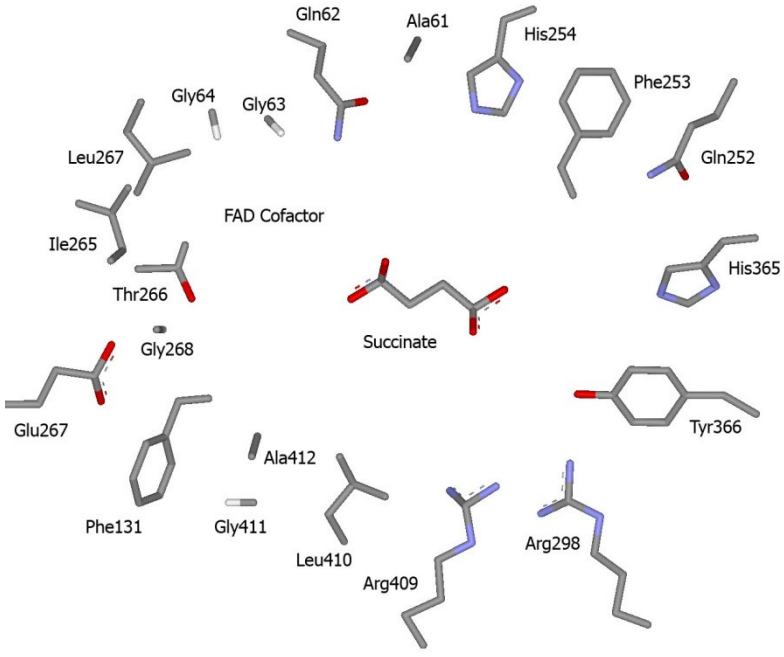

Figure 13 Structural schematic representation for model of succinate.

3.3 Cyclooxygenase

The ONIOM2 method was used to investigate the interaction between flurbiprofen and the residues in the COX-2 binding site (see Figure 14). In this study, we focused on the interactions between flurbiprofen and three important residues, Arg120, Tyr355 and Val523. The Arg120 is a key amino acid of the active site of substrate which guanidinium group has function to stabilize the carboxylate of the inhibitor, while Tyr355 is a key amino for flurbiprofen binding site. Both residues are located near the hydrophobic channel binding region of protein. Moreover, Val523 is considered as the amino acid which makes the difference between COX-1 and COX-2 isozymes. Therefore, these three residues were particularly focused.

The ONIOM2 systems were set up by separation of the model studied to be two layers in order to investigate individual interactions. The inner layer or the interaction region composed of flurbiprofen with interested residues Arg120, Tyr355 and Val523 was treated at inner model layer (high level of ONIOM calculations), while the outer layer or the environmental region consisting of the rest residues was treated at a lower level of calculation. Therefore different ONIOM2 methods, *ab initio* and density functional theory combined with PM3, were applied to calculate the structural information and estimate interaction energies between flurbiprofen and the COX-2 binding site. The setting up of calculations are described with the combination of methods and the partitioning of model layer and real layer, heavy atoms fixing.

The combination of different level of theory, HF/6-31G(d), HF/6-31G(d,p), B3LYP/6-31G(d) and B3LYP/6-31G(d,p), with PM3 for ONIOM2 set up were performed, resulting in the Model A, B C and D as following

Model A ONIOM2(HF/6-31G(d):PM3)
Model B ONIOM2(HF/6-31G(d,p):PM3)
Model C ONIOM2(B3LYP/6-31G(d):PM3)
Model D ONIOM2(B3LYP/6-31G(d,p):PM3)

In addition, ionic system was also considered and calculated by ONIOM2 with B3LYP/6-31G(d):PM3 method of calculation. In this case, flurbiprofen was set to be ionic charge form with ionic residue system which calculated as similar criteria in neutral system. Moreover, systems of cyclooxygenase complexed with SC558 and flurbiprofen were compared. Focusing high level region comprised inhibitor and Tyr355 residue was due to this residue presented very strong interaction with SC558. Therefore, ONIOM calculation of SC558 was set up as shown in Figure 15.

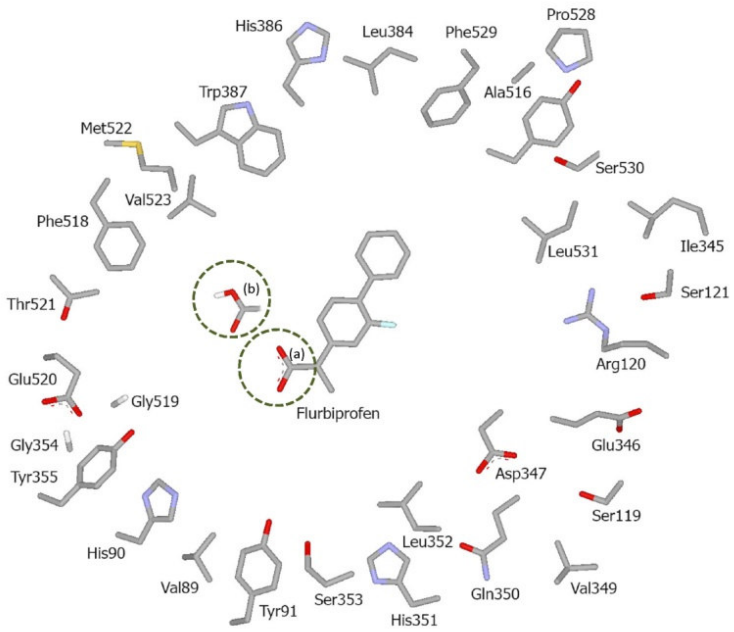

Figure 14 Structural schematic representation for model of cyclooxygenase with (a) charged of flurbiprofen and (b) neutral of flurbiprofen.

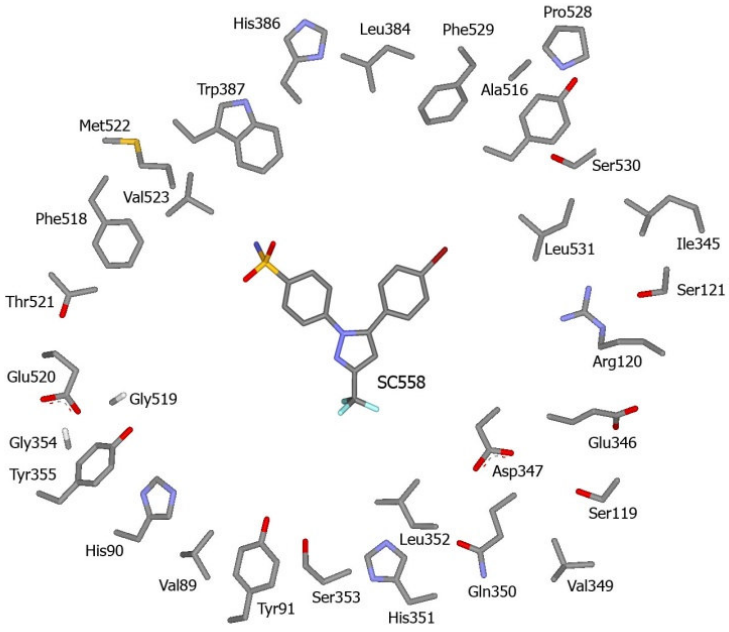

Figure 15 Structural schematic representation for model of cyclooxygenase with SC558.

RESULTS AND DISCUSSION

Quantum Chemical Calculation and ONIOM Study of S-adenosyl-L-methionine and S-adenosyl-L-homocysteine Cofactors of Cyclopropane Synthase in *M.tuberculosis*

1. Inhibitor-enzyme interaction

Comparison of the relative affinities for homologous residues between cofactor and binding site provides direction in terms of drug design by highlighting differences that can be potentially exploited for selectivity. Comparison of the interaction energies of SAM cofactor, the reaction product SAH cofactor and sinefungin inhibitor with the three cyclopropane synthases are investigated using *ab initio* and DFT method of calculations. These calculations were divided into three parts within 7 Å from ligand at substrate binding site including (i) calculation including three water molecules of PcaA with each of ligand (SAM+PcaA, SAH+PcaA and sinefungin+PcaA); (ii) calculation including thirteen water molecules of CmaA1 with each of ligand (SAM + CmaA1, SAH + CmaA1 and sinefungin+ CmaA1); and (iii) calculation including six water molecules of CmaA2 with each of ligand (SAM + CmaA2, SAH + CmaA2 and sinefungin + CmaA2). The positions of water molecules are shown in Figure 16. Moreover, the interactions of these enzyme systems in the absence of water molecules were also performed. However, results of these systems are not shown because the energies give similar trends with including water molecules in the system.

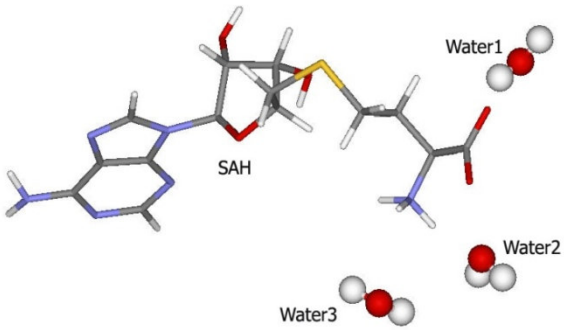

(a)

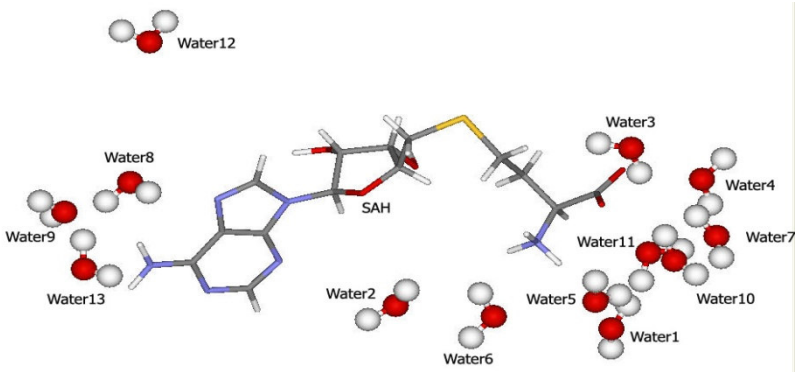

(b)

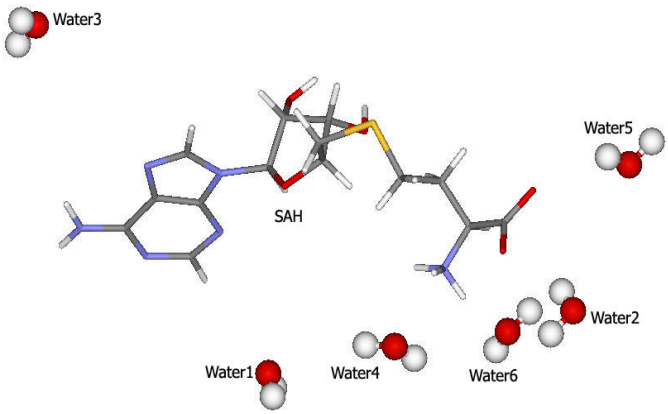

(c)

Figure 16 Position of water molecules bound in the PcaA (a), CmaA1 (b) and CmaA2 (c) within 7Å of cofactor binding site.

B3LYP with 6-31G(d) and 6-31G(d,p) basis sets and MP2/6-31G(d) methods were used and the results were compared in order to search for appropriate method. The interaction energies of SAH cofactor with zwitterionic form of residues in PcaA cofactor binding site are presented in Table 4. Comparison of energies by B3LYP method with 6-31G(d) and 6-31G(d,p) gives an insight into quality of the basis sets. The results do not show significantly different energies which are less than 0.3 kcal/mol. Consideration on B3LYP and MP2 with 6-31G(d) basis set, it was found that residues that show different interaction energy between these two methods higher than 3 kcal/mol are Leu95 and Trp123 with energy difference 5.19 and 3.02 kcal/mol, respectively. The reason might be from the ability of the method, as B3LYP calculations cannot present energy from H-pi interaction or pi-pi interaction (Kuno *el al.,* 2006). Therefore, in this study we select MP2 method to investigate deeper understanding on interaction of inhibitor-enzyme due to the electron correlation found to be important in the ionic system.

Table 4 Interaction energies (INT) of zwitterionic form of SAH cofactor with individual amino acids (X_i) (in ionic system) in kcal/mol, calculated at the B3LYP/6-31G(d), B3LYP/6-31G(d,p) and MP2/6-31G(d) level of theory.

	Interaction energies (kcal/mol)		
	B3LYP		MP2
	6-31G(d)	6-31G(d,p)	6-31G(d)
Thr32	-4.86	-4.83	-6.05
Tyr33	-6.42	-6.50	-8.29
Ser34	-8.17	-8.14	-8.56
Cys35	-0.29	-0.28	-0.38
Asp70 (charge -1)	-16.69	-16.65	-17.61
Ile71	-1.63	-1.62	-2.73
Gly72	-5.91	-6.21	-7.95
Cys73	2.03	2.05	0.13
Gly74	0.11	0.18	-2.20
Trp75	-0.33	-0.32	-1.05
Leu93	-0.70	-0.68	-1.95
Thr94	-1.51	-1.44	-3.58
Leu95	1.92	1.92	-3.27
Ser96	-0.05	-0.03	-0.54
Gln99	-0.90	-0.84	-1.36
Glu121(charge -1)	-1.23	-1.33	-1.61
Gly122	1.22	1.16	0.10
Trp123	1.04	1.05	-1.98
Glu124	-13.77	-13.75	-13.81
Ser135	1.31	1.30	1.16
ILE136	-7.77	-7.90	-9.02
Gly137	1.00	0.93	-0.08
Ala138	1.75	1.74	-0.61
His141	-1.09	-1.08	-3.41
Phe142	0.73	0.70	-1.73
Arg146 (charge +1)	4.34	4.36	3.71
Water1	-6.28	-6.27	-5.54
Water2	-11.91	-11.77	-11.99
Water3	-3.35	-3.31	-3.51

1.1 Identification of key residues of PcaA cofactor binding site

In PcaA cofactor binding site, three water molecules are located within 7Å from SAH cofactor. The results of individual interaction energies of SAM, SAH and sinefungin in PcaA enzyme are shown in Table 5. All residues are assigned to be at pH 7.0, therefore Arg, Asp, Glu and Lys residues are ionized. In this calculations, MP2/6-31G(d) method of calculation was used. First, considering SAM substrate cofactor, three residues showing very strong interaction with SAM are Asp70, Glu124 and Glu121 (-54.55, -53.80 and -23.31 kcal/mol, respectively). Among three water molecules, water2 shows the highest interaction of about -14.53 kcal/mol.

Second, SAH product cofactor was examined. The strongest two residues are similar to SAM cofactor while the third water molecule (water2). However, the interaction energy of Asp70 with SAM is twice time higher than that of SAH (-54.55 and -21.29 kcal/mol, respectively). SAM substrate expresses strong interaction in the substrate binding pocket, especially with Asp70, Glu124, Glu121 and water molecule. Conversely, Ser34, Trp123 and water molecule (water1) act with SAH stronger than SAM cofactor with energy different of about 6.38, 4.16 and 3.99 kcal/mol, respectively. Using the same model system, sinefungin was then calculated and compared with other two cofactors. The interaction results of sinefungin and SAM are quite similar. A reason is due to positively charged molecule in both SAM and sinefungin. Excepting, Tyr33 and Gly72 residues perform big different compared to SAM cofactor with ΔE 11.78 and 7.23 kcal/mol, respectively. Sinefungin strongly interacts with Tyr33 by positively charged at nitrogen atom of cofactor which is located close phenyl ring of tyrosine while decreasing interaction with Gly72 compared with SAM by steric effect between glycine side chain and hydroxyl of ribose moiety in sinefungin. Consequently, the obtained results demonstrate that Asp70 and Glu124 are main contribution in the cofactor binding site of PcaA enzyme. Asp70 shows the strongest interaction to SAM, SAH and SIN of about -54.55, -21.29 and -54.99 kcal/mol, respectively. This residue lays its orientation next to amino group and forms strong electrostatic interaction despite bond distance quite far approximately 4 Å. Another residue, Glu124 shows strong interaction to SAM, SAH

and SIN of about -53.80, -18.85 and -46.93 kcal/mol, respectively. Carboxylate group of glutamate forms hydrogen bonding with adenine moiety of cofactor or inhibitor that consistent with experiment result form Guérard *et al* report. In addition, the results imply that at least one water molecule plays important role in the binding site of cofactor.

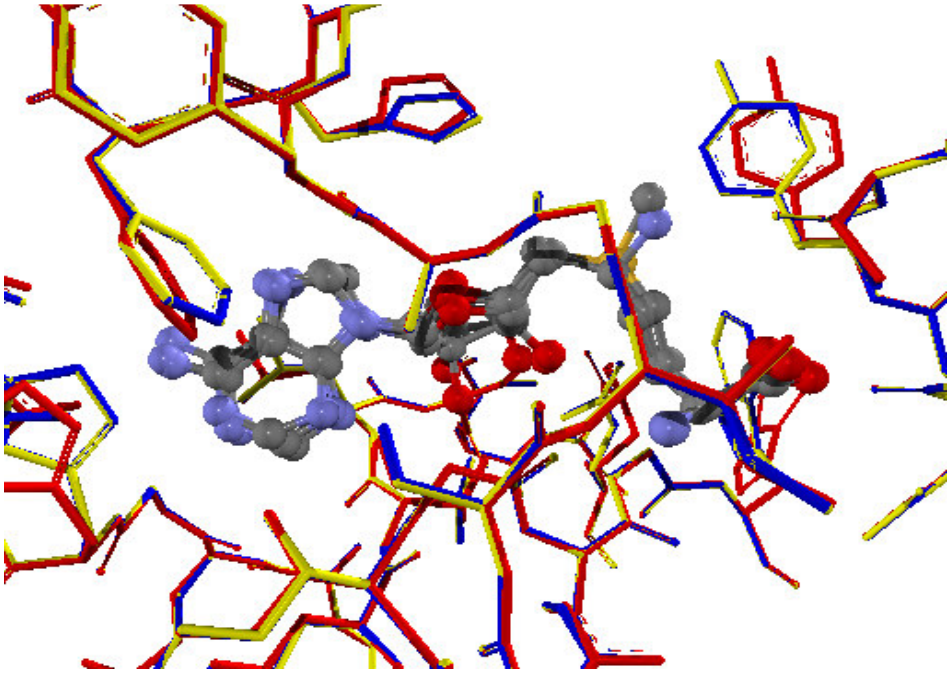

Figure 17 Overlay structure of PcaA (blue), CmaA1 (red), and CmaA2 (yellow) followed in Table 5.

Table 5 Individual interaction energy of cofactors (SAM and SAH) and sinefungin (SIN) with individual residues of PcaA calculated by MP2/6-31G (d,p) with BSSE-CP method (in kcal/mol).

PcaA	SAM	SAH	Sinefungin
Thr32	-2.28	-4.74	-2.36
Tyr33	-16.97	-7.27	-28.75
Ser34	-2.39	-8.77	-2.31
Cys35	0.38	-0.50	0.53
Asp70	-54.55	-21.29	-54.99
Ile71	-4.29	-2.61	-4.37
Gly72	-16.08	-10.53	-8.85
Cys73	1.10	0.89	1.23
Gly74	-3.33	-3.41	-2.79
Trp75	-0.55	-0.13	-0.48
Leu93	-2.66	-1.89	-3.75
Thr94	-2.07	-4.08	0.67
Leu95	-0.97	-3.72	-1.07
Ser96	0.91	-0.07	0.62
Gln99	-0.51	-0.56	0.59
Glu121	-23.31	-1.45	-23.57
Gly122	0.79	-0.82	1.53
Trp123	0.70	-3.46	0.82
Glu124	-53.8	-18.85	-46.93
Ser135	1.19	1.44	1.25
Ile136	-11.4	-6.94	-10.88
Gly137	-5.97	1.95	-4.35
Ala138	-0.19	-0.70	0.04
His141	-8.63	-2.86	-6.46
Phe142	-1.28	-1.66	-1.06
Arg146	28.68	0.31	28.48
Water1	-6.35	-9.74	-6.18
Water2	-14.53	-10.76	-13.48
Water3	-6.13	-3.12	-4.73

1.2 Identification of key residues of CmaA1 cofactor binding site

Study series of cyclopropane synthase, the SAM, SAH cofactors and sinefungin with CmaA1 were investigated. As expected, the results show similar trend as PcaA enzyme because of 60% identity of the enzyme. Additional residues or different residues as compared with PcaA are Pro7, His8, Val12, Tyr16, Cys35, Ala77, Thr78 and Arg146 while side chains at position 121, Glu in PcaA and Ala in CmaA1enzyme is different. Moreover, substrate binding site from X-ray structure of this enzyme within 7 Å consists of water molecules more than that of PcaA binding site. Perusal of SAM cofactor results, the data obtained form Table 6 gives similar tendency to interaction between SAM and PcaA, excepting Gln99 residue. The carbonyl of amide side chain of glutamine in CmaA1 forms hydrogen bonding with hydroxyl group of ribose moiety of cofactor with bond distance 1.87Å. At position 121 in PcaA enzyme, SAM and sinefungin strongly act with its residue while CmaA1 enzyme interaction is decreased. As side chain at this position between two these enzymes is different, glutamate shows strong interaction due to electrostatic interaction from negatively charged of residue and positively charged of cofactors while alanine residue gives regular van der Waals interaction in both cofactors.

In case of SAH, the main contribution residue is also Asp70 and three water molecules play an important role in CmaA1 substrate binding site. These waters are water5, water10 and water3. Comparison of water molecule positions, it was found that water3, water5 and water6 in CmaA1 are equal to water1, water2 and water3 in PcaA enzyme, respectively. The results can be implied that at least two water molecules are important for substrate binding site.

Table 6 Individual interaction energy of cofactors (SAM and SAH) and inhibitor (Sinefungin) with individual residues of CmaA1 calculated by MP2/6-31G (d,p) with BSSE-CP method (in kcal/mol).

CmaA1	SAM	SAH	Sinefungin
Tyr16	-4.02	-1.67	-18.53
Thr32	-2.59	-5.54	-2.91
Tyr33	-16.68	-9.04	-17.76
Ser34	-2.82	-8.86	-3.93
Asp70	-53.51	-15.36	-49.72
Val71	-4.71	-2.97	-4.61
Gly72	-14.16	-7.63	-12.84
Cys73	1.27	0.68	1.37
Gly74	-2.26	-2.00	-2.64
Trp75	-0.88	-1.24	-1.09
Leu93	-2.31	0.04	-1.95
Thr94	1.28	1.27	1.75
Leu95	-1.52	-3.68	-1.49
Ser96	-0.34	-0.81	0.00
Gln99	-7.85	-6.10	-5.59
Ala121	-1.01	-0.21	-0.99
Gly122	0.70	0.89	1.30
Trp123	-0.91	-3.09	-0.68
Glu124	-49.01	-19.20	-49.14
Ser135	1.35	1.09	0.99
Ile136	-13.51	-7.87	-11.43
Gly137	-4.38	0.18	-12.76
Ala138	0.57	-0.13	1.96
His141	-9.62	-4.04	-12.37
Phe142	-1.30	-1.74	-1.25
Water1	2.48	1.46	2.26
Water2	-1.53	-0.09	-1.82
Water3	-4.47	-7.62	-4.57
Water4	0.05	-1.39	-0.07
Water5	-12.39	-11.52	-12.8
Water6	-8.30	-5.75	-7.80
Water7	-1.28	-3.68	-1.17
Water8	-6.03	8.80	-5.98
Water9	4.47	0.50	4.64
Water10	-3.48	-8.74	-4.36
Water11	-5.53	0.66	-4.67
Water12	-1.46	-0.44	-1.63
Water13	-1.03	-0.26	-1.52

Sinefungin was then examined with this enzyme; the interaction energies are similar to SAM results excepting Tyr16 and Gly137. These show stronger interaction when compared to SAM results of about 3-5 fold. The reason are due to two hydrogen bonding with peptide bond of glycine and hydroxyl group of tyrosine, respectively whereas it was not found in case of SAM cofactor. Three water molecules also show significant interaction with sinefungin it similar as SAM cofactor. Based on theoretical interaction results of cofactors or sinefungin with CmaA1, it can be concluded that Asp70, Glu124 and at least two water molecules are necessary for the binding in the substrate binding site.

1.3 Identification of key residues of CmaA2 cofactor binding site

Although the sequence numbering of CmaA2 differs from PcaA and CmaA1, there is high sequence homology in the cofactor binding site. The calculated interaction energies of this energy with the cofactors and sinefungin are shown in Table 7. The highest interaction energies with SAM are with the same residues as SAH, namely Asp78, Glu132, Gly80 and Tyr41. The methylated tertiary sulfur of SAM that is positively charged clearly has a significant impact on the magnitude of the interaction with these residues and total interaction energy is more than for SAH and sinefungin, respectively. In all cases, Asp78 (residue 70 in PcaA numbering) and Glu132 (residue 124 in PcaA numbering) are the main contributors to binding with SAM, SAH and sinefungin, although the energies are different. However, some interactions of SAH with binding pocket is distinctive from SAM or sinefungin, especially in Ser42, SAH shows stronger interaction than SAM or sinefungin with interaction energy -8.69, -2.67 and -3.37 kcal/mol, respectively, because carboxylate moiety of SAH is far more negatively charged than SAM cofactor.

Comparing the interaction energies of SAM and sinefungin, two residues show distinct difference. These residues are Tyr24 and Gly145 where sinefungin shows higher attractive energy. In addition, two remarkable water molecules, water4 and water6 (water3 and water2 numbering of PcaA enzyme) show strong interaction with SAM, SAH and sinefungin.

Consequently, with all interaction energy results, these can be concluded that the main residues for the cofactor binding site of cyclopropane synthase enzyme are Asp70 and Glu124. Moreover, at least two water molecules play significant role in the binding of cofactors or inhibitor. In addition, energetically highly more favorable interactions with SAM and sinefungin are due to charge distribution of the positive charges of these ligands which will be discussed in next section.

Table 7 Individual interaction energies of cofactors (SAM and SAH) and inhibitor (sinefungin) with individual residues of CmaA2 calculated by MP2/6-31G(d,p) with BSSE-CP method (in kcal/mol).

CmaA2	SAM	SAH	Sinefungin
Tyr24	-3.94	-5.57	-17.91
Met39	-0.55	1.16	-0.23
Thr40	-2.11	-5.51	-2.23
Tyr41	-15.96	-8.51	-15.76
Ser42	-2.67	-8.69	-3.37
Asp78	-53.99	-15.33	-50.82
Ile79	-4.33	-2.65	-4.39
Gly80	-16.15	-11.33	-14.1
Cys81	1.47	1.17	1.59
Gly82	-0.22	-1.68	-2.29
Trp83	-1.20	-1.58	-1.32
Gly84	1.12	-0.17	1.04
Ser85	-0.71	-1.30	-0.66
Thr86	3.24	2.09	2.97
Leu101	-2.52	-1.07	-2.50
Thr102	-0.14	-1.65	0.45
Leu103	-1.30	-4.65	-1.43
Ser104	-0.43	0.01	-0.34
Gln107	-7.12	-6.59	-6.31
Gln129	-1.12	-0.36	-1.08
Gly130	0.05	-0.73	1.47
Trp131	-0.29	-2.58	1.05
Glu132	-41.06	-17.72	-48.5
Ser143	1.32	1.12	1.00
Leu144	-10.39	-6.38	-8.18
Gly145	-5.57	-0.16	-14.57
Ala146	0.00	-0.35	2.78
His149	-7.67	-4.20	-9.56
Phe150	-1.50	-1.93	-1.60
Water1	-1.77	-0.32	-2.01
Water2	1.03	1.19	0.97
Water3	-1.22	-0.17	-1.39
Water4	-10.53	-6.74	-9.95
Water5	-0.79	-3.17	-0.84
Water6	-10.23	-9.76	-11.05
Total	-197.25	-124.11	-219.07

2. Charge distributions of Cofactors

Additionally of the methyl group on the sulfur atom of SAM or the amine group on the carbon atom of sinefungin have an effect on the charge distributions, particularly in neighboring atoms surrounding the positively charged atoms of cofactors or inhibitor. Mulliken atomic charges calculated by ONIOM2 (B3LYP/6-31G(d):PM3) were employed to analyze charge distribution of SAM, SAH and sinefungin for which the atomic numbering is present in Figure 10. Considering atomic charges as shown in Table 8 and Table 9, electron density distributions of SAM and sinefungin are not widely different, expecting positively atomic charge of methyl sulfur moiety or amine moiety of SAM and sinefungin, respectively. The positively charged sulfur moiety of SAM consists of S, C_{16}, H_{21}, H_{22} and H_{23} atoms while the positively charged carbon moiety of sinefungin consists of C_{15}, N_7, H_{21}, H_{22}, $H_{23,}$ and H_{24}. The mulliken atomic charges for SAM and sinefungin are 0.758 and 0.824, respectively. The only moiety of SAM and sinefungin show different charge distribution whereas other moieties show similar charge values. Tiny differences of charges distribution for these ligands are caused by similar interaction energies shows in previous section whereas sulfur atom of SAH gives an atomic charge 0.013.

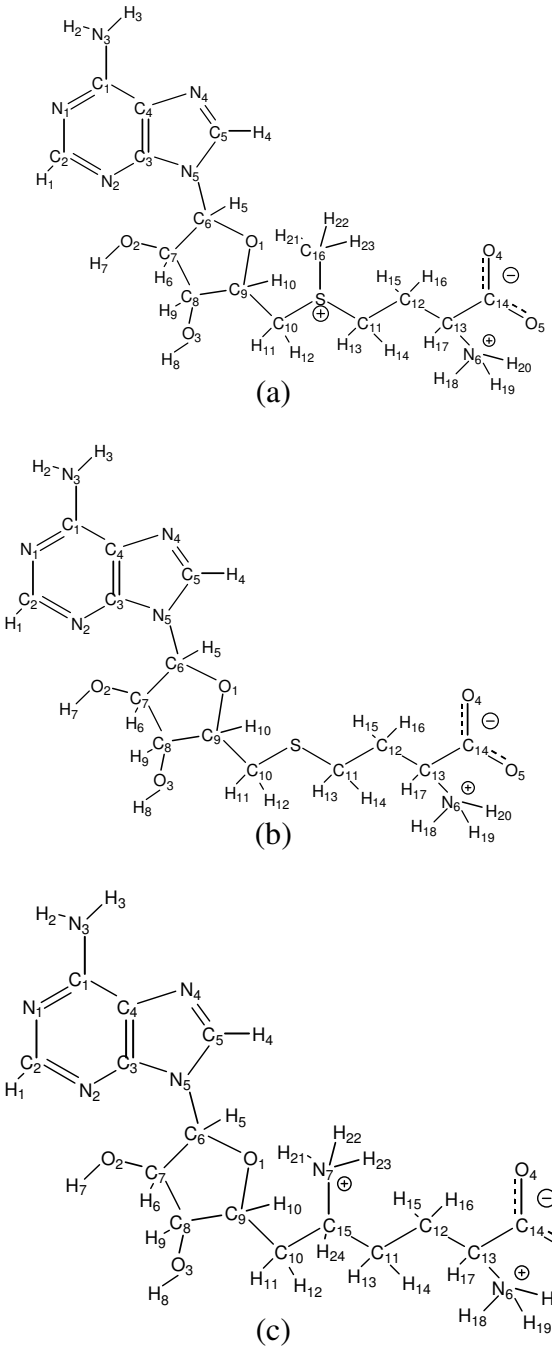

Figure 18 Atomic numbering of SAM (a), SAH (b) cofactor and sinefungin(c) inhibitor.

Table 8 Mulliken atomic charges of SAM, SAH and sinefungin calculated by B3LYP/6-31G(d) method.

	SAM	SAH	sinefungin		SAM	SAH	sinefungin
C1	0.071	0.072	0.078	S	0.622	0.013	
C2	0.063	0.037	0.075				
C3	-0.090	-0.096	-0.107	H1	0.125	0.116	0.124
C4	-0.268	-0.230	-0.256	H2	0.077	0.067	0.087
C5	-0.206	-0.177	-0.185	H3	0.086	0.063	0.077
C6	0.032	0.067	0.072	H4	0.151	0.162	0.157
C7	0.012	0.005	0.021	H5	0.126	0.109	0.082
C8	0.050	0.010	0.041	H6	0.071	0.075	0.092
C9	0.058	0.051	0.035	H7	0.228	0.211	0.261
C10	-0.221	-0.205	-0.106	H8	0.244	0.186	0.241
C11	-0.215	-0.191	-0.141	H9	0.072	0.109	0.082
C12	-0.091	-0.090	-0.107	H10	0.075	0.051	0.057
C13	-0.307	-0.357	-0.303	H11	0.116	0.107	0.083
C14	0.410	0.410	0.412	H12	0.125	0.097	0.082
C15			-0.172	H13	0.083	0.051	0.07
C16	-0.233			H14	0.156	0.140	0.101
				H15	0.075	0.038	0.076
O1	-0.249	-0.263	-0.273	H16	0.129	0.126	0.114
O2	-0.296	-0.293	-0.340	H17	0.128	0.017	0.126
O3	-0.324	-0.278	-0.329	H18	0.016	0.036	0.014
O4	-0.478	-0.506	-0.499	H19	0.085	-0.020	0.081
O5	-0.583	-0.588	-0.583	H20	0.047	0.021	0.043
				H21	0.103		0.041
N1	-0.225	-0.235	-0.230	H22	0.142		0.037
N2	-0.197	-0.152	-0.242	H23	0.124		0.075
N3	0.19	0.153	0.199	H24			0.136
N4	-0.015	-0.059	-0.025				
N5	0.225	0.221	0.23				
N6	0.673	0.818	0.682				
N7			0.707				

Table 9 Mulliken atomic charges grouping of SAM, SAH and sinefungin calculated by B3LYP/6-31G(d) method.

	SAM	SAH	sinefungin
Adenine[(a)]	-0.013	-0.058	-0.018
Ribose[(b)]	0.099	0.040	0.042
Amino[(c)]	0.821	0.855	0.820
Carboxylate[(d)]	-0.651	-0.684	-0.670
α-C[(e)]	-0.179	-0.340	-0.177
β-C[(f)]	0.113	0.074	0.083
C_{10}[(g)]	0.020	-0.001	0.059
C_{11}[(h)]	0.024	0.000	0.030
Sulfur(SAM and SAH) / Carbon (SIN)[(i)]	0.622	0.013	-0.172
Sulfur(SAM and SAH) / Carbon (SIN) moiety[(j)]	0.758	0.013	0.824

(a) Comprise of C1-C5, N1-N5 and H1-H4 atomic numbering
(b) Comprise of C6-C9, O1-O3 and H5-H10 atomic numbering
(c) Comprise of N6 and H18-H20 atomic numbering
(d) Comprise of C14 and O4-O5 atomic numbering
(e) Comprise of C13 and H17 atomic numbering
(f) Comprise of C12 and H15-H16 atomic numbering
(g) Comprise of C10 and H11-H12 atomic numbering
(h) Comprise of C11 and H13-H14 atomic numbering
(i) Comprise of S atom (for SAM and SAH) and C15 (for sinefungin) atomic numbering
(j) Comprise of S, C16 and H21-H23 (for SAM), S (for SAH) and C15, N7 and H21-H24 (for sinefungin) atomic numbering

Figure 19 shows the molecular atomic charges of three ligands. Negatively charge are found on the adenine and very strong localized on the carboxylate moiety and the positive unit charge placed around sulfur moiety of SAM whereas the sulfur moiety of SAH is not changed. Moreover, the positively charged sulfur atom or protonated nitrogen moiety of sinefungin results in diffusion of charge to neighboring atom in that way the interaction energies are then different.

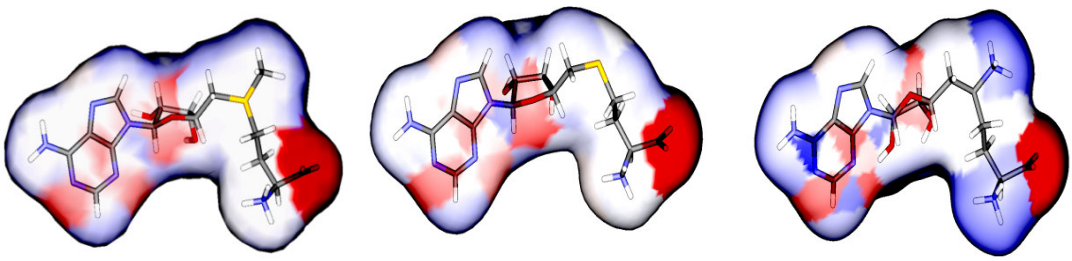

(a) (b) (c)

Figure 19 Charge distribution surface of SAM (a), SAH (b) and sinefungin (c).

In order to understand more deeper the interaction of SAM and SAH cofactors with their cofactor binding sites, each cofactor is separated into four fragments, adenine, ribose, sulfur, and amino moieties. In this fragment study, sinefungin was not included SAM can represent for this inhibitor due to the similar interaction energy and charge distribution results.

3. Fragment interaction

3.1 Adenine moiety

The interaction energies between adenine moiety and residues (the same residue series with previous inhibitor-enzyme interaction parts) are given in Figure 20. Although the adenine fragments of SAM and SAH are the same, the interaction energies of the fragment and residues in the pocket cofactors are diffent in binding with Glu124. It appears that the interaction energies between these moieties of SAM/SAH cofactors and Glu124 contribute to about -16 and -10 kcal/mol, respectively. This observation is due to the hydrogen bonding, occurred by carboxylate anion of glutamate and pyrimidine ring of the cofactors. The interaction between adenine of SAM and Glu124 is larger than that of SAH because of a closer hydrogen bond distance of about 0.4 Å. For other residues, the interactions are similar for both, SAM and SAH. Considering water molecules found in former studies, it was

found that these molecules cannot influence the interaction energies between water molecules and the adenine fragment (less than 0.14 kcal/mol). Therefore, the obtained results indicate that adenine moiety of cofactors establish the main interaction with Glu124 which is the key residue in the binding pocket.

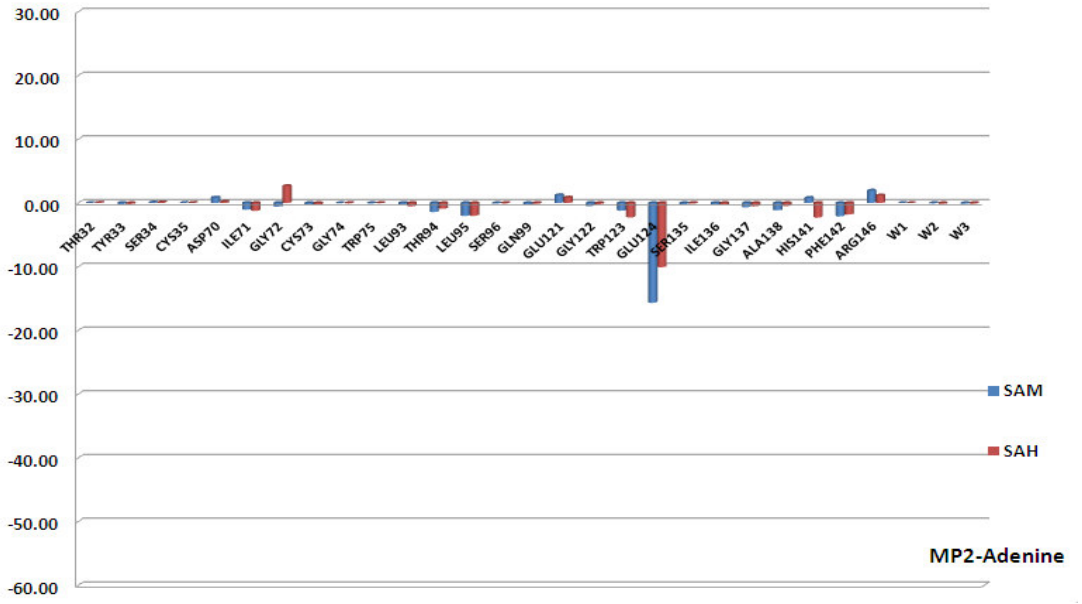

Figure 20 Interaction energies of the adenine moiety (in kcal/mol) with SAM (in blue color) and SAH (in red color) calculated using MP2/6-31G(d) method.

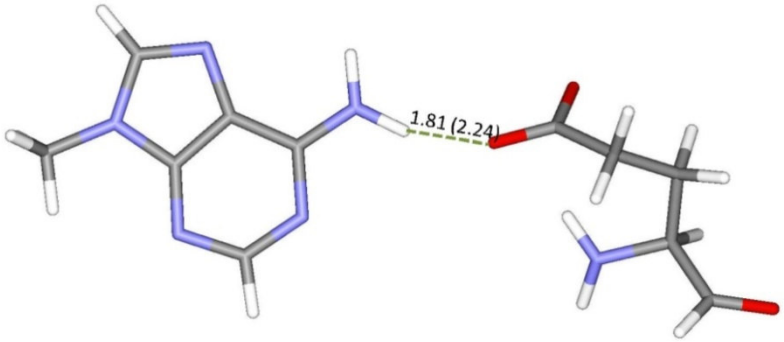

Figure 21 Hydrogen bond distances of adenine moiety with SAM and SAH (in parenthesis) with Glu124.

3.2 Ribose moiety

Next the ribose moiety was investigated in a similar fashion as the adenine moiety. This moiety is composed of five membered ring and two hydroxyl group. Surprisingly, it does not establish the main interaction between residues with this fragment of both cofactors. However, there is different energy with the key residue, Glu124, in which the ribose part of SAM gives a higher interaction than SAH of about 2 kcal/mol. Moreover, we notice the difference of repulsive energies between the ribose fragment and Gly137. The ribose fragment of SAM shows repulsive interactions but not that of SAH. This may be explained by the fact that charges distributions of SAM and SAH are different, evidently in different interaction of ribose moiety. This is demonstrated more cleanly by a graphically representation as shown in Figure 22.

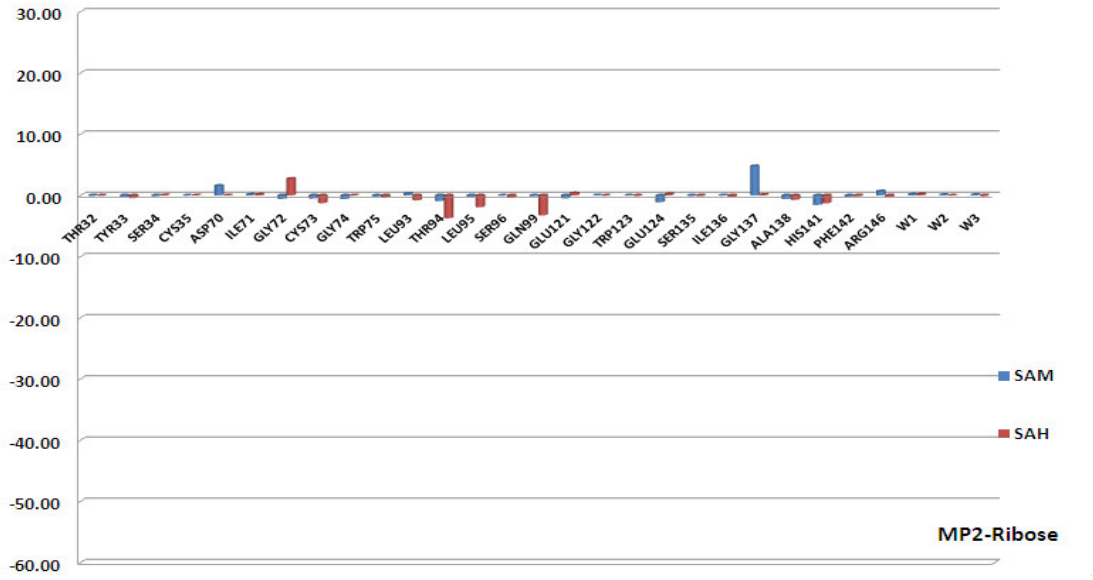

Figure 22 Interaction energies of the ribose moiety (in kcal/mol) with SAM (in blue color) and SAH (in red color) calculated using MP2/6-31G(d) method.

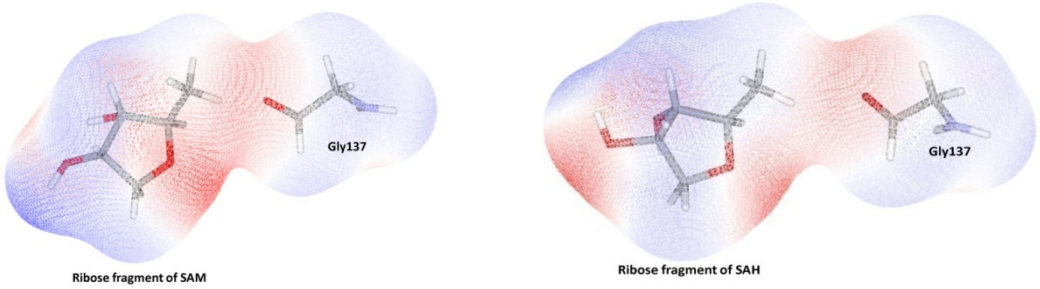

(a) (b)

Figure 23 Charge surface interactions between the ribose fragment of SAM and Gly137 (a), SAH and Gly137 (b).

3.3 Sulfur moiety

Considering calculated interaction energies from the sulfur moiety as shown in Figure 24, this plot suggested that the relatively significant interactions of

sulfur fragment and residues in the cofactor active site are of much higher energy differences compared with those of other fragments, especially with this moiety in SAM. The sulfur fragment of SAM displays strong attractive interactions with Asp70, Glu124 and Glu121, moderate interactions with His141 while the sulfur fragment of SAH cofactor shows weak interactions with these residues. Moreover, most of the fragments show repulsive interactions with Arg146, this particularly repulsive interaction are found in sulfur moiety of SAM cofactor with values of 22 kcal/mol. These indicate that positively charged sulfur moiety plays a significant role that allows a stronger interaction in the substrate binding site than the neutral sulfur moiety of SAH. Therefore, this structural information can be helpful for the design new serial inhibitors of the cyclopropane synthase enzyme. The modification can be made on this moiety by keeping the positive charge of inhibitor.

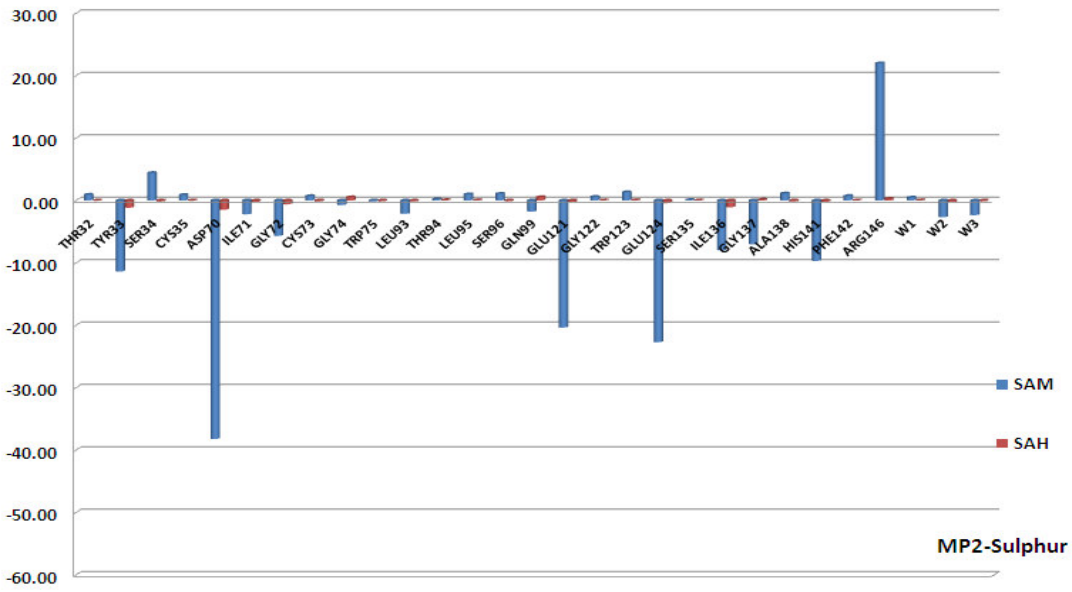

Figure 24 Interaction energies of sulfur moiety (in kcal/mol) with SAM (in blue color) and SAH (in red color) calculated using MP2/6-31G(d) method.

3.4 Amino moiety

In case of interactions between the amino fragment and surrounding residues as shown in Figure 25, Asp70 shows the strongest interaction and gives similar energies in both cofactors with 18-19 kcal/mol. Other residues give lower interactions with tiny differences between the amino moiety of SAM and SAH such as Ser34, Gly72, and water2 molecule. Some residues, Gly137 and water1 show different energies with two types of cofactors. Interestingly, water molecules have effect on to this moiety due to hydrogen bond linkage with Asp70 and amino moiety. It is implied that the amino fragment can be considered as an important part for cofactors caused by Coulomb interaction between zwitterionic form of the amino moiety and the surrounding residues. However, calculated energies given in Figure 18 display not significant differences between SAM and SAH, indicating that this moiety is not appropriate for modification for new potent inhibitor.

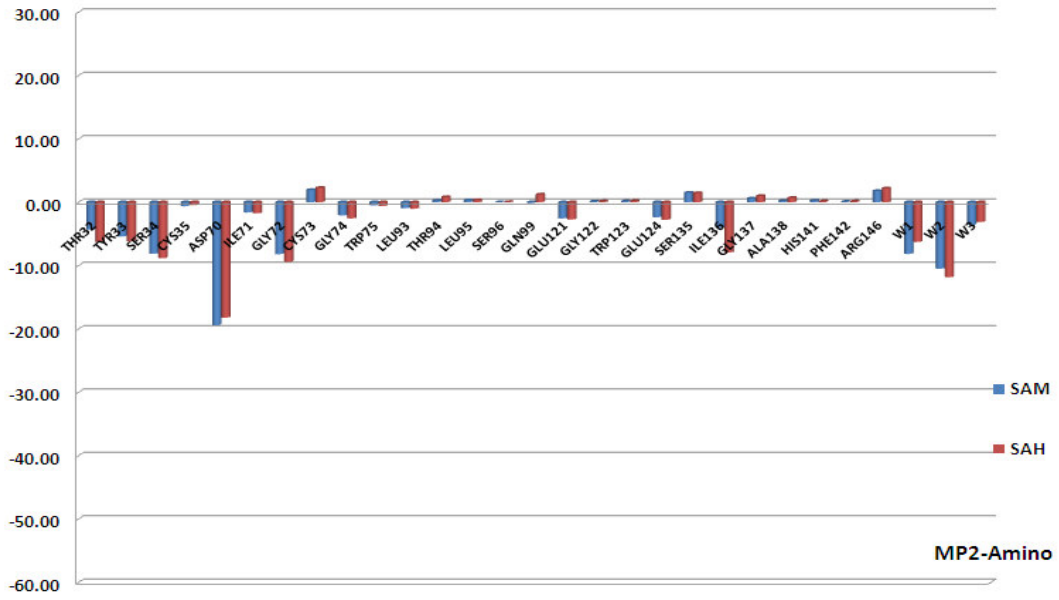

Figure 25 Interaction energies of amino moiety (in kcal/mol) with SAM (in blue color) and SAH (in red color) calculated using MP2/6-31G(d) method.

3.5 Comparison between each fragment with the whole SAM/SAH cofactors

Sums of interaction energies derived from each fragment, adenine, ribose, sulfur and amino moiety, are shown in Table 10. Slightly different energies between the sum of interaction energies from each fragment and calculated interaction energies from the whole cofactor imply that hydrogen linked atoms take little effect to the total interaction energies. In addition, individual fragment interactions show the same trend with the whole cofactor calculations in which the key residues are Asp70, Glu124, Glu121, and the water2 molecule.

Considering surrounding residues within 6 Å, centered at each fragment, can be separated in to four components shown in Figure 27, as following

Residues surrounding adenine moiety: Ile71, Gly72, Leu93, Thr94, Leu95, Glu121, Gly122, Trp123, Glu124, Ala138, His141, Phe142 and Arg146

Residues surrounding ribose moiety: Gly72, Cys73, Gly74, Thr94, Leu95, Ser96, Gln99, Gly137, Ala138 and His141

Residues surrounding sulfur moiety: Tyr33, Ser34, Gly72, Cys73, Gly74, Trp75, Ile136, Ala138 and His141

Residues surrounding amino moiety: Thr32, Tyr33, Ser34, Asp70, Gly72, Cys73, Gly74, Ser135, Ile136, Gly137 and Ala138

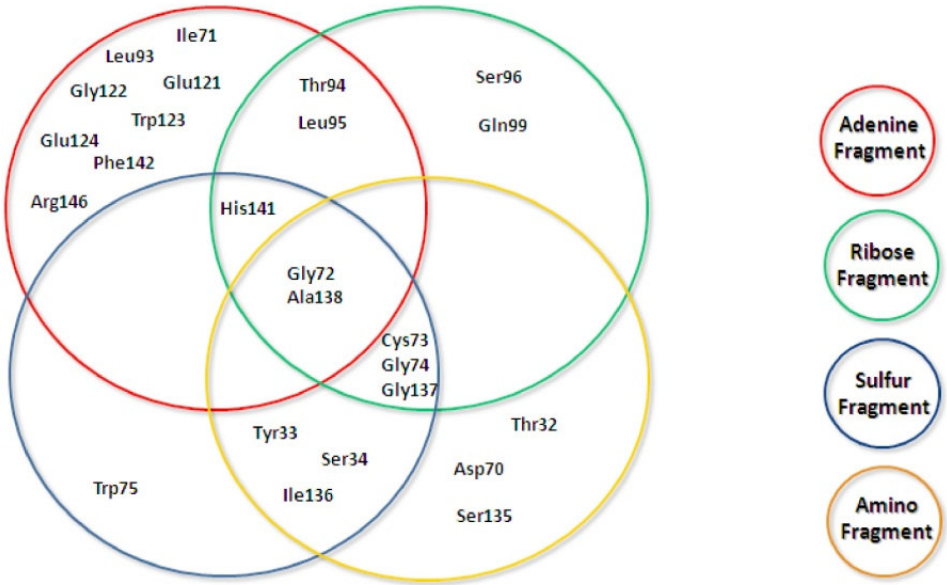

(a)

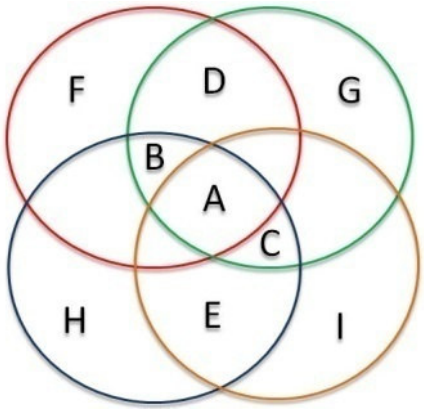

(b)

Figure 26 (a) Four components diagram of residues surrounding 6 Å from each fragment of the cofactor

(b) Separate region numbering of the diagram

Interestingly, Gly72 and Ala138 are common residues located within 6 Å of all fragments (region A). However, the interaction energies of both residues are less than that of Asp70 or Glu124 which are located in region I and F, respectively. Even, Gly72 pays attention to amino moiety of SAM and SAH and the sulfur moiety of SAM, it is not prominent when compared with the interaction energy of Asp70 (see Table 10). In addition, Ala138 does not significantly contribute to total interaction energy, though it places close to all fragments. Overlapping residue in the three fragments; adenine, ribose and sulfur (see Figure 26), is His141 (region B). It shows remarkable interaction energies only with sulfur moiety of SAM. These data can be interpreted for the message that high potent inhibitors should interact with particular residues in order to make specific interactions.

Next, Cys73, Gly74 and Gly137 are located close to ribose, sulfur and amino fragments (region C). The results show that the interaction of Cys73 and Gly74 with both cofactors are not distinctive. The sum of the fragment interaction energies is 1.10 and 0.89 kcal/mol for Cys73 and -3.33 and -3.41 kcal/mol for Gly74 for the interactions with SAM and SAH cofactors, respectively. As for Gly137, the energy of ribose and sulfur fragments of SAM is contrasted with SAH. The repulsive interaction of ribose moiety of SAM is expressed with 4.79 kcal/mol whereas the ribose moiety of SAH shows a tiny interaction only. Considering the interaction of the sulfur fragment with Gly137, the interaction energies are -7.00 and 0.14 kcal/mol for SAM and SAH moieties, respectively. The result indicated that Gly137 is one of the residues which show significant difference between SAM and SAH cofactors.

Thr94 and Leu95 residues are located near adenine and ribose moiety (region D). Interactions of adenine moiety of both cofactors are not different whereas ribose moiety of SAH shows stronger binding with the two residues. For Thr94, energies are -0.94 and -3.73 kcal/mol for SAM and SAH, respectively. In case of Leu95, the energies are -0.24 and -1.93 kcal/mol for SAM and SAH, respectively. Even, the no largely different energy between the two cofactors, the results revealed that SAH shows stronger binding than SAM cofactor.

The overlap region E covers Tyr33, Ser34 and Ile136 residues which are part of sulfur and amino fragments. Considering Thr33 and Ile136, the sulfur fragment of SAM gives attractive interaction whereas Ser34 shows repulsive interaction in which energies are -11.38, -7.98 and 4.43 kcal/mol, respectively. It means that Ser34 residue does not need a positive charges close to its residue.

The large region which comprises eight residues; Ile71, Leu93, Glu121, Gly122, Trp123, Glu124, Phe142 and Arg146, interacted on the only adenine fragment is region F. Ile71 and Leu93 give similar results which the sulfur fragment of SAM and can bind slightly stronger than to SAH whereas the interaction between adenine moiety with both of cofactors is not different. Glu121 and Glu124 residues present large attractive interaction energies with the sulfur moiety of SAM by the coulomb interaction. Moreover, the adenine moiety of SAM and SAH give strong binding with Glu124, but small repulsive interaction with Glu121. In addition, all fragments of SAM show repulsive energies with Arg146 especially the sulfur moiety. It was also found that Gly122 and Phe142 give similar results in both cofactors. Interactions of the adenine moiety and Phe142 are of distinguishable energy compared to other moieties, however, there is a slight difference similar to that found in the case of Trp123.

Region G consists of Ser96 and Gln99 in which these residues are located in only ribose fragment. Interactions of SAM and SAH cofactors with Ser96 are not significant different whereas interaction of Gln99 residue with ribose fragment of the SAH gives attractive interaction with moderate hydrogen bonding, resulting in lower energy than SAM cofactor.

Trp75 is a residue close to the sulfur moiety and its position is far from other fragments (see region H). The results show that the residue does not play any important interaction in the sulfur moiety with energy less than 1 kcal/mol in both of SAM and SAH cofactors. Interactions between other fragments and this residue are not varying from the sulfur fragment. It means that Trp75 is not an interesting residue to be focused on the cyclopropane synthase enzyme.

Finally, region I, comprised of three residues; Thr32, Asp70 and Ser135, is then focused. For Thr32, the amino fragment of SAH performs favorable interaction than SAM of about 2 kcal/mol because a hydroxyl group of Thr32 locates closer the carboxylate group of SAH than SAM cofactor. The leading residue, Asp70 also presents strong interactions with the amino moiety similar to both cofactors. However, the charge distribution of SAM reacts upon the interaction with the sulfur moiety as charge polarization which does not appearance in SAH cofactor. Considering Ser135 residue, amino moiety gives small repulsive interaction in both fragment of SAM and SAH. Whatever it is very tiny energy compared with other residues.

The Sum of interaction energies of all four fragments and surrounding residues (in column Total [(a)]), are compared with the energies from the whole cofactor (in column Total [(b)]) as shown in Table 10. The results show that the summed energies of each fragment and of the whole cofactor are comparable. If the energies are different for Glu124 in two columns, this is also in line with the same tendency in both show high energy value. Taken into account, it means that cutting the cofactor into fragments can present important interaction of moiety with it surrounding residues. This structural information of the fragment can be useful for the design of new cyclopropane synthase inhibitor.

Table 10 Total interaction energies between cofactors (SAM and SAH) with residues in kcal/mol calculated by MP2/6-31G(d) method with BSSE-CP correction

	SAM		ΔE	SAH		ΔE
	Total[(a)]	Total[(b)]		Total[(a)]	Total[(b)]	
Thr32	-3.42	-2.28	-1.14	-6.29	-4.74	-1.55
Tyr33	-17.31	-16.97	-0.34	-7.90	-7.27	-0.63
Ser34	-3.73	-2.39	-1.34	-8.81	-8.77	-0.04
Cys35	0.29	0.38	-0.09	-0.42	-0.50	0.08
Asp70	-55.17	-54.55	-0.62	-19.46	-21.29	1.83
Ile71	-4.71	-4.29	-0.42	-3.04	-2.61	-0.43
Gly72	-15.01	-16.08	1.07	-4.60	-10.53	5.93
Cys73	1.82	1.10	0.72	0.53	0.89	-0.36
Gly74	-3.43	-3.33	-0.10	-2.09	-3.41	1.32
Trp75	-0.88	-0.55	-0.33	-1.11	-0.13	-0.98
Leu93	-3.01	-2.66	-0.35	-2.47	-1.89	-0.58
Thr94	-1.88	-2.07	0.19	-3.73	-4.08	0.35
Leu95	-0.96	-0.97	0.01	-3.54	-3.72	0.18
Ser96	0.97	0.91	0.06	-0.55	-0.07	-0.48
Gln99	-2.33	-0.51	-1.82	-1.62	-0.56	-1.06
Glu121	-22.15	-23.31	1.16	-1.77	-1.45	-0.32
Gly122	0.22	0.79	-0.57	-0.03	-0.82	0.79
Trp123	0.29	0.70	-0.41	-2.10	-3.46	1.36
Glu124	-41.85	-53.8	11.95	-13.06	-18.85	5.79
Ser135	1.29	1.19	0.10	1.28	1.44	-0.16
Ile136	-12.26	-11.4	-0.86	-9.56	-6.94	-2.62
Gly137	-2.30	-5.97	3.67	0.73	1.95	-1.22
Ala138	-0.40	-0.19	-0.21	-0.65	-0.70	0.05
His141	-10.15	-8.63	-1.52	-3.62	-2.86	-0.76
Phe142	-1.48	-1.28	-0.20	-1.81	-1.66	-0.15
Arg146	26.41	28.68	-2.27	3.42	0.31	3.11
Water1	-7.51	-6.35	-1.16	-6.01	-9.74	3.73
Water2	-13.1	-14.53	1.43	-12.3	-10.76	-1.54
Water3	-5.96	-6.13	0.17	-3.43	-3.12	-0.31
Total	-197.69	-204.49	6.80	-114.02	-125.32	11.30

[(a)] Total : sum of interaction energies from each fragment

[(b)] Total : calculated interaction energies from the whole cofactor

4. ONIOM calculation

In order to investigate the binding energies of SAM and SAH cofactors and sinefungin inhibitor in the PcaA binding site, ONIOM calculations were performed. B3LYP method in combination of PM3 semiempirical calculations were used in this study. As there are several conditions that may affect the binding energies, therefore, several different effects were investigated and the results are shown separately. Consequently, 24 ONIOM models were generated and specific definition of inner and outer layers of each ONIOM model is shown in Table 3.

4.1 Effect of HAF and BBF approach

In this study, two approximations; heavy atoms fixed (HAF) and backbone fixed (BBF), are performed to optimize the structure of the SAH cofactor and its binding site. In HAF, all heavy atoms of the residues in the binding pocket are fixed to the X-ray structure co-ordinates, only the structure of SAH and hydrogen atom geometries are optimized. In BBF, only the backbone atoms of the residues are fixed to the X-ray structure co-ordinates, with all structures of SAH and the side chain atoms free to optimize. In addition, models which included water molecules had the water oxygen atom fixed. Following this approach, four ONIOM systems, ONIOM 2A, 2B, 2C and 2D, were investigated. The results as shown in Table 11 indicated that the BBF optimization produces an improvement in the calculated energies for all systems, and imply that relaxation of residues during optimization has an effect on the interaction energy that in turn affects the binding energy. The BBF approach gives lower binding energies than HAF approach for about 6 – 7 kcal/mol for HF/6-31G(d):PM3 and B3LYP/6-31G(d):PM3 level of calculations. Superimpositions of the complex structures after HAF and BBF optimization protocols (see Figure 27) indicate slight displacements of the side-chains of Tyr33, Trp75, Leu93, Leu95, Gln99, Trp123, Glu121, His141, and Phe142, with an overall RMSD value of all the heavy atoms of 0.981 Å. Furthermore, RMS differences between HAF and BBF with X-ray structure are 0.979 and 0.238 Å, respectively. Therefore, the results show different energies and structural geometries obtained from the two approaches. In

further study, the ONIOM calculations were performed using BBF optimization procedure for the relaxation of the side chains of the amino acids in order to investigate an interaction of the cofactors in the cofactor binding site.

Table 11 Interaction energies (INT) of SAH with 26 residues, calculated by HF/6-31G(d):PM3 and B3LYP/6-31G(d):PM3 calculations (in kcal/mol) .

	HF/6-31G(d):PM3			B3LYP/6-31G(d):PM3		
Systems	HAF	BBF	ΔE	HAF	BBF	ΔE
ONIOM 2A	-16.40	-23.50	7.10	-20.87	-27.11	6.24
ONIOM 2B	-17.29	-23.25	5.96	-21.12	-27.30	6.18
ONIOM 2C	-61.48	-68.28	6.80	-65.26	-72.05	6.79
ONIOM 2D	-89.79	-95.34	5.55	-91.14	-98.77	7.63

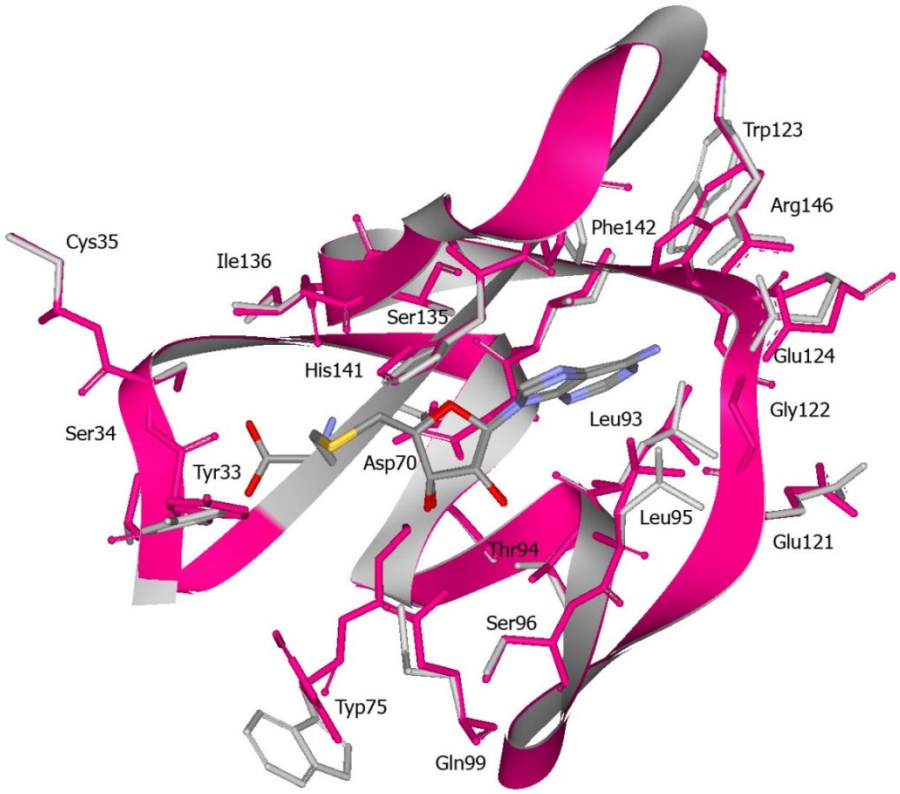

Figure 27 Superimposition of the backbone for the BBF approach (in red color) and HAF (in blue color) approach in ONIOM2 model

4.2 Effect of the cutting model of SAH

In the ONIOM calculations, the cutting molecule is very important, concerning accuracy of the combined methods and computational time. In this study, two models of SAH cofactor are investigated. In the first model, only the 6-amino pyrimidine ring of SAH was considered as inner region together with Glu124 (see Figure 28a), while in the second model, all parts of SAH cofactor were selected with Glu124 (see Figure 28b) in order to investigate an effect of the inner layer size. Considering Table 3, ONIOM 2B compared with ONIOM 2J and ONIOM 2E, compared with ONIOM 2L models, were picked up to analyze an effect of the model of cofactors. The results show that the first model of both compared systems give lower binding energies than that of the second model. Considering deeper information, interaction energies of these models are of quite similar value. For example, the interaction energy difference of ONIOM 2B and 2J are about 1.90 kcal/mol and interaction energy differences of ONIOM 2E and 2L are about 2.66 kcal/mol. The detail of deformation energies can be divided into two parts, deformation energies of the ligand and deformation of the pocket. Both type of deformation energy can lead to the difference of two models. We found that the energy difference of both models comes from the deformation part of the ligands (13.88 and 27.25 kcal/mol for ONIOM 2B and 2J and 18.40 and 29.06 kcal/mol for ONIOM 2E and 2L, respectively). The models of the second systems (ONIOM 2J and 2L) need more energy to deform their structures. Suggesting that all atoms of cofactor should be included in the high level part in order to get more reliable interaction.

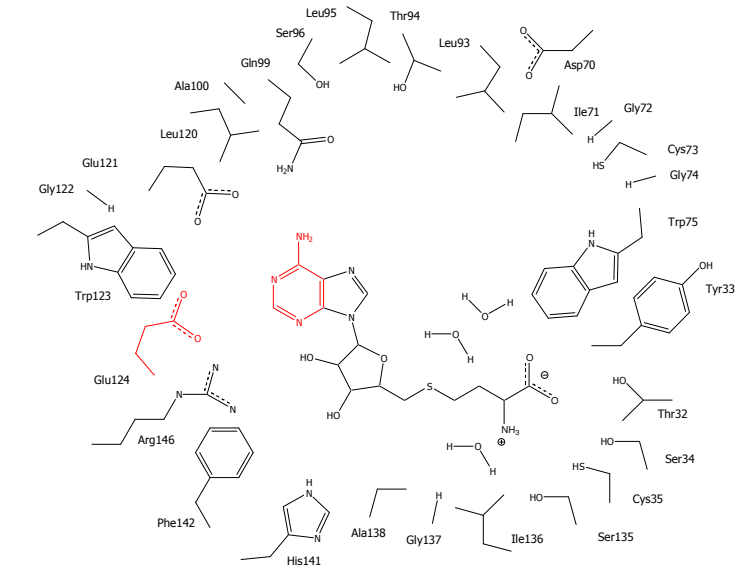

(a)

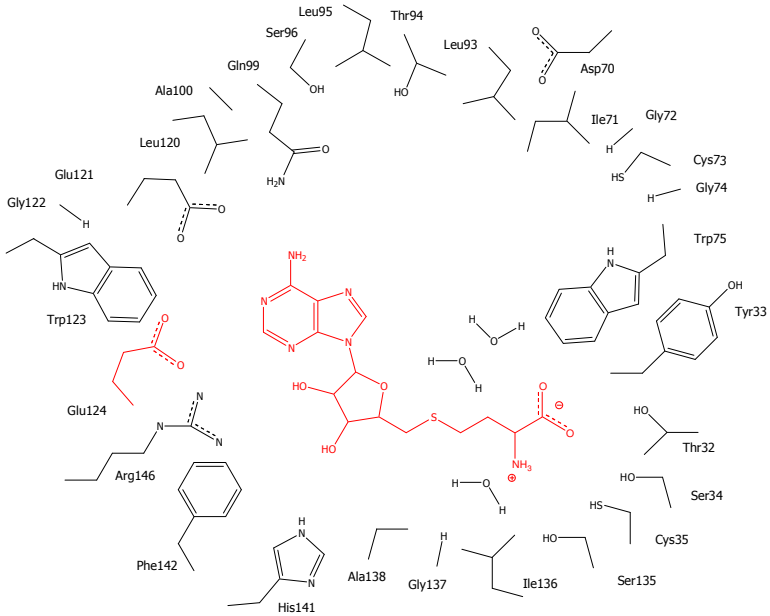

(b)

Figure 28 Model (a) comprises 6-amino-pyrimidine of SAH cofactor and Glu124 in high level (in red color), model (b) comprises cofactor and Glu124 in high level of the ONIOM2 system (in red color) and rest residues shown in black color.

Table 12 Binding energies (BE), Interaction energies (INT), Deformation energies (DEF) from ONIOM2(B3LYP/6-31G(d):PM3) calculations (in kcal/mol).

	ONIOM 2B	ONIOM 2J	ONIOM 2E	ONIOM 2L
BE	-51.22	-34.70	-57.10	-45.99
INT	-73.40	-70.74	-94.46	-92.56
DEF	2.19	36.04	37.35	46.57

4.3 Neutral vs. zwitterionic form of SAH

In this section, the SAH cofactor is considered and divided into two states, neutral and zwitterionic form (See Figure 29). To predict the suitable form of the cofactor in the cofactor binding site, the performance of the ONIOM method was used. Different structures of the two states are negatively and positively charged at the carboxylic and amine position for zwitterionic form, respectively, whereas, neutral carboxylic acid and amine group was assumable to be a neutral form. In this study three model systems were examined, ONIOM 2A/ONIOM 2B, ONIOM 2C/ONIOM 2D, and ONIOM 2F/ONIOM 2G.

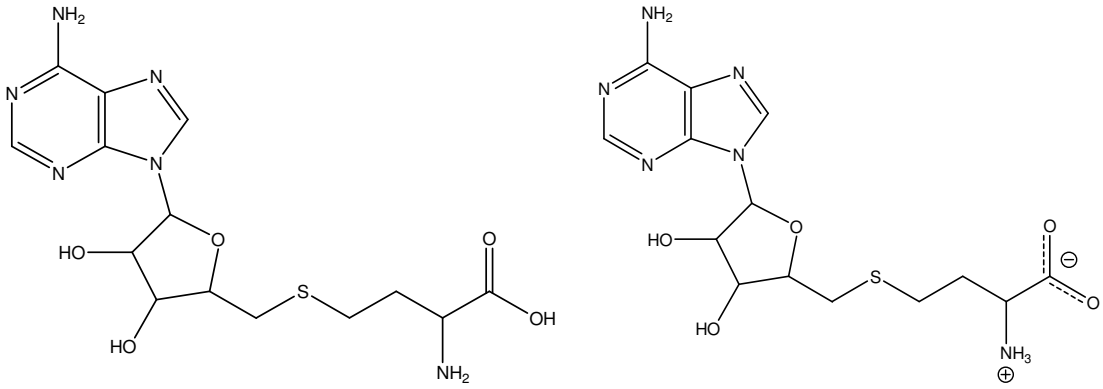

(a) (b)

Figure 29 Neutral (a) and zwitterionic form (b) of SAH cofactor.

The results as shown in Table 13, document that the zwitterionic form of SAH cofactor establishes more favorable interaction than that of the neutral form of about 10 times. This large difference comes from large interaction energy and deformation energy of the ligand and their residues of zwitterionic form. The interaction energy (INT) and deformation energy (DEF) of zwitterionic state show of about 3 times and 2 times higher amount thereof the neutral form of SAH, respectively. These results demonstrate that the electrostatic interaction plays important role in this system studied. Thus, in next investigation zwitterionic form of cofactors will be focused.

Table 13 Binding energies (BE), Interaction energies (INT), Deformation energies (DEF) from ONIOM2(B3LYP/6-31G(d):PM3) calculations (in kcal/mol)

	ONIOM 2A	ONIOM 2B	ONIOM 2C	ONIOM 2D	ONIOM 2F	ONIOM 2G
BE	-12.67	-51.202	-9.38	-53.48	-11.07	-56.98
INT	-28.26	-73.400	-28.42	-94.49	-30.13	-95.23
DEF	15.59	2.109	19.04	41.01	19.06	38.25

4.4 Comparison of the interaction between SAM and SAH cofactor

S-adenosyl-L-methionine (SAM) and S-adenosyl-L-homocysteine (SAH) are substrate and product cofactors, respectively, of the methylation of cyclopropane reaction. Both cofactors have only one sub strut at sulfur atom. Different atom plays dramatically effect in its cofactor binding site as show in section 3.3.3. In order to explain is phenomenon, the ONIOM calculations are investigated by selection of three model systems, ONIOM 2S/ONIOM 2I, ONIOM 2R/ONIOM 2H and ONIOM 2X/ONIOM 2P. The results show that the binding energies of SAM models are dramatically lower than that of SAH cofactor. For example, in ONIOM 2R/ONIOM 2H as shown in Table 14, even as hydrogen bond distance is not different, large different energy comes from positively charged sulfur moiety of SAM cofactor. The interaction energies resulting from ONIOM 2X and ONIOM 2P suggest that sulfur moiety represents a very important part that affects the interaction with Asp70,

Glu121 and Glu124 residues. Considering ONIOM 2X, including SAM cofactor, Thr32, Ser34, Asp70, Glu124 and three water molecules in the high level, compared with ONIOM 2P, SAM cofactor gives higher different binding energy than that of SAH cofactor with an energy difference of about 70 kcal/mol ,while other systems give energy differences of about 60 kcal/mol. It means that these four residues have effect to the binding energy of about 10 kcal/mol. The explanation for the large energy of SAM comes from the interaction of the residues surrounding the cofactor site (more than 2 times for SAM), while, deformation energy of the binding pocket are quite similar in both SAM and SAH cofactor. Moreover, sinefungin was also considered (ONIOM 2Y) to be compared with both cofactors (ONIOM 2R and ONIOM 2H). The results show that binding energy of sinefungin with the cofactor binding site is stronger than that of SAM of about 8 kcal/mol in which NH_2 of the adenine moiety of SAM does not undergo hydrogen bonding whereas sinefungin performs hydrogen bonding with carboxylate group of Glu124 (Table 15), having distance of about 1.83 Å. It suggests that sulfur moiety perform very important part for further inhibitor modification.

Table 14 Binding energies (BE), Interaction energies (INT), Deformation energies (DEF) from ONIOM2(B3LYP/6-31G(d):PM3) calculations (in kcal/mol)

	ONIOM 2S	ONIOM 2I	ONIOM 2R	ONIOM 2H	ONIOM 2Y	ONIOM 2X	ONIOM 2P
BE	-100.87	-43.742	-111.98	-52.26	-119.41	-135.77	-67.05
INT	-159.54	-86.79	-176.00	-100.12	-180.57	-206.85	-120.8
DEF	58.67	43.059	64.02	47.86	61.17	71.08	53.75

Table 15 Hydrogen bond distances (Å) of SAM (ONIOM 2R), SAH (ONIOM 2H) and sinefungin (ONIOM 2Y) with surrounding atoms

Hydrogen bond distance	SAM	SAH	sinefungin
NH_2 adenine moiety --- COO^- side chain of Glu124	-	1.83	1.83
OH ribose moiety --- NH_2 side chain of Glu124	2.48	2.38	2.37
NH_3 sulfur moiety --- CO backbone of Tyr33	-	-	1.81
COO^- amino moiety --- Water1	1.86	1.82	1.86
COO^- amino moiety --- OH side chain of Ser34	1.76	1.76	1.75
NH_3 amino moiety --- Water2	1.65	1.74	1.64
NH_3 amino moiety --- CO backbone of Gly72	1.79	1.80	1.80
NH_3 amino moiety --- CO backbone of Ile136	1.92	1.90	1.90

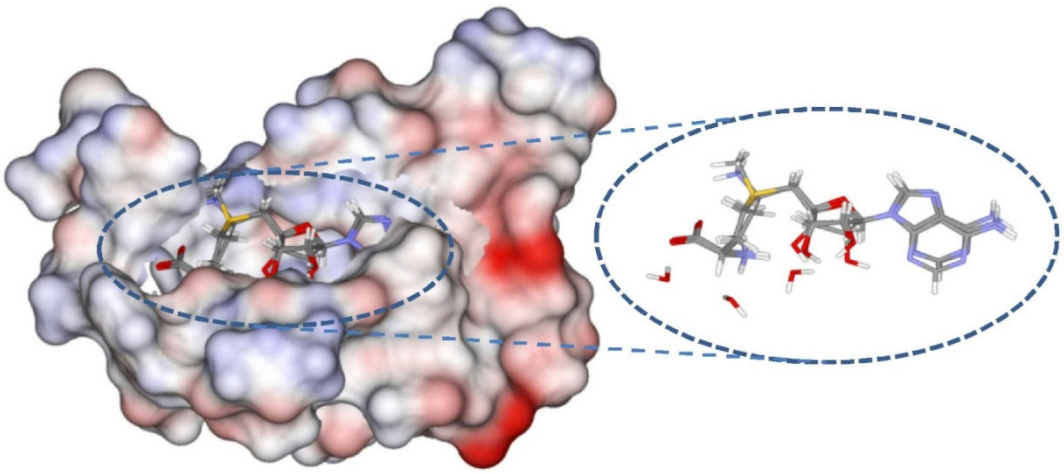

Figure 30 Overlay structures of SAM, SAH and sinefungin from ONIOM 2R, 2H and 2Y.

4.5 Effect of water molecules in the binding site

The X-ray structures of cyclopropane synthase includes of some water molecules in the crystal. In addition, it was found that the cofactor binding site includes more than three water molecules around its site. From the results shown in Table 16, these indicate the important contribution to the binding. For example, hydrogen bond linkage with the cofactor and Asp70 appear in all systems of SAM, SAH and sinefungin. To see more effects of water molecules, some models were studied, within the region around 7Å of the binding site and the results are separated as following.

Table 16 Hydrogen bond distances (Å) of SAM (ONIOM 2R), SAH (ONIOM 2H) and sinefungin (ONIOM 2Y), including water molecules in its binding site

Hydrogen bond distance atom	SAM	SAH	sinefungin
Water 1 --- COO^- amino moiety of cofactor/inhibitor	1.86	1.82	1.86
Water 1 --- CO backbone of Gln31	1.79	1.80	1.79
Water 1 --- NH backbone of Trp75	2.01	2.01	2.01
Water 2 --- NH_3^+ amino moiety of cofactor/inhibitor	1.65	1.74	1.64
Water 2 --- COO- side chain of Asp70	1.74	1.75	1.73
Water 3 --- COO^- side chain of Asp70	1.73	1.73	1.72
Water 3 --- CO backbone of Ile71	2.18	2.21	2.21
Water 3 --- NH backbone of Ile136	1.70	1.70	1.71

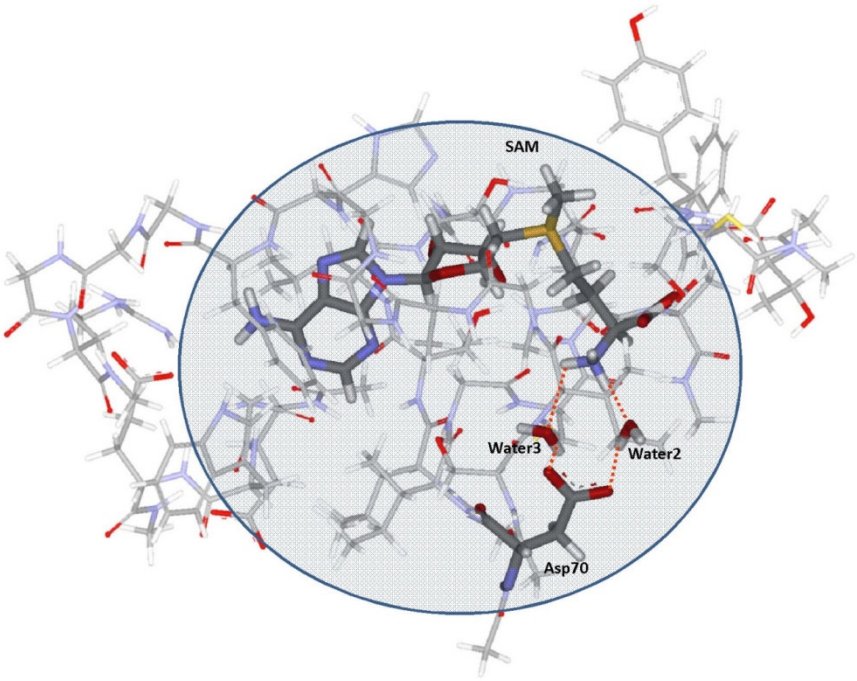

Figure 31 Hydrogen bond between SAM cofactor, water molecules and Asp70, obtained from ONIOM 2R model calculations

4.5.1 Effect of water molecules in the inner layer

In this section, the aim was to investigate the role of water, mapping in a binding site for potential interaction. Three compared models were set up to examine with varying condition in the high layer of ONIOM system in which presence and absence the water molecules, resulting in ONIOM 2R/ONIOM 2Q, ONIOM 2K/ONIOM 2J and ONIOM 2N/ONIOM 2M for comparison (see Table 3 and Table 17). Three water molecules are included in the ONIOM 2R, ONIOM 2K and ONIOM 2N models removed in the ONIOM 2Q, ONIOM 2J and ONIOM 2M, consecutively. From Table 17, the results indicate that includes water molecules in the systems (ONIOM 2R, ONIOM 2K and ONIOM 2N) gives lower binding energies than those obtained in the absence water molecules by 20- 25 kcal/mol (energy differences of binding energies of each compared system). These results that interaction of three water molecules in the cofactor binding site of about 20-25 kcal/mol is in consistent with individual interaction energy of PcaA (as shown in

Table 5) by sums of interaction energy of three waters are -27.01 and -23.62 kcal/mol for SAM and SAH cofactor, respectively. Moreover, it was found the former section (Table 15) that at least two water molecules present significant importance. Concluding from the obtained results, the water molecules are considered as one of the main contributions in the cofactor binding site that requires including them in the model systems.

Table 17 Binding energies (BE), Interaction energies (INT), Deformation energies (DEF) from ONIOM2(B3LYP/6-31G(d):PM3) calculations (in kcal/mol). Including water molecules in the inner layer (ONIOM 2R, ONIOM 2K and ONIOM 2N) and excluding water molecules (ONIOM 2Q, ONIOM 2J and ONIOM 2M)

	ONIOM 2R	ONIOM 2Q	ONIOM 2K	ONIOM 2J	ONIOM 2N	ONIOM 2M
BE	-111.98	-86.77	-54.62	-34.70	-51.26	-27.47
INT	-176.00	-135.83	-105.78	-70.74	-98.48	-57.92
DEF	64.02	49.06	51.16	36.04	47.21	30.46

4.5.2 Stabilized cofactor by water molecules

From previous part, the water molecules in the cofactor binding site show important function. To define role of the water molecules if they stabilize the systems, two approaches were modeled, setting up the water molecules in part of the cofactor and in part of the pocket of the cofactor binding site. The calculated results are given in Table 18. Calculated water molecules as part of cofactor of SAM give lower binding energy than that of part of binding pocket and the different binding energy is about 4.90 kcal/mol. Different energy of about 5 kcal/mol means surrounding water molecules seem to more stabilization of the carboxylate and the amino groups of the cofactors, however, they also play an important role in the surrounding residues, for example, water numbering 2 (water2) stabilizes the carboxylate side chain of Asp70. Considering the SAH cofactor, the result show the

same tendency which the binding energies of the water molecules as part of cofactor are lower than those of the water molecules as part of the binding pocket, -65.97 and -52.26 kcal/mol, respectively. However, large different energy between these two approaches of SAH in comparison to that of SAM cofactor (13.71 kcal/mol) implies that the charge distribution of the SAM cofactor decrease stabilization of the water molecules on the system.

Table 18 Binding energies of SAM and SAH cofactor in the cofactor binding site, calculated by ONIOM2(B3LYP/6-31G(d):PM3) calculations (in kcal/mol)

	SAM			SAH		
	H_2O stabilize cofactor	H_2O stabilize binding pocket	ΔE	H_2O stabilize cofactor	H_2O stabilize binding pocket	ΔE
BE	-116.88	-111.98	4.9	-65.97	-52.26	13.71

4.5.3 Important water molecules

Considering 7 Å around the SAM cofactor binding site including of five water molecules, it can be shown that these water molecules are essential for stabilized complexes. Results of individual interaction energies of SAM with PcaA enzyme show that at least two molecules have strong interaction with SAM cofactor. In this section, the aim is to find an important water molecule by ONIOM calculations, considering each water molecule together with the SAM cofactor in inner layer and the rest of water molecules in outer layer. The relative energies of the SAM complexes are shown in Table 19. Water2 and water5 show prominent energies with -9.68 and -8.16 kcal/mol, respectively. Water1 (H_2O^1) forms hydrogen bond with carboxylate group of the SAM cofactor, peptide bond of Gln31 and Gly75 by bond distances of 1.85, 1.79 and 2.01 Å, respectively. Water2 (H_2O^2) forms a hydrogen bond with the amino group of the SAM cofactor and the carboxylate group of Asp70 by bond distance of 1.66 and 1.73 Å, respectively. Water3 (H_2O^3) forms a hydrogen bond with carboxylate group of Asp70, the peptide bond of Ile71 and Ile136 by bond

distances of 1.70, 2.19 and 1.70 Å, respectively. Water4 (H_2O^4) forms only one hydrogen bond with the peptide bond of Gly137 by a bond distance of 1.83 Å. At Last, water5 (H_2O^5) forms only one hydrogen bond with the hydroxyl group of the ribose moiety of the SAM cofactor by a bond distance of 1.74 Å. However, water4 and water5 are excluded from other ONIOM systems. Consequently, only three water molecules, water1, water2 and water3 are considered, at the same position as in the SAH cofactor binding site. Water2 shows the lowest binding energy which is consistent with individual interaction energy results. This can be explained from strong hydrogen bridge linkage between negatively charged carboxylate group of Asp70 and positively charged amino group of SAM cofactor.

Table 19 Relative binding energy differences of each water molecule (in kcal/mol) in the SAM cofactor binding site, using ONIOM2(B3LYP/6-31G(d):PM3) calculations

	All H_2O as part of Low level	H_2O^1 as part of High level	H_2O^2 as part of High level	H_2O^3 as part of High level	H_2O^4 as part of High level	H_2O^5 as part of High level
ΔΔE	0	-5.90	-9.68	-5.01	-4.00	-8.16

Next, the complex of SAH with its cofactor binding site including three water molecules was investigated. The relative energy results of SAH complexes are shown in Table 20. Water2 shows the lowest interaction energy similar as obtained from the SAM cofactor. Water1 (H_2O^1) forms hydrogen bonds with carboxylate group of SAH cofactor, which the peptide bond of Gln31 and Gly75 by bond distances of 1.83, 1.80 and 2.00 Å, respectively. Water2 (H_2O^2) forms hydrogen bonds with amino group of the SAH cofactor and carboxylate group of Asp70 by bond distances of 1.73 and 1.74 Å, respectively. Finally, water3 (H_2O^3) forms hydrogen bonds with the amino group of the SAH cofactor and carboxylate group of Asp70 by bond distances of 1.73 and 1.74 Å, respectively. The relative binding energies of water molecules following by strong interaction are $H_2O^2 > H_2O^1 > H_2O^3$. It was found from the results

that both cofactors show consistent relative strong binding energies by water molecule.

Table 20 Relative binding energy differences of each water molecule (in kcal/mol) in SAH complexed to the cofactor binding site, using ONIOM2(B3LYP/6-31G(d):PM3) calculations

	All H_2O as part of Low level	H_2O^1 as part of High level	H_2O^2 as part of High level	$H2O^3$ as part of High level
ΔΔE	0	-5.21	-6.93	-3.15

4.5.4 Water molecules in inner/outer layer of system

In this section, a comparison of water molecules in the inner and the outer layers of ONIOM model was investigated in the combined ONIOM model. ONIOM 2H/ONIOM 2I and ONIOM 2K/ONIOM 2L used two different approachs, setting up water molecules in the inner layer (ONIOM 2H and ONIOM 2K) and setting up water molecule in the outer layer (ONIOM 2I and ONIOM 2L). The calculated energy results are shown in Table 21. It was found that binding energy difference there two approaches are of about 9 kcal/mol in which energy differences come from parts of interaction energies of the complex, while, the deformation energy shows small. For example, the binding energy different of ONIOM 2H/ONIOM 2I system are about 8.52 kcal/mol while interaction energy difference is 13.33 kcal/mol as quite similar as that of obtained from ONIOM 2K/ONIOM 2L. The different binding energies come from part of the interaction energies where ONIOM 2H and ONIOM 2K are included water molecules in the high level and give lower energies than that of ONIOM 2I and ONIOM 2L, where deformation of the ligand are small (47.86, 43.05, 51.16 and 46.57 kcal/mol for ONIOM 2H, ONIOM 2I, ONIOM 2K and ONIOM 2L, respectively). This different energies come from the deformation energy part of the pocket (17.48, 13.87, 21.23 and 17.50 kcal/mol for ONIOM 2H, ONIOM 2I, ONIOM 2K and ONIOM 2L, respectively) where deformation energy part of the

ligand is similar (30.38, 29.18, 29.93 and 29.36 kcal/mol for ONIOM 2H, ONIOM 2I, ONIOM 2K and ONIOM 2L, respectively). Considering the obtained results these indicated that the different binding energies of two approaches are quite different. We conclude that water molecules affect of the interaction between cofactor and surrounding residues, thus, water molecules should be added in the inner layer of ONIOM models to represent the role of waters on this system studied.

Table 21 Binding energies (BE), Interaction energies (INT), Deformation energis (DEF) from ONIOM2(B3LYP/6-31G(d):PM3) calculations (in kcal/mol).

	ONIOM 2H	ONIOM 2I	ONIOM 2K	ONIOM 2L
BE	-52.26	-43.74	-54.62	-45.99
INT	-100.12	-86.79	-105.78	-92.56
DEF	47.86	43.05	51.16	46.57

4.5.5 Constraint water molecule: fix or relax water molecule

In this section, we focused mainly on the water molecules. The optimization including water molecules at high level of calculation were performed by constraint of the water molecules compared with relaxation of the water molecule. ONIOM 2C/ONIOM 2F, ONIOM 2D/ONIOM 2G and ONIOM 2O/ONIOM 2P were picked up to explain the role of constrained water molecules. Table 22 presents the energies of these compared systems. No significant energy value between two approaches is found. The constrained water models have binding energies less than those obtain upon relaxation of water molecules of about 3 kcal/mol while the deformation is very similar. A slightly different energy of these systems proceeds from interaction among water molecules in the high region. These findings suggested that constrained water molecules can be used to represention for reliable system.

Table 22 Binding energies (BE), Interaction energies (INT), Deformation energies (DEF) from ONIOM2(B3LYP/6-31G(d):PM3) calculations (in kcal/mol).

	ONIOM 2C	ONIOM 2F	ONIOM 2D	ONIOM 2G	ONIOM 2O	ONIOM 2P
BE	-9.38	-11.07	-53.48	-56.98	-63.40	-67.05
INT	-28.42	-30.13	-94.49	-95.23	-117.37	-120.80
DEF	19.04	19.06	41.01	38.25	53.98	53.75

4.6 Effect of residues in high level of calculation

Extended important residues are included in the inner layer of ONIOM calculation. Thr32, Ser34, Asp70 and Glu124 are considered and suitable models for representative interactions as shown in Table 23, are found. Firstly, Asp70 is considered. The SAH cofactor and three water molecules are treated at of the high level of calculation compared with a model system consisting of cofactor, Asp70 and three water molecules (ONIOM 2H/ONIOM 2N). The binding energies of these two models are quite similar in which energy difference is of about 1 kcal/mol. This difference comes partly of form the interaction energy whereas the deformation energy is similar value. In addition, ONIOM 2K was investigated and compared with ONIOM 2H as test effect of Glu124 in the inner layer. The interaction energy of ONIOM 2K model is decreased to 5.66 kcal/mol, however, deformation energy is also increased by 3.3 kcal/mol, resulting in different binding energy of about 2.3 kcal/mol. It means that adding Asp70 or Glu124 in the inner layer does not affect the binding energy obtain from the ONIOM systems. Thr32, Ser34, Asp70 and Glu124 are found to be the key interactions according to results in Table 5, therefore, they were added in the model system in order to explore the effect of these residues. ONIOM 2O was compared with ONIOM 2H. The results show that the energy was decreased to 11.14 kcal/mol when Thr32, Ser34, Asp70 and Glu124 were added in the inner layer.

Table 23 Binding energies (BE), Interaction energies (INT), Deformation energies (DEF) from ONIOM2(B3LYP/6-31G(d):PM3) calculations (in kcal/mol) of SAH cofactor

	ONIOM 2H	ONIOM 2N	ONIOM 2K	ONIOM 2O
BE	-52.26	-51.26	-54.62	-63.40
INT	-100.12	-98.48	-105.78	-117.37
DEF	47.86	47.21	51.16	53.98
DEF(L)	30.38	29.36	29.93	31.24
DEF(P)	17.48	17.86	21.23	22.74

In addition, Thr32, Ser34, Asp70, Glu124, three water molecules with the SAM cofactor were defined in ONIOM 2X, and compared with ONIOM 2R as shown in Table 24. A different binding energies, of about 24 kcal/mol in observed, mostly comes from the interaction energy (30.85 kcal/mol), with a smaller contribution from the deformation energy (7.06 kcal/mol). It implies that increasing a number of residues in the inner layer of ONIOM model for SAM system affects the energies more than that found in the SAH system. From these results can be concluded that only the cofactor and water molecules in high level of calculation is an alternative representative for the model system while the rest of residues can be included in the low level of calculation.

Table 24 Binding energies (BE), Interaction energies (INT), Deformation energies (DEF) from ONIOM2(B3LYP/6-31G(d):PM3) calculations (in kcal/mol) of SAM cofactor.

	ONIOM2R	ONIOM 2X
BE	-111.98	-135.77
INT	-176.00	-206.85
DEF	64.02	71.08
DEF(L)	43.58	47.21
DEF(P)	20.44	23.87

Table 25 Summary of Energies of 25 ONIOM models (in kcal/mol), calculated by B3LYP/6-31G(d):PM3

	HIGH			LOW		BE	INT	DEF	DEF(L)	DEF (P)
ONIOM 2A	PYR-SAH(N)	Glu124		Rest Residues		-12.67	-28.26	-15.59	9.28	6.31
ONIOM 2B	PYR-SAH(Z)	Glu124		Rest Residues		-51.22	-73.4	22.19	13.88	8.31
ONIOM 2C	PYR-SAH(N)	Glu124	$3H_2O$(F)	Rest Residues		-9.38	-28.42	19.04	10.65	8.39
ONIOM 2D	PYR-SAH(Z)	Glu124	$3H_2O$(F)	Rest Residues		-53.48	-94.49	41.01	18.40	22.61
ONIOM 2E	PYR-SAH(N)	Glu124		Rest Residues	$3H_2O$(F)	-57.10	-94.46	37.35	18.40	18.96
ONIOM 2F	PYR-SAH(N)	Glu124	$3H_2O$(R)	Rest Residues		-11.07	-30.13	19.06	10.59	8.48
ONIOM 2G	PYR-SAH(Z)	Glu124	$3H_2O$(R)	Rest Residues		-56.98	-95.23	38.25	18.85	19.40
ONIOM 2H	SAH(Z)		$3H_2O$(F)	Rest Residues		-52.26	-100.12	47.86	30.38	17.48
ONIOM 2I	SAH(Z)			Rest Residues	$3H_2O$(F)	-43.74	-86.79	43.05	29.18	13.87
ONIOM 2J	SAH(Z)	Glu124		Rest Residues		-34.70	-70.74	36.04	27.25	8.79
ONIOM 2K	SAH(Z)	Glu124	$3H_2O$(F)	Rest Residues		-54.62	-105.78	51.16	29.93	21.23
ONIOM 2L	SAH(Z)	Glu124		Rest Residues	$3H_2O$(F)	-45.99	-92.56	46.57	29.06	17.50
ONIOM 2M	SAH(Z)	Asp70		Rest Residues		-27.47	-57.92	30.46	25.54	4.92
ONIOM 2N	SAH(Z)	Asp70	$3H_2O$(F)	Rest Residues		-51.26	-98.48	47.21	29.36	17.86
ONIOM 2O	SAH(Z)	Thr32 Ser34 Asp70 Glu124	$3H_2O$(F)	Rest Residues		-63.40	-117.37	53.98	31.24	22.74
ONIOM 2P	SAH(Z)	Thr32 Ser34 Asp70 Glu124	$3H_2O$(R)	Rest Residues		-67.05	-120.80	53.75	31.75	22.00
ONIOM 2Q	SAM(Z)			Rest Residues		-86.77	-135.83	49.06	41.15	7.91
ONIOM 2R	SAM(Z)		$3H_2O$(F)	Rest Residues		-111.98	-176.00	64.02	43.58	20.44
ONIOM 2S	SAM(Z)			Rest Residues	$3H_2O$(F)	-100.87	-159.54	58.67	42.23	16.44
ONIOM 2T	SAM(Z)			Rest Residues	$5H_2O$(F)	-102.99	-166.36	63.37	43.02	20.35
ONIOM 2U	SAM(Z)			Rest Residues	$5H_2O$(R)	-102.04	-169.28	67.24	43.86	23.38
ONIOM 2V	SAM(Z)	Asp70		Rest Residues		-87.87	-135.84	47.98	40.75	7.23
ONIOM 2W	SAM(Z)	Asp70	$5H_2O$(F)	Rest Residues		-124.95	-198.69	73.74	46.56	27.18
ONIOM 2X	SAM(Z)	Thr32 Ser34 Asp70 Glu124	$3H_2O$(F)	Rest Residues		-135.77	-206.85	71.08	47.21	23.87
ONIOM 2Y	Sinefungin		$3H_2O$(F)	Rest Residues		-119.41	-180.57	61.17	38.99	22.18

Quantum Chemical Calculations on Succinate dehydrogenase/ Substrate-Inhibitor Interactions

1. Ligand-Enzyme Interaction

The present studies are concerned with the effect of the substrate upon the respiration cycle of succinate dehydrogenase in the TCA cycle. The calculated interaction energies between substrate, succinate and inhibitor, 3-nitropropionate (structural orientation from X-ray) to each residue that surrounds the binding pocket are shown in Table 26, In this calculation succinate and 3-nitropropinonate are charged forms will minus two charge for succinate and minus one for 3-nitropropionate, respectively. The calculation demonstrates that there are more attractive interactions between both ligands with residues surrounding the substrate binding pocket for SDH, especially, the interactions with Arg409 and Arg298. However, considering attractive interactions, it is found that the total interactions energies indicate that attractive interactions play a significant role of carboxylate ligands in the binding site. It is important to note that the main contribution is due to the electrostatic interaction and two hydrogen bonds. Considering hydrogen bond distance show that hydrogen bond distance between Arg409 and carboxylate group of succinate is shorter than for 3-nitropropionate (1.78 and 2.01,respectively). For the Arg298 residue, no hydrogen bond is detected. However, this residue is positioned as a acid-base catalyst abstracting a proton for succinate to fumarate conversion.(Huang *et al.*, 2006) A largely repulsive energy of Glu267 is due to nearest distance between residue and ligand. Moreover, this repulsion comes from interaction between negative charge of Glu267 and the carboxylate of succinate or 3-nitropropionate.

Table 26 Particular interaction energies of succinate and 3-nitropropionate with individual residues (in kcal/mol) calculated by MP2/6-31G(d) with BSSE-CP methods Interaction energies (INT)

Residues	Succinate	3-Nitropropionate
Ala61	-4.03	-1.37
Gln62	-11.56	-3.18
Gly63	-9.69	-4.03
Gly64	0.77	0.56
Phe131	-10.98	-0.71
Gln252	-18.68	-18.77
Phe253	0.77	0.68
His254	-2.50	1.35
Leu264	-5.41	-2.28
Ile265	-0.22	1.55
Thr266	-27.12	0.63
Glu267	90.92	60.67
Gly268	-8.25	-3.01
Arg298	-115.47	-70.94
His365	3.44	9.55
Tyr366	-1.41	-0.82
Arg409	-162.34	-94.00
Leu410	-0.78	-0.68
Gly411	-7.72	-1.76
Ala412	-8.6	-3.28

2. ONIOM Calculation

Conversion of succinate to fumarate by succinate dehydrogenase relates to transfers of two electrons of succinate to the FAD. Therefore, an investigation of succinate and 3-nitropropionate in the substrate binding site was performed in this study, FAD is included in the system. First of all, we perform two approachs, heteroatom fix (HAF) and back bone fix (BBF) to find an appropriate methodology.

2.1 The susceptibility of HAF and BBF Methodology

Investigation For effect of HAF and BBF methodology, system comprises succinic and residues with in 7Å show similar interaction energy with ΔE 0.03 kcal/mole while the zwiiter ionic of succinic give quite different energy with ΔE about 15.35 kcal/mole that calculated using ONIOM2 with B3LYP/6-31G(d):PM3 method. This different energy might be from relaxation of side chain of amino acid taken effect to interaction of systems. However, the calculations of this system were studied using BBF methodology to investigate interaction of ligand and inhibitor with succinate dehydrogenase enzyme in order to have an unbiased structure of residues surrounding succinate binding site.

2.2 Search for Basis Set

Density functional theory hybrid B3LYP with three basis sets, polarization only heavy atom 6-31G(d), polarization both heavy atom and hydrogen atom 6-31G(d,p) and diffusion 6-31G+(d,p) have been used for calculations. In this ONIOM systems, 3-nitropropionate and flavin are treated in high level with B3LYP and rest residues and rest FAD cofactor are treated with PM3 methods. Because all residues are set up at pH 7.0, some residues such as Arg or Glu are ionized. In accuracy, the calculation could be performed with diffusion of basis set. However, cost of calculation also important. Interaction energy of these systems are -60.40, -63.52 and -63.35 kcal/mol with 6-31G(d), 6-31G(d,p) and 6-31+G(d,p), respectively. The same model of succinate shows similar trend with 3-nitropropionate. Thus, in next studies in this system at least basis set is 6-31G(d,p) that can represent for diffuse function of basis set.

2.3 Comparison interaction energy between succinate and 3-NP

Four models of succinate and 3-nitropropionate are set up as shown in Figure 32. The calculated interaction energy of model A, B, C and D are -143.93,

-155.64, -61.77, -63.52, kcal/mol, respectively. The data suggests that succinate complexed with substrate binding site has quite stabilize it structure than 3-nitropropionic. Interesting results of 3-nitropropinate, structure of 3-nitropropionate from ONIOM calculation adopt it structure, nitrogen sp^3 of 3-nitropropionate geometry from x-ray crystal to planar nitrogen. However, the interaction significant different between succinate and 3-nitropropionate, the hydrogen bonding detected are similar. The carboxylate of the ligands form a salt bridge with guanidinium group of Arg409 with bond distance 1.79 and 1.72 Å for succinate and 1.76 and 1.81 Å for 3-nitropropionate. Additional hydrogen bonding is Glu267. Nitro group of 3-nitropropionate is formed hydrogen bond with 1.90 Å, while another carboxylate group of succinate form is formed hydrogen bond with 1.76 Å as shown in Figure 33 . Inspire of including flavin of FAD into high region of ONIOM2, interaction energy of system not significantly different in 3-nitropropinate system. On the other hand, ΔE is about 10 kcal/mol in succinate system. It is import that succinate interacts with flavin, which is reduced by the addition of two hydrogen atoms to become FADH2 while 3-nitropropinate not involve in this reaction. Then, 3-nitropropionate is a respectable inhibitor in succinate dehydrogenase confirmed by this calculation.

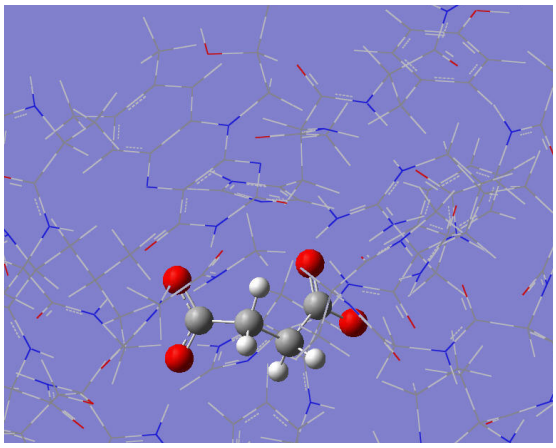

Model A High : Succinate
Low : Rest residues + Flavin

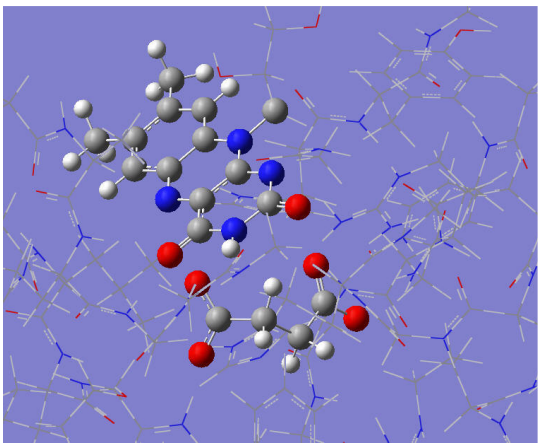

Model B High : Succinate + Flavin
Low : Rest residues

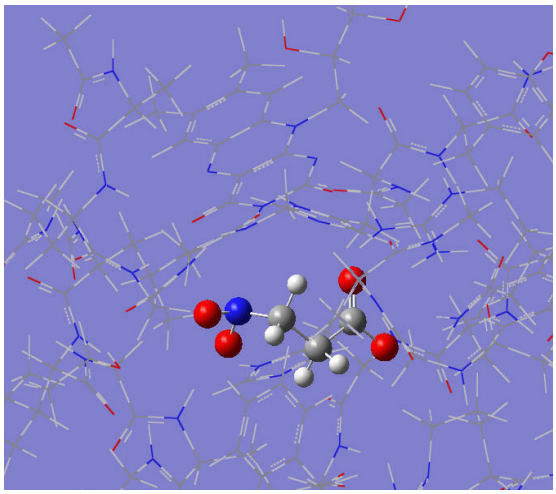

Model C High : 3-Nitropropionate
Low : Rest residues + Flavin

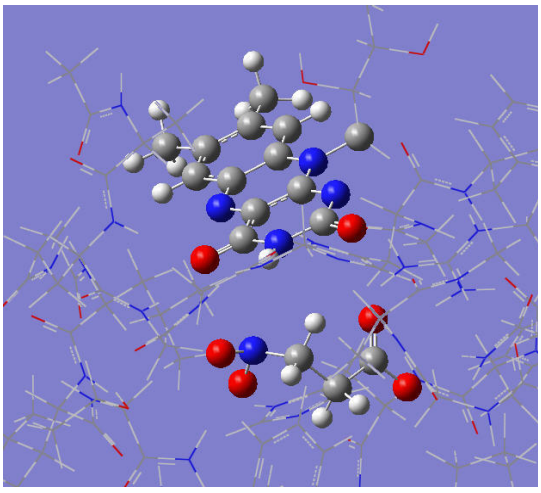

Model D High : 3-Nitropropionate + Flavin
Low : Rest residues

Figure 32 Two layer ONIOM system, model A and B for succinate system and model C and D for 3-nitropropionate system

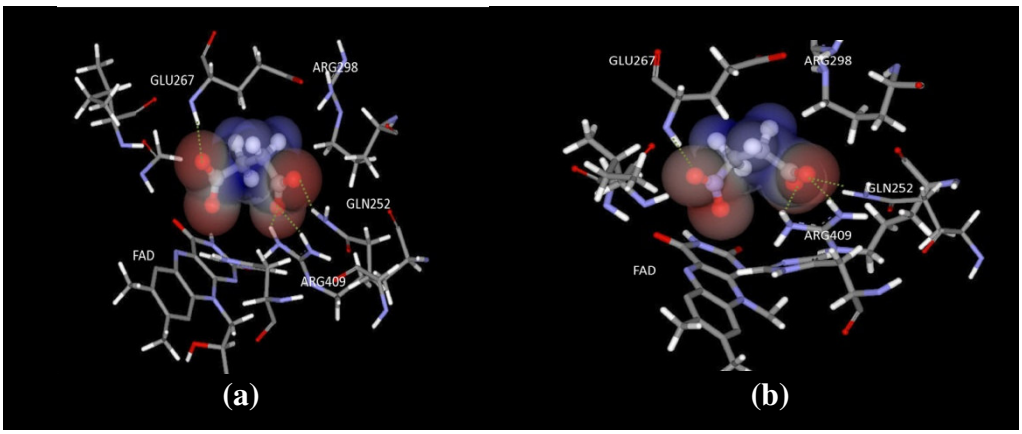

Figure 33 Bound complex conformations of succinate (a) and 3-nitropropionate (b) including hydrogen bonding with key residues.

Role of Key Residues Specific to Cyclooxygenase II

1. Inhibitor-enzyme interaction

1.1 Identify method

Two methods of calculations, B3LYP with 6-31G(d) and 6-31G(d,p) and MP2 with 6-31G(d) basis sets were applied. The calculated interaction energies between neutral forms of flurbiprofen to each residue in the neutral system of binding pocket are shown in Table 27. The results demonstrate that B3LYP/6-31G(d) and B3LYP/6-31G(d,p) do not present significantly different interaction energies with ΔE less than 0.12 kcal/mol. These results show that the polarization of hydrogen atoms does not affect the system. Therefore, 6-31G(d) basis set was employed in next calculations on this system. On the contrary, B3LYP and MP2 methods give different energy with range between 0.6 – 4.6 kcal/mol. Anyway, the results from two different theories lead to the same flurbiprofen key residues, Arg120 and Tyr355 important for attractive and repulsive interaction, respectively. Considering Ala527 residue, it performs opposite trend between B3LYP and MP2 calculations showing higher repulsive interaction with B3LYP whereas attractive interaction with MP2. However, in this study we select MP2 method to deeply understand the interaction of inhibitor-enzyme as this methods sensitive for H---π interaction as *Kuno et al*. proposed (Kuno *et al.*, 2006).

Table 27 Interaction energies (INT) of neutral form of flurbiprofen with individual amino acids (X_i) in the neutral system (in kcal/mol), calculated at the B3LYP/6-31G(d), B3LYP/6-31G(d,p) and MP2/6-31G(d) level of theory

	Interaction energies (kcal/mol)		
	B3YLP		MP2
	6-31G(d)	6-31G(d,p)	6-31G(d)
Val116	3.13	3.05	2.50
Arg120	-2.70	-2.58	-3.97
Val349	3.75	3.72	-0.09
Leu352	0.53	0.53	-1.33
Ser353	0.26	0.27	-0.96
Tyr355	5.30	5.30	3.45
Leu359	3.07	2.95	2.27
Tyr385	3.58	3.48	1.77
Met522	-0.35	-0.32	-1.24
Val523	0.67	0.71	-1.44
Gly526	0.18	0.18	-1.09
Ala527	2.61	2.58	-1.96
Ser530	0.32	0.34	-1.62
Leu531	1.20	1.15	-1.38

1.2 Particular interaction energy of flurbiprofen with COX-2 binding site

The result of the calculate of the particular interaction of neutral form of flurbiprofen to each residue in the binding pocket using MP2/6-31G(d) are given in Table 27. From the consideration on attractive interactions, it appears that the total interactions energies indicate that attractive interaction plays significant role for flurbiprofen in the binding site. It is important to note that the main contributions are due to the interaction with Arg120 as indicated by the interaction energy of about -3.97 kcal/mol. In addition, Val523 is also contributed as shown by the interaction energy about -1.44 kcal/mol. However, there are more repulsive interactions especially with Tyr355 and Val116 (3.45 and 2.50 kcal/mol, respectively). A graphical representation of attractive and repulsive interaction of flurbiprofen with COX2 binding site is shown in Figure 34.

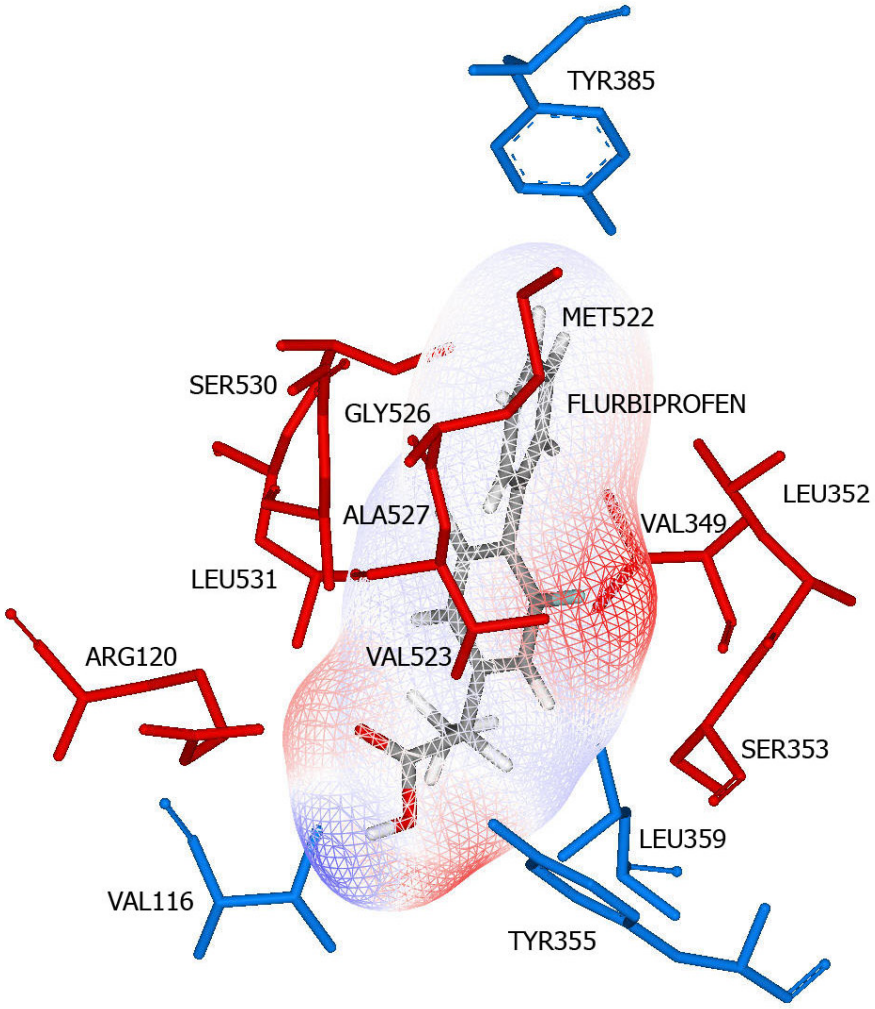

Figure 34 Attractive interactions (red) and repulsive interactions (blue) of flurbiprofen with individual residue (X_i)

1.3 State of flurbiprofen in COX-2 binding pocket

Two forms of flurbiprofen, neutral and ionic states, were investigated. As a result, the ionic form of the inhibitor gives higher interaction than the neutral form of flurbiprofen with Arg120. This large different interact comes from the Coulomb attraction caused by the positively charged guanidinium cation and negatively charged carboxylate of flurbiprofen.

1.4 Comparison energies of the interaction of flurbiprofen with COX-1 and COX-2

In addition, we set up systems using the neutral system of residues surrounding flurbiprofen to compare interactions with two COX isoforms. The calculated results obtained from MP2/6-31G(d) method are shown in Table 28. Large different interaction energies between COX-1 and COX-2 come from the Arg120 residue interactioning with a ΔE value of about 8.0 kcal/mol. This result is consistent with X-ray data where, Arg120 is the key residues in the COX active site. Flurbiprofen with Arg120 in COX-1 performs stronger interaction than the COX-2 due to appropriate orientation of the carboxylic group of flurbiprofen and the guanidine side chain of Arg120 with two hydrogen bonds (1.80 and 1.86 Å). Tyr385 shows an opposite trend in COX-1 and COX-2. In COX-1, flurbiprofen gives energetically favorable attractive interaction with this residue (-1.94 kcal/mol) whereas COX-2 shows repulsive interaction (1.77 kcal/mol). Considering Tyr355 residue, COX-2 enzyme provides higher repulsive interaction than COX-1 about 2 kcal/mol. The last residue that shows different interaction energy is found to be Ser530. Complexed of flurbiprofen with Ser530 in COX-2 enzyme gives higher attractive energy than in the complex in COX-1 of about 1.61 kcal/mol. Van der Waals surfaces of three residues are show in Figure 35, the orientation of the hydroxyl group of tyrosyl are difference affect on the energy of this complexes. Even COX-1 and COX-2 have different amino acid such as at position 523, their interaction energies with at their will perform quite similar energy between Ile in COX-1 and Val in COX-2 with flurbiprofen.

Table 28 Interaction energies (INT) of the neutral form of flurbiprofen with individual amino acids (X_i) in the neutral system (in kcal/mol) of COX-1 and COX-2 binding pocket, calculated MP2/6-31G(d) level of theory.

	Interaction energies(kcal/mol)	
	COX-1	COX-2
Val116	1.85	2.50
Arg120	-12.04	-3.97
Val349	-0.86	-0.09
Leu352	-1.23	-1.33
Ser353	-0.84	-0.96
Tyr355	1.90	3.45
Leu359	-0.17	2.27
Tyr385	-1.94	1.77
Met522	-1.49	-1.24
Ile/Val523	-1.57	-1.44
Gly526	-1.71	-1.09
Ala527	-1.98	-1.96
Ser530	-0.01	-1.62
Leu531	-1.35	-1.38

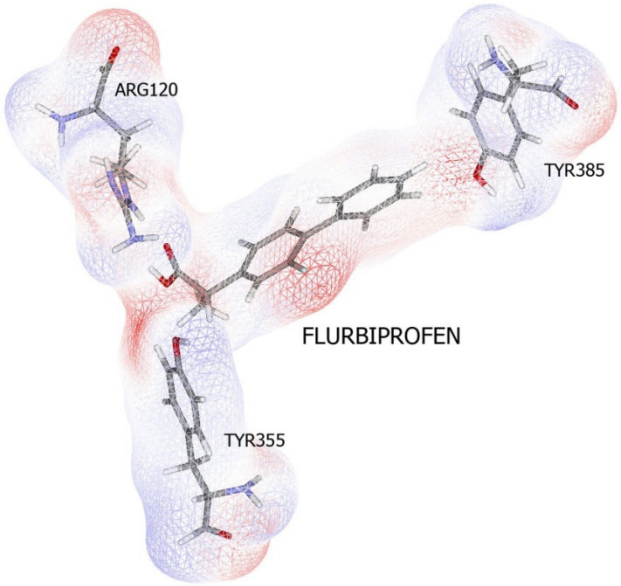

(a)

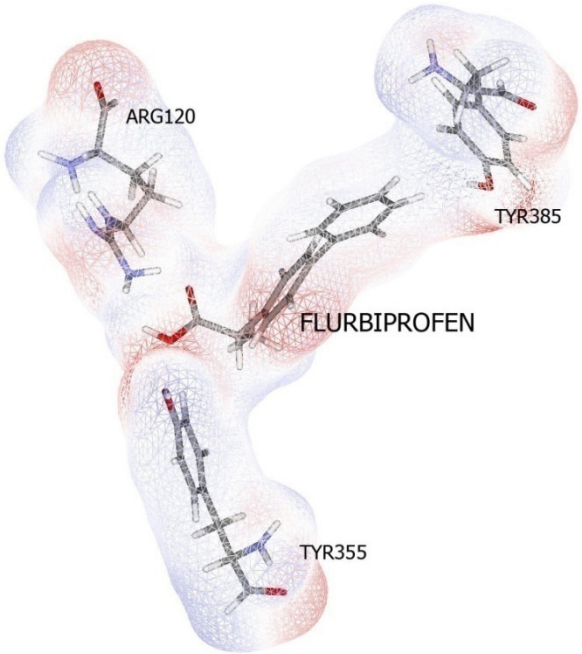

(b)

Figure 35 Van der Waals surfaces of flurbiprofen with Arg120, Tyr355, Tyr385 in COX 1 (a) and in COX-2 (b).

1.5 Effect of neutral and ionic system in COX-2

Surrounding residues of flurbiprofen within 6 Å were divided into two systems, neutral and charged environment at pH 7.0 to compare the effect of states of the residues in the binding site. Our results (see Table 29) provide that all of residues do not represent significantly different energies with ΔE less than 0.3 kcal/mol. In exception, Arg120 shows dramatically different interaction energies with -3.97 and -9.36 kcal/mol for neutral and charged environments, respectively. As a result, the ionic system of COX-2 binding site provides stronger interaction with flurbiprofen than the neutral system. Although the results give different values in two systems, Arg120 is an important residue which shows significantly different interactions from others residues.

Table 29 Interaction energies (INT) of the neutral form of flurbiprofen with individual amino acids (X_i) (in kcal/mol) in neutral and ionic system in COX-2 binding pocket, calculated MP2/6-31G(d) level of theory.

	Interaction energies with different of COX-2 binding site (kcal/mol)		
	Neutral	Ionic	ΔE
Val116	2.50	0.21	2.29
Arg120	-3.97	-9.36	5.39
Val349	-0.09	-0.14	0.05
Leu352	-1.33	-1.33	0.00
Ser353	-0.96	-0.96	0.00
Tyr355	3.45	3.08	0.37
Leu359	2.27	3.24	-0.97
Tyr385	1.77	1.70	0.07
Met522	-1.24	-1.22	-0.02
Val523	-1.44	-1.41	-0.03
Gly526	-1.09	-0.83	-0.26
Ala527	-1.96	-1.97	0.01
Ser530	-1.62	-1.57	-0.05
Leu531	-1.38	-1.41	0.03

1.6 Comparison of the interaction energies between flurbiprofen and SC558 with COX-2

Structures of flurbiprofen and SC558 are roughly equivalent in the binding site as the fluorphenyl ring of flurbiprofen overlaps with the bromophenylring of SC558. The sulphonamide moiety of SC558 attached to pyrazole ring lead to the selective of the inhibitor. Arg120, Tyr355, Leu359, Val523 and Glu524 residues show widely different interaction energies between flurbiprofen and SC558 (see Table 30). There is more attractive interaction between flurbiprofen with Arg120 while Tyr355 favorably interacts with SC558 in comparison to flurbiprofen. Considering, the Val523 residue, it shows a selective with the sulphonyl phenyl ring of SC558. These results indicate clearly that SC558 can bind to COX-2 better than flurbiprofen. However considering attractive interactions, it was found that the total interaction energies indicate that attractive interaction plays significant role of both inhibiters.

Table 30 Interaction energies (INT) of flurbiprofen and SC558 with individual amino acids (X_i) (in kcal/mol) in the ionic system of COX-2 binding pocket, calculated by MP2/6-31G(d) level of theory.

	Interaction energies (kcal/mol)	
	Flurbiprofen	SC558
His90	0.04	3.30
Val116	0.21	-0.54
Arg120	-9.36	-3.87
Gln192	-0.05	1.98
Val349	-0.14	-0.83
Leu352	-1.33	1.54
Ser353	-0.96	-2.17
Gly354	-0.10	-0.57
Tyr355	3.08	-3.63
Leu359	3.24	-0.51
Tyr385	1.70	2.66
Trp387	-0.76	-0.09
Arg513	-0.58	21.45
Ala516	-0.03	-1.41
Ile517	-0.07	-1.80
Phe518	-0.56	4.47
Gly519	0.03	-0.81
Met522	-1.22	-1.79
Val523	-1.41	1.57
Gly526	-0.83	-0.82
Ala527	-1.97	-0.67
Ser530	-1.57	-0.86
Leu531	-1.41	-0.48

2. ONIOM calculations

2.1 Neutral system

The main focus of our study is the specific interaction the flurbiprofen with Arg120, Tyr355 and Val 523, respectively. The results of binding energies obtained from ONIOM2 calculations are given in Table 31. The results show that the binding energies of flurbiprofen/Arg120 are higher than that for flurbiprofen/Val523. This suggests that the effect of hydrogen bonding between hydroxyl carboxylic group of flurbiprofen and guanidine group of Arg120 causes stronger interaction. The length of hydrogen bond distances are 2.24, 2.28, 1.97 and 1.99 Å for model A, model B, model C and model D, respectively, whereas no hydrogen bonding was observed between Tyr355 and flurbiprofen.

Table 31 Binding energies and bond distances of flurbiprofen bound to Arg120, Tyr355 and Val523 in the COX-2 binding pocket, together with Hydrogen bond distances.

ONIOM2 method	Binding energy (kcal/mol)			Bond distance (Å)	
	Arg120	Tyr355	Val523	N_{Arg120}--H-O_{FLP}	O_{Tyr355}--H-O_{FLP}
Model A	-9.49	-10.75	-9.33	2.243	4.169
Model B	-9.83	-8.61	-9.37	2.279	4.176
Model C	-12.97	-11.48	-10.38	1.973	4.096
Model D	-12.53	-13.63	-10.30	1.988	4.091

The results from Table 31 show in case of the interaction between flurbiprofen and Tyr355 that the bond distance between O_{TYR355}--H-O_{FLP} from the model D is longer than that observed in X-ray crystallographic structure (3.09 Å) for about 1.4 Å. This result indicates no hydrogen bond formation between the side chain of tyroxyl of Tyr355 and flurbiprofen (see Figure 36). In addition, it is known that the significant

difference between COX-1 and COX-2 is the difference at position 523, Ile in COX-1 and Val in COX-2.

Deletion of a methylene group at 523 in COX-2 allows access to an additional pocket. Considering van der Waals interactions between Val523 and flurbiprofen implies that this interaction might not be significant to the binding with COX-2. Therefore, selective COX-2 inhibitor exploits the additional pocket for enhanced binding through the sulphonamide or methylsulfone moiety that a clearly different for selective COX-2 inhibitor in compares to non-selective COX inhibitor.

Moreover, the four models of ONIOM2 results can also provide the suggestion to select the combined method between high and low level of calculations. The lower level of calculations that could be combined with the B3LYP/6-31G(d) is PM3 from the significantly binding energies and hydrogen bond distances. However, the combination with other higher levels of calculations can also be considered to get more information on particular interactions.

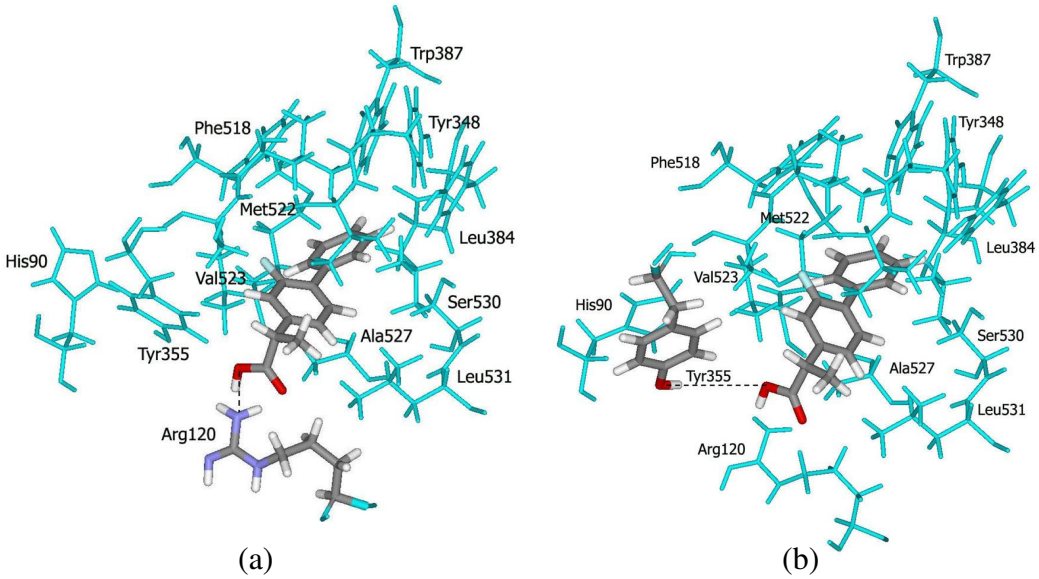

Figure 36 Hydrogen bonding between flurbiprofen/Arg120 (a) and flurbiprofen/Tyr355 (b), obtained from model D.

2.2 Comparison neutral and ionic system

The aim of this study is to compare the interaction of flurbiprofen with two state of COX-2 binding site, neutral and ionic residues environment. The combine ONIOM2(B3LYP/6-31G(d) with PM3 was used to calculate two different state on the same criteria environment.

2.2.1 Interaction of Arg120 with flurbiprofen

First for the neutral system, flurbiprofen in neutral form and Arg at position 120 were included at high level of ONIOM while the other rest residues were calculated at low level. Second ionic system, flurbiprofen in ionic form and Arg at position 120 (positively charged) were included in high level of ONIOM while the other rest residues were calculated at low level. The calculated results show that the ionic system gives strong binding interaction between flurbiprofen with its pocket. (see Table 32). Considering hydrogen bonding interactions, the ionic system performs shorter hydrogen bond distances of about 1.68(2.65) and 1.98(2.69) Å. For the neutral system hydrogen bond distances of about 1.97(2.90) Å are obtained, while structure from x-ray crystal data provides hydrogen bond distance (2.96Å) where the value data in parentheses are the intermolecular distance between hetero atom of the hydrogen bond donors and hetero atoms of the hydrogen bond acceptor. A superimposition of neutral, ionic system and x-ray structure is shown in Figure 37.

Table 32 Binding energies of flurbiprofen bound to Arg120, Tyr355 and Val523 in the COX-2 binding pocket in neutral and ionic states (in kcal/mol), calculated by ONIOM(B3LYP/6-31G(d):PM3) method

States	**Inner layer**	Flurbiprofen Arg120	Flurbiprofen Tyr355	Flurbiprofen Val523
	Outer layer	Rest residues	Rest residues	Rest residues
Neutral		-12.97	-11.48	-10.38
Ionic		-102.58	-34.72	-42.15

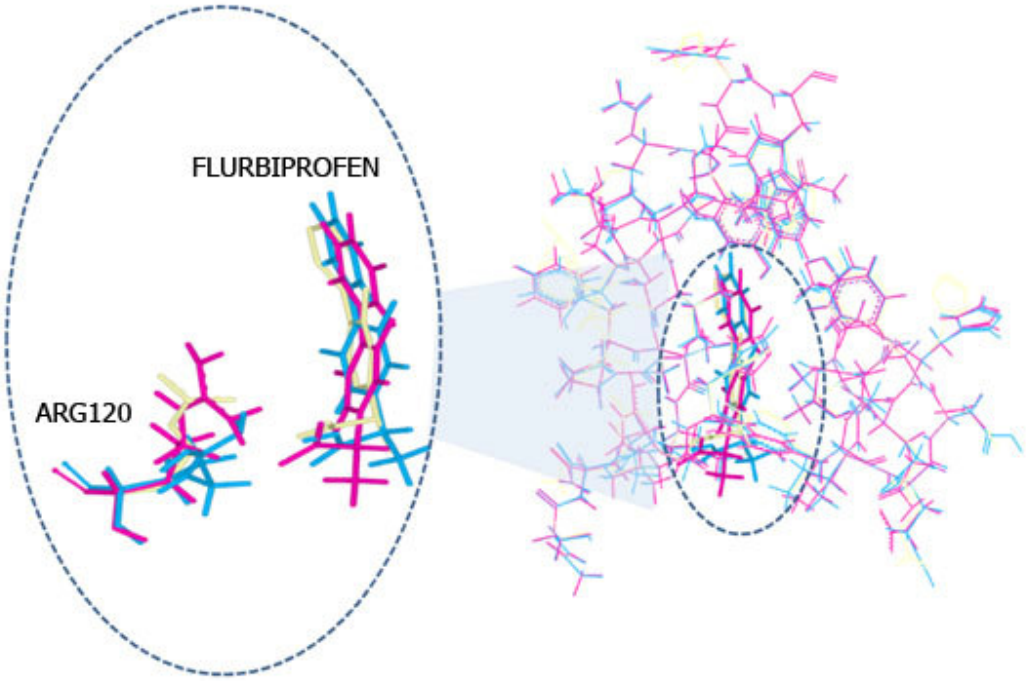

Figure 37 Superimposition structures of neutral system (in blue color), ionic system (in red color) and X-ray structure (in yellow color) in ONIOM2 system which Arg120 and flurbiprofen located in inner layer and rest residues located in outer layer.

2.2.2 Interaction of Tyr355 with flurbiprofen

Calculation of Tyr355 and flurbiprofen in ionic system gives hydrogen bonding between the carboxylate of inhibitor and the hydroxyl group of the tyrosine residue with a distance of which 1.77(2.76) Å, while neutral system does not show any hydrogen bonding. Considering binding energies of the ionic system shows over estimating same as in Arg120/flurbiprofen ONIOM system.

2.2.3 Interaction of Val523 with flurbiprofen

The largest binding energy of this system comes from the interaction with Arg120 included in the low layer. Hydrogen bonding is not detected

between flurbiprofen and Val523 in both systems because this residue is specific for selective COX-2 inhibition. Finally, the comparison of energies of all three above systems between neutral and ionic state can implied that ionic system gives higher binding energies. This reason may arrive from electrostatic interaction between charge-charge of pair ligand and residue that we will investigate in further work.

2.3 Comparison of Interactions between flurbiprofen and SC558

Comparing the structures of flurbiprofen, a non selective COX inhibitor, and SC558, a selective COX-2 inhibitor, show rough equivalents in binding site with the fluorphenyl ring of flurbiprofen overlapping with the bromophenylring of SC558. Different by the sulphonamide of SC558 attached to pyrazole ring introduces the selectively of this inhibitor. The optimized structure of 32 amino acids residues was performed on these different structures. Firstly, the calculated interaction energies between flurbiprofen and SC558 to each residue that surrounds the binding pocket were compared as shown in Table 33.

Main distribution of comparing systems are Arg120, Tyr355 and Val523.The Arg120 position is a long channel cavity where Tyr355 has a position near Val523 which has a larger pocket on COX-1. There are more attractive interactions between flurbiprofen with Arg residues while Tyr355 interacts with SC558 more than flurbiprofen. The Val523 residue show selective interaction with sulphonyl phenyl ring of SC558. The interactions with Arg120 and Tyr355 with flurbiprofen and SC558 are -6.13 and -1.86 kcal/mol and for Arg120, 1.23 and -5.33 for Tyr355, respectively. These results indicate clearly that SC558 can bind to COX-2 better than flurbiprofen. However, consideration on attractive interactions, it was found that the total interactions energies indicate that attractive interaction play significant role of both inhibiters.

Table 33 Interaction energies (INT) of flurbiprofen and SC558 with surrounded residues, calculated by B3LYP/6-31G(d, p) method (in kcal/mol).

Residues	Flurbiprofen	SC558
Met113	0.08	-0.92
Val116	0.84	-1.39
Arg120	-6.13	-1.86
Tyr348	0.20	-0.40
Val349	2.15	-0.82
Leu352	-0.20	6.38
Ser353	0.07	-0.50
Tyr355	1.23	-5.33
Leu359	3.67	-1.72
Phe381	-0.57	-1.66
Leu384	-0.12	-1.44
Trp387	-0.23	-1.82
Phe518	-0.15	4.33
Met522	-1.38	-2.82
Val523	-2.79	2.63
Ala527	-0.03	-0.36
Ser530	-1.61	-1.56
Leu531	-0.69	-1.56

However, ONIOM study are picked up to understand the interaction at the Tyr 355 position with show the highest interaction energy with SC558. In the Figure 38, the hydrogen bonding interactions between SC558 and Tyr355 are shown, as indicated by the $O\text{-}H_{Tyr355}\text{--}F_3C_{SC\text{-}558}$ distance of about 2.3 Å whereas no hydrogen bonding observed in flurbiprofen. The obtained results can be explained for the selectivity of the SC558 inhibitor to the COX-2 enzyme.

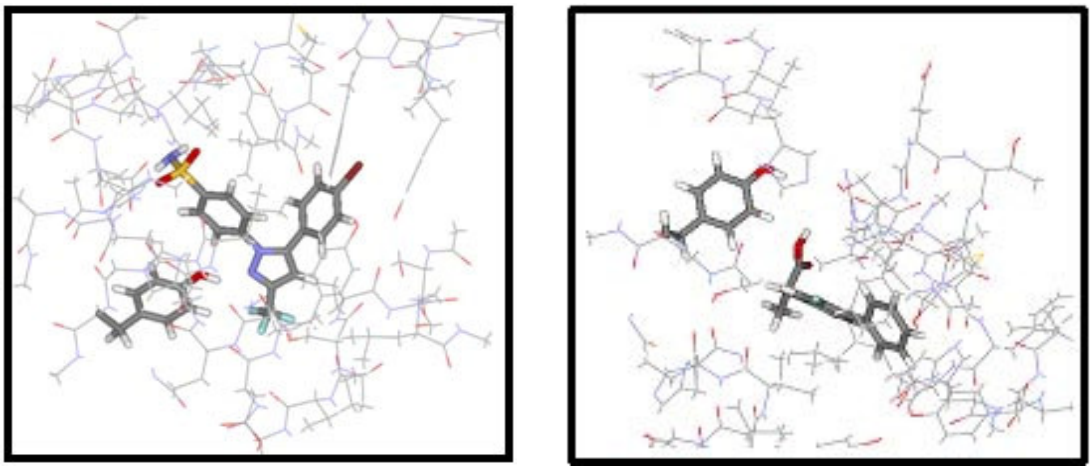

(a) **(b)**

Figure 38 The two layers in the ONIOM model. The high level of calculation represented in stick with SC558/Tyr355 residue (a), flurbiprofen Tyr355 residue (b) and the low level of calculation represented in line.

In order to study why flurbiprofen is not selective in COX-2, the interaction of flurbiprofen between COX-1 and COX-2 was calculated in charged environment of residues at pH 7.0 and the results are given in Table 34. In addition, we set up a system using the neutral form of amino acids with flurbiprofen. Largely different interaction energies between COX-1 and COX-2 were obtained from the interaction of the key residue Arg120. Later a residue is Tyr355 shows different interaction energies of about 2 kcal/mol. On the contrary, Tyr385 shows opposite trend in COX-1 and COX-2. In COX-1, flurbiprofen shows attractive interaction with this residue of about -2 kcal/mol) while in COX-2 shows a repulsive interaction.

Table 34 Particular interaction energies between flurbiprofen with COX1 and COX2, calculated by MP2/6-31G (d,p) with BSSE-CP methods (in kcal/mol).

Residues	COX-1	COX-2	ΔE
Ile/Val89	-0.02	-0.01	0.01
His90	0.11	0.05	-0.06
Phe/Typ91	0.02	0.01	-0.01
Val/Ser119	-0.04	0.17	0.21
Arg120	-12.04	-3.97	8.07
Ser121	-0.09	-0.07	0.02
Ile345	-0.17	-0.26	-0.09
Glu346	0.00	0.02	0.02
Glu/Asp347	0.02	0.03	0.01
Tyr348	-0.48	-0.17	0.31
Val349	-0.86	-0.09	0.77
Gln350	-0.20	-0.31	-0.11
Gln/His351	-0.06	-0.09	-0.03
Leu/Ile352	-1.23	-1.33	-0.10
Ser353	-0.84	-0.96	-0.12
Gly354	-0.07	-0.10	-0.03
Tyr355	1.90	3.45	1.55
Leu384	-0.37	-0.51	-0.14
Tyr385	-1.94	1.77	3.71
His386	0.03	0.02	-0.01
Trp387	-0.37	-0.77	-0.40
Phe518	-1.03	-0.55	0.48
Gly519	0.02	0.02	0.00
Glu520	-0.08	0.02	0.10
Ser/Thr521	-0.05	-0.02	0.03
Met522	-1.49	-1.24	0.25
Ile/Val523	-1.57	-1.44	0.13
Ala527	-1.98	-1.96	0.02
Pro528	-0.48	-0.55	-0.07
Phe529	-0.34	-0.45	-0.11
Ser530	-0.01	-1.62	-1.61
Leu531	-1.35	-1.38	-0.03

From the van der Waals surface shown in Figure 39, it can been seen that the orientation of hydroxyl group of tyroxyl are different affecting the energy of this complex. Moreover, the calculation of position 523, the different residue within active site of the inhibitor, gave similar energies between Ile in COX-1 and Val in COX-2.

The total energies of interaction between residues within 7 Å of COX-1 and COX-2 are -25.06 and -12.29 kcal/mol, respectively.

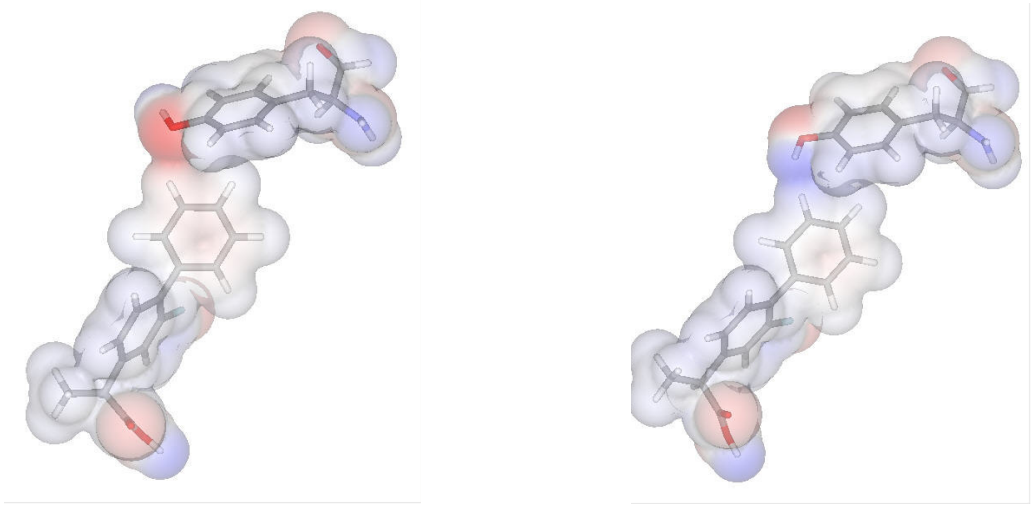

(a) **(b)**

Figure 39 Van der Waals surface of (a) flurbiprofen with Tyr355 in COX-1 and (b) flurbiprofen with Tyr355 in COX-2.

CONCLUSIONS

Quantum Chemical Calculation and ONIOM Study of *S*-adenosyl-L methionine and *S*-adenosyl-L-homocysteine Cofactors of Cyclopropane Synthase in *M.tuberculosis*

The interaction energies of the cofactor in the methylation with the cyclopropane synthase, S-adenosyl-L-methionine (SAM), S-adenosyl-L-homocysteine (SAH), and sinefungin have been calculated by B3LYP/6-31G(d), B3LYP/6-31G(d,p) and MP2/6-31G(d). Consistent data trends results for B3LYP and MP2 methods and similar quality by 6-31G(d) or 6-31G(d,p) basis sets with B3LYP method. For the interaction results, the important residues are found to be Asp70 and Glu121 in which SAM shows a stronger interaction than sinefungin and SAH, respectively, by cutting the cofactor molecule into fragments was performed to investigate the role of residues in each of the fragments of the cofactor, adenine, ribose, sulfur and amino moieties. The results show that Glu124 residue plays an important role for the interacting with adenine moiety while no residues had any effect on the ribose moiety. Considering the sulfur moiety, this fragment presents largely different in energies between SAM and SAH. At last, the amino fragment establishes hydrogen bond linkage with Asp70 and water molecules. Moreover, twenty five systematic ONIOM2 calculations were performed with B3LYP/6-31G(d,p):PM3 combinations for the cyclopropane synthase system with various model sizes. The SAM cofactor obviously strongly interacts in the cofactor binding site than SAH product as a consequent of the from methyl group at the sulfur atom resulting in positive charge around sulfur and neighboring atoms. In addition, water molecules observed in X-ray crystal structures form hydrogen bond between the cofactor and Asp70, thus water molecules were added in the system study. The results show the requirement of these water molecules to be included in the high level of calculations. Including of Asp70 or Glu124 residues with the cofactor and water molecules in the inner layer show no significantly different energy. In order to set up an ONIOM model with many atoms in the system of the cyclopropane synthase

system studied, adding the cofactor with water molecules in the inner layer or high level of calculation can represent the interaction with appropriate energies.

Quantum Chemical Calculations on Succinate dehydrogenase/Substrate-Inhibitor Interaction

An ONIOM calculation of succinate dehydrogenase enzyme and its inhibitor, 3-NPA, has been investigated and compared with substrate, succinate, within 7 Å of the substrate site of succinate dehydrogenase flavoprotein subunit (SdhA). The calculations showed that the succinate has more tight binding than 3-nitropropionate about 3 times. In addition, double polarization of basis set, 6-31G(d,p) can represent for diffuses function basis set, 6-31G(d,p). From individual interaction calculations between ligand, FAD, and various amino acids could be shown that the interaction energy with Arg409 is the main contributors. Moreover, it is important to note that the hydrogen bonding between the oxygen atom of the ligand (3-nitropropionic acid or succinate) and the flavin derivatives FAD play an important role in the binding pocket of the complex.

Role of Key Residues Specific to Cyclooxygenase II

Individual interaction energies of flurbiprofen with the COX-2 binding pocket were investigated. The results show that MP2/6-31G(d) is appropriate to study this system. Similarly, Arg120 seem to be an important residue in the two COX isoforms in both neutral and ionic system. Comparison of the interactions between flurbiprofen and SC558 with COX-2 binding site shows that Arg120 also plays an important role in the interactions. In addition, the ONIOM2 calculation has been useful to investigate the interaction between flurbiprofen and key amino acid in binding pocket. The obtained results indicate that flurbiprofen can produce moderate hydrogen bonding with Arg120 while no hydrogen bond is detected with Tyr355 or Val523. By the way, the combination of different levels of theory with ONIOM studies in four models shows that the combine method with ONIOM2(B3LYP/6-31G(d):PM3) is the best method to investigate the interaction between inhibitor-COX2 enzyme. ONIOM study

with B3LYP/6-31G(d):PM3 was performed for ionic systems. All results indicate an over binding energy due to electrostatic interactions.

An investigation on inhibitor-enzyme interactions of a non-selective COXs inhibitor; flurbiprofen and a selective COX-2 inhibitor; SC558 to the binding pocket of COX-2 enzyme were performed, based on ONIOM method. The interaction energies of flurbiprofen and SC-558 particularly interacting with Tyr355 in the COX-2 enzyme pocket, using B3LYP/6-31G(d,p)//PM3 are 1.23 and -6.13 kcal/mol, respectively. These results indicate clearly that SC558 can bind to COX-2 better than flurbiprofen. Moreover, there is hydrogen bonding interaction between SC-558 and Tyr355, as indicated by the $O\text{-}H_{Tyr355}\text{--}F_3C_{SC558}$ distance of about 2.3 Å whereas no hydrogen bonding observed in flurbiprofen. The obtained results can explain the selectivity of the SC558 inhibitor to the COX-2 enzyme.

LITERRATURE CITED

Akaho, E., C. Fujikawa, I. H. Runion, C. R. Hill and H. Nakano 1999. A study on binding modes of nonsteroidal antiinflammatory drugs to COX-1 and COX2 as obtained by Dock4.0. **Journal of Chemical Software.** 5: 147-162.

Albert, P., J. J. Pe´rez, N. Susana, L. Oriol, P. Jaume, L. Garcý´a and D. Mauleo´n. 2000. Modeling cyclooxygenase inhibition. Implication of active site hydration on the selectivity of ketoprofen analogues. **J. Med. Chem.** 43: 2280-2284.

Alexander, W., A. Casini, A. Heine, D. Kuhn, C. T. Supuran, A. Scozzafava, and G. Klebe. 2004. Unexpected nanomolar inhibition of carbonic anhydrase by COX-2-selective celecoxib: New pharmacological opportunities due to related binding site Recognition. **J. Med. Chem.** 47: 550-557.

Alston, T.A., L. Mela and H.J. Bright. 1977. 3-Nitropropionate, the toxic substance of Indigofera, is a suicide inactivator of succinate dehydrogenase. **Proceedings of the National Academy of Sciences of the United States of America** 74(9):3767-3771.

Barry, C.E., R.E. Lee, K. Mdluli, A.E. Sampson, B.G. Schroeder, R.A. Slayden and Y. Ying. 1998. Mycolic acids: structure, biosynthesis and physiological functions. **Progress in Lipid Research** 37(2-3):143-179.

Bloom, B.R. and P.M. Small. 1998. The Evolving Relation between Humans and Mycobacterium tuberculosis. **N Engl J Med** 338(10):677-678.

Boys, S.F. and F. Bernardi. 1970. The calculation of small molecular interactions by the differences of separate total energies. Some procedures with reduced errors. **Molecular Physics** 19(4):553 - 566.

Brouillet E, J.B., Hyman BT, Ferrante RJ, Kowall NW, Srivastava R, Roy DS, Rosen BR, and Beal MF. 1993. Age-dependent vulnerability of the striatum to the mitochondrial toxin 3-nitropropionic acid **Journal of neurochemistry** 60356-359.

Chomcheon, P., S. Wiyakrutta, N. Sriubolmas, N. Ngamrojanavanich, D. Isarangkul and P. Kittakoop. 2005. 3-Nitropropionic Acid (3-NPA), a Potent Antimycobacterial Agent from Endophytic Fungi: Is 3-NPA in Some Plants Produced by Endophytes? **Journal of Natural Products** 68(7):1103-1105.

Cole, S.T., R. Brosch, J. Parkhill, T. Garnier, C. Churcher, D. Harris, S.V. Gordon, K. Eiglmeier, S. Gas, C.E. Barry, F. Tekaia, K. Badcock, D. Basham, D. Brown, T. Chillingworth, R. Connor, R. Davies, K. Devlin, T. Feltwell, S. Gentles, N. Hamlin, S. Holroyd, T. Hornsby, K. Jagels, A. Krogh, J. McLean, S. Moule, L. Murphy, K. Oliver, J. Osborne, M.A. Quail, M.A. Rajandream, J. Rogers, S. Rutter, K. Seeger, J. Skelton, R. Squares, S. Squares, J.E. Sulston, K. Taylor, S. Whitehead and B.G. Barrell. 1998. Deciphering the biology of Mycobacterium tuberculosis from the complete genome sequence. **Nature** 393(6685):537-544.

Copeland, R.A., J.M. Williams, J. Giannaras, S. Nurnberg, M. Covington, D. Pinto, S. Pick and J.M. Trzaskos. 1994. Mechanism of selective inhibition of the inducible isoform of prostaglandin G/H synthase. **Proceedings of the National Academy of Sciences of the United States of America** 91(23):11202-11206.

Dapprich, S., I. Komaromi, K.S. Byun, K. Morokuma and M.J. Frisch. 1999. A new ONIOM implementation in Gaussian98. Part I. The calculation of energies, gradients, vibrational frequencies and electric field derivatives. **Journal of Molecular Structure: THEOCHEM** 461-4621-21.

Dye, C. 2006. Global epidemiology of tuberculosis. **The Lancet** 367(9514):938-940.

Dye, C., S. Scheele, P. Dolin, V. Pathania, M.C. Raviglione, f.t.W.G. Surveillance and Monitoring Project. 1999. Global Burden of Tuberculosis: Estimated Incidence, Prevalence, and Mortality by Country. **JAMA** 282(7):677-686.

Feliu Maseras, K.M. 1995. IMOMM: A new integrated <I>ab initio</I> + molecular mechanics geometry optimization scheme of equilibrium structures and transition states. **Journal of Computational Chemistry** 16(9):1170-1179.

Futaki, N., S. Takahashi, M. Yokoyama, I. Arai, S. Higuchi and S. Otomo. 1994. NS-398, a new anti-inflammatory agent, selectively inhibits prostaglandin G/H synthase/cyclooxygenase (COX-2) activity in vitro. **Prostaglandins** 47(1):55-59.

Gaussian 03, R.C., M. J. Frisch, G. W. Trucks, H. B. Schlegel, G. E. Scuseria, M. A. Robb, J. R. Cheeseman, J. A. Montgomery, Jr., T. Vreven, K. N. Kudin, J. C. Burant, J. M. Millam, S. S. Iyengar, J. Tomasi, V. Barone, B. Mennucci, M. Cossi, G. Scalmani, N. Rega, G. A. Petersson, H. Nakatsuji, M. Hada, M. Ehara, K. Toyota, R. Fukuda, J. Hasegawa, M. Ishida, T. Nakajima, Y. Honda, O. Kitao, H. Nakai, M. Klene, X. Li, J. E. Knox, H. P. Hratchian, J. B. Cross, V. Bakken, C. Adamo, J. Jaramillo, R. Gomperts, R. E. Stratmann, O. Yazyev, A. J. Austin, R. Cammi, C. Pomelli, J. W. Ochterski, P. Y. Ayala, K. Morokuma, G. A. Voth, P. Salvador, J. J. Dannenberg, V. G. Zakrzewski, S. Dapprich, A. D. Daniels, M. C. Strain, O. Farkas, D. K. Malick, A. D. Rabuck, K. Raghavachari, J. B. Foresman, J. V. Ortiz, Q. Cui, A. G. Baboul, S. Clifford, J. Cioslowski, B. B. Stefanov, G. Liu, A. Liashenko, P. Piskorz, I. Komaromi, R. L. Martin, D. J. Fox, T. Keith, M. A. Al-Laham, C. Y. Peng, A. Nanayakkara, M. Challacombe, P. M. W. Gill, B. Johnson, W. Chen, M. W. Wong, C. Gonzalez, and J. A. Pople. 2004. **Gaussian, Inc., Wallingford CT**

George, K.M., Y. Yuan, D.R. Sherman and C.E. Barry, , III. 1995. The Biosynthesis of Cyclopropanated Mycolic Acids in Mycobacterium tuberculosis. **J. Biol. Chem.** 270(45):27292-27298.

Glickman, M.S., J.S. Cox and W.R. Jacobs. 2000. A Novel Mycolic Acid Cyclopropane Synthetase Is Required for Cording, Persistence, and Virulence of Mycobacterium tuberculosis. **Molecular Cell** 5(4):717-727.

Guérard, C., M. Bréard, F. Courtois, T. Drujon and O. Ploux. 2004. Synthesis and evaluation of analogues of S-adenosyl--methionine, as inhibitors of the E. coli cyclopropane fatty acid synthase. **Bioorganic & Medicinal Chemistry Letters** 14(7):1661-1664.

Huang, C.-c., C.V. Smith, M.S. Glickman, W.R. Jacobs, Jr. and J.C. Sacchettini. 2002. Crystal Structures of Mycolic Acid Cyclopropane Synthases from Mycobacterium tuberculosis. **J. Biol. Chem.** 277(13):11559-11569.

Huang, L.-s., G. Sun, D. Cobessi, A.C. Wang, J.T. Shen, E.Y. Tung, V.E. Anderson and E.A. Berry. 2006. 3-Nitropropionic Acid Is a Suicide Inhibitor of Mitochondrial Respiration That, upon Oxidation by Complex II, Forms a Covalent Adduct with a Catalytic Base Arginine in the Active Site of the Enzyme. **J. Biol. Chem.** 281(9):5965-5972.

Hunt, R.H., S. Harper, D.J. Watson, C. Yu, H. Quan, M. Lee, J.K. Evans and B. Oxenius. 2003. The gastrointestinal safety of the COX-2 selective inhibitor etoricoxib assessed by both endoscopy and analysis of upper gastrointestinal events. **Am J Gastroenterol** 98(8):1725-1733.

Katori, M., M. Majima and Y. Harada. 1998. Possible background mechanisms of the effectiveness of cyclooxygenase-2 inhibitors in the treatment of rheumatoid arthritis. **Inflammation Research** 47(14):107-111.

Kujubu, D., B. Fletcher, B. Varnum, R. Lim and H. Herschman. 1991. TIS10, a phorbol ester tumor promoter-inducible mRNA from Swiss 3T3 cells, encodes a novel prostaglandin synthase/cyclooxygenase homologue. **J. Biol. Chem.** 266(20):12866-12872.

Kuno, M., R. Hongkrengkai and S. Hannongbua. 2006. ONIOM-BSSE scheme for H...[pi] system and applications on HIV-1 reverse transcriptase. **Chemical Physics Letters** 424(1-3):172-177.

Lemire, B.D. and K.S. Oyedotun. 2002. The Saccharomyces cerevisiae mitochondrial succinate:ubiquinone oxidoreductase. **Biochimica et Biophysica Acta (BBA) - Bioenergetics** 1553(1-2):102-116.

Mantri, P. and D. T.Witiak. 1994. Inhibitors of COX and 5-lipoxygenase. **Curr. Med. Chem.** 1328-355.

McKinney, J.D., K.H. zu Bentrup, E.J. Munoz-Elias, A. Miczak, B. Chen, W.-T. Chan, D. Swenson, J.C. Sacchettini, W.R. Jacobs and D.G. Russell. 2000. Persistence of Mycobacterium tuberculosis in macrophages and mice requires the glyoxylate shunt enzyme isocitrate lyase. **Nature** 406(6797):735-738.

Meade, E., W. Smith and D. DeWitt. 1993. Differential inhibition of prostaglandin endoperoxide synthase (cyclooxygenase) isozymes by aspirin and other non-steroidal anti- inflammatory drugs. **J. Biol. Chem.** 268(9):6610-6614.

Mitchison, D. 1992. The Garrod Lecture. Understanding the chemotherapy of tuberculosis: current problems. **J Antimicrob Chemother** 29477 - 493.

Mitchison, D.A. 2004. The search for new sterilizing anti-tuberculosis drugs. **Frontiers in Bioscience** 91059-1072.

Nielsen, K.F. and J.r. Smedsgaard. 2003. Fungal metabolite screening: database of 474 mycotoxins and fungal metabolites for dereplication by standardised liquid chromatography-UV-mass spectrometry methodology. **Journal of Chromatography A** 1002(1-2):111-136.

Paterson, R.R.M. and C. Kemmelmeier. 1990. Neutral, alkaline and difference ultraviolet spectra of secondary metabolites from Penicillium and other fungi, and comparisons to published maxima from gradient high-performance liquid chromatography with diode-array detection. **Journal of Chromatography A** 511195-221.

Patocka, J., J. Bielavsky, J. Cabal and J. Fusek. 2000. 3-Nitropropionic acid and similar nitrotoxins. **Acta-Medica-(Hradec-Kralove)** 43(1):9-13.

Salem, M.A., J. Michael Williams, S.J. Wainwright and C.R. Hipkin. 1995. Nitroaliphatic compounds in Hippocrepis comosa and other legumes in the European flora. **Phytochemistry** 40(1):89-91.

Salvatore, F., Borek, E., Zappia, V., Williams-Ashman, H. G., Schlenk, F., Eds. 1977. The Biochemistry of Adenosylmethionine. **Columbia University Press** New York

Schmidt, F., S. Donahoe, K. Hagens, J. Mattow, U.E. Schaible, S.H.E. Kaufmann, R. Aebersold and P.R. Jungblut. 2004. Complementary Analysis of the Mycobacterium tuberculosis Proteome by Two-dimensional Electrophoresis and Isotope-coded Affinity Tag Technology. **Mol Cell Proteomics** 3(1):24-42.

Sharma, V., S. Sharma, K.H. zu Bentrup, J.D. McKinney, D.G. Russell, W.R. Jacobs and J.C. Sacchettini. 2000. Structure of isocitrate lyase, a persistence factor of Mycobacterium tuberculosis. **Nat Struct Mol Biol** 7(8):663-668.

Simmons, D.L., D.B. Levy, Y. Yannoni and R.L. Erikson. 1989. Identification of a phorbol ester-repressible v-src-inducible gene. **Proceedings of the National Academy of Sciences of the United States of America** 86(4):1178-1182.

Smith, C.V., C.-c. Huang, A. Miczak, D.G. Russell, J.C. Sacchettini and K. Honer zu Bentrup. 2003. Biochemical and Structural Studies of Malate Synthase from Mycobacterium tuberculosis. **J. Biol. Chem.** 278(3):1735-1743.

Smith, D.D. and S.J. Norton. 1980. Inhibition of cyclopropane fatty acid synthase by sinefungin and A9145C. **Biochemical and Biophysical Research Communications** 94(4):1458-1462.

Smith, H.S. and W. Baird. 2003. Meloxicam and selective COX-2 inhibitors in the management of pain in the palliative care population. **American Journal of Hospice and Palliative Medicine** 20(4):297-306.

Smith, W.L., R.M. Garavito and D.L. DeWitt. 1996. Prostaglandin Endoperoxide H Synthases (Cyclooxygenases)-1 and -2. **J. Biol. Chem.** 271(52):33157-33160.

Sun, F., X. Huo, Y. Zhai, A. Wang, J. Xu, D. Su, M. Bartlam and Z. Rao. 2005. Crystal Structure of Mitochondrial Respiratory Membrane Protein Complex II. **Cell** 121(7):1043-1057.

Svensson, M., S. Humbel, R.D.J. Froese, T. Matsubara, S. Sieber and K. Morokuma. 1996. ONIOM: A multilayered integrated MO + MM method for geometry optimizations and single point energy predictions. A test for Diels-Alder reactions and Pt(P(t-Bu)3)2 + H2 oxidative addition. **Journal of Physical Chemistry** 100(50):19357-19363.

SYBYL 7.3, T.I., 1699 South Hanley Rd., St. Louis, Missouri, 63144, USA

Vane, J.R. and R.M. Botting. 1996. Mechanism of Action of Anti-Inflammatory Drugs. **Scandinavian Journal of Rheumatology** 25(6 supp 102):9 - 21.

Williams, M.C., F.R. Stermitz and R.D. Thomas. 1975. Nitro compounds in Astragalus species. **Phytochemistry** 14(10):2306-2308.

Xie, W.L., J.G. Chipman, D.L. Robertson, R.L. Erikson and D.L. Simmons. 1991. Expression of a mitogen-responsive gene encoding prostaglandin synthase is regulated by mRNA splicing. **Proceedings of the National Academy of Sciences of the United States of America** 88(7):2692-2696.

Yankovskaya, V., R. Horsefield, S. Tornroth, C. Luna-Chavez, H. Miyoshi, C. Leger, B. Byrne, G. Cecchini and S. Iwata. 2003. Architecture of Succinate Dehydrogenase and Reactive Oxygen Species Generation. **Science** 299(5607):700-704.

Yuan, Y., R.E. Lee, G.S. Besra, J.T. Belisle and C.E. Barry. 1995. Identification of a gene involved in the biosynthesis of cyclopropanated mycolic acids in Mycobacterium tuberculosis. **Proceedings of the National Academy of Sciences of the United States of America** 92(14):6630-6634.

CURRICULUM VITAE

NAME : Miss Darinee Sae-Tang

BIRTH DATE : March 1, 1982

BIRTH PLACE : Bangkok, THAILAND

NATIONALITY : Thai

EDUCATION :

YEAR	INSTITUTION	DEGREE/DIPLOMA
2002	Kasetsart Univ.	B.Sc.(Chemistry)
2004	Kasetsart Univ.	M.S.(Physical Chemistry)

SCHOLASHIP : Higher Education Development Project Scholarship Postgraduate Education and Research Program in Physical Chemistry (2002-2003)

Thai Graduate Institute of Science and Technology(TGIST) (2004-2009)

Research Assistant Scholarship, Kasetsart University. (2007-2009)

PUBLICATIONS

1. Saiphon Songarsa, Shuleewan Rajviroongit, Darinee Sae-Tang, Supa Hannongbua, Kanyawim Kirtikara, and Prasat Kittakoop :New Racemosol Derivatives as Potent Cyclooxygenase (COX) Inhibitors. *CHEMISTRY & BIODIVERSITY* , Vol. 2 (2005) 1635-1647.

2. Darinee Sae-Tang, Prasat Kittakoop and Supa Hannongbua. Role of Key Residue Specific to Cyclooxygenase II : An ONIOM Study (submitted)

3. Darinee Sae-Tang, Nahoum Antony, Sumalee Kamchonwongpaisan, Simon Mackay and Supa Hannongbua. Comparison Interaction Energy of Mycolic Acid Cyclopropane Synthase as Tuberculosis Target with SAM and SAH cofactors and Sinefungin Inhibitor: A Quantum Chemical Calculation (to be submitted)

4. Darinee Sae-Tang and Supa Hannongbua. An ONIOM Study of Interaction of Mycolic Acid Cyclopropane Synthase with SAM and SAH cofactors and Sinefungin Inhibitor by B3LYP method of calculations (to be submitted)

5. Darinee Sae-Tang, Prasat Kittakoop and Supa Hannongbua. Quantum Chemical Calculations of 3-Nitropropionate Inhibitor of Succinate Dehydrogenase (to be submitted)

CONFERENCES (ORAL AND POSTER PRESENTATIONS) :

1. Darinee Sae-Tang, Supa Hannongbua, Saiphon Songarsa, Shuleewan Rajviroongit and Prasat Kittakoop. Molecular Docking of COX-2 Inhibitors: Racemosol and Demethylracemosol. The abstract of 29th Congress on Science and Technology of Thailand (STT2003), Khon Kaen University, Khon Kaen, Thailand, 20-22 October 2003.

2. Darinee Sae-Tang and Supa Hannongbua. Quantum Chemical Calculations Investigated COX-2/Flurbiprofen Interactions. The 8th Annual National Symposium on Computational Science and Engineering, Suranaree University of Technology , Nakhon Ratchasima, Thailand, 21-23 July 2004.

3. Darinee Sae-Tang, Saiphon Songarsa, Chuleewan Rajviroongit, Prasat Kittakoop, Kanyawim Kirtikara and Supa Hannongbua. Theoretical Investigation and Molecular Modeling Study on Cyclooxygenase-2/Inhibitors Interaction, The 15th European Symposium on Quantitative Structure Activity Relationship & Molecular Modelling, Istanbul, Turkey, 5-10 September 2004.

4. Darinee Sae-Tang and Supa Hannongbua Structural Conformational Analysis of SC558 : The Inhibitor of Cyclooxygenase-2, Based on Quantum Chemical Calculations, 30th Congress on Science and Technology of Thailand, IMPACT Exhibition and Convention Center, Nonnthaburi, Thailand, 19-21 October 2004.

5. Darinee Sae-Tang, Supa Hannongbua, Saiphon Songarsa, Shuleewan Rajviroongit and Prasat Kittakoop. Docking studies of Racemosol and Derivatives as a search for Cyclooxygenase-2 selective enzyme inhibitors The Petroleum and Petrochemical Technology Consortium 2005.

6. Darinee Sae-Tang, Prasat Kittakoop and Supa Hannongbua. Investigation on the Cyclooxygenase-2/SC558 Interactions, Based on Quantum Chemical Calculations, NSTDA Annual Conference: NAC 2005, Thailand Science Pack, Pathumthani, Thailand, 27-30 March 2005.

7. Darinee Sae-Tang, Prasat Kittakoop and Supa Hannongbua. A comparison of Interactions between Flurbiprofen and SC558 with Tyr355 in Cyclooxygenase-2 Using ONIOM2 Method, 2ndAsian Pacific Conference on Theoretical and Computational Chemistry (APACTC), Chulalongkorn University, Thailand, 2-6 May 2005.

8. Darinee Sae-Tang, Prasat Kittakoop and Supa Hannongbua. Molecular Docking of 3-Nitropropionic Acid in Succinate Dehydrogenase ComplexII, 31th Congress on Science and Technology of Thailand, Suranaree University of Technology, Nakornratchasima, Thailand,18-20 October 2005.

9. Darinee Sae-Tang, Prasat Kittakoop and Supa Hannongbua. Theoretical Study on the Inhibition of Succinate Dehydrogenase by 3-nitropropionic acid, International Conference on Modeling in Chemical and Biological Engineering Science, Bangkok, 25-27 October 2006.

10. Darinee Sae-Tang, Nahoun Anthony, Sumalee Kamchonwongpaisan, Supa Hannongbua, G.D. Coxon and Simon Mackay. Cyclopropane Synthases as Targets in Antituberculosis Drug Design Key Residue Identification Using *Ab initio* Methodologies, ScotCHEM Computional Chemistry Symposium , St Andrews university, Scotland , 4 April 2007.

11. Darinee Sae-Tang, Nahoun Anthony, Sumalee Kamchonwongpaisan, Supa Hannongbua and Simon Mackay. Quantum Chemical Calculations Study of Cofactors Fragment in Interaction Energy of Cyclopropane Synthase, German-Thai Symposium on nanoscience and nanotechnogy, The Tide resort, Chonburi, Thailand, 26-28 September 2007.

12. Darinee Sae-Tang, Prasat Kittakoop, Sumalee Kamchonwongpaisan and Supa Hannongbua. Quantum Chemical Calculations on Succinate dehydrogenase/ Substrate-Inhibitor Interaction, Second Annual Symposium of Protein Society of Thailand, Chulabhorn Research Institute Conference Center Bangkok, Thailand, 20-21 September 2007.

13. Darinee Sae-Tang, Nahoun Anthony, Sumalee Kamchonwongpaisan, Simon Mackay and Supa Hannongbua. Binding Energy Calculation of CyclopropaneSynthase Enzymes between Cofactors and Their Active Site: ONIOM Study, Pure and Applied Chemistry International Conference2008, Sofital Centara Grand Bangkok, Thailand, 30 January – 1 February 2008.

14. Pongthep Prajongtat, Darinee Sae-Tang, Phronphimon Maitarad, Patchreenart Saparpakorn and Supa Hannongbua. Interaction Energies of Oxaloacetate and Binding Site of Phosphoenolpyruvate Carboxykinase(PEPCK) by MP2 Calculations, Pure and Applied Chemistry International Conference2008, ,Sofital Centara Grand Bangkok, Thailand, 30 January – 1 February 2008.

15. Darinee Sae-Tang, Prasat Kittakoop, Supa Hannongbua. An ONIOM Study on Succinate Dehydrogenase/Substrate-Inhibitor Interaction, The 12th Annual Symposium on Computational Science and Engineering, Ubon Rajathanee University, Thailand, 27-29 March 2008.

16. Darinee Sae-Tang, Sumalee Kamchonwongpaisan, Nahoum Anthony, Simon Mackay and Supa Hannongbua. Effect of Water Molecule in Cyclopropane Synthase Cofactor Binding Site by Quantum Chemical Calculations, The 13th Annual Symposium on Computational Science and Engineering, Kasetsart University, Thailand, 25-27 March 2009.

.